DEVELOPMENT OF PAPER-BASED BIOSENSORS FOR POINT-OF-CARE NUCLEIC ACID TESTING

CHOI JANE RU

THESIS SUBMITTED IN FULFILMENT OF THE REQUIREMENTS FOR THE DEGREE OF DOCTOR OF PHILOSOPHY

FACULTY OF ENGINEERING
UNIVERSITY OF MALAYA
KUALA LUMPUR

2016

UNIVERSITY OF MALAYA

ORIGINAL LITERARY WORK DECLARATION

Name of Candidate: **CHOI JANE RU**

Matric No: **KHA140065**

Name of Degree: **DOCTOR OF PHILOSOPHY**

Title of Thesis:

DEVELOPMENT OF PAPER-BASED BIOSENSORS FOR POINT-OF-CARE NUCLEIC ACID TESTING

Field of Study: **BIOMEDICAL ENGINEERING**

I do solemnly and sincerely declare that:

(1) I am the sole author/writer of this Work;
(2) This Work is original;
(3) Any use of any work in which copyright exists was done by way of fair dealing and for permitted purposes and any excerpt or extract from, or reference to or reproduction of any copyright work has been disclosed expressly and sufficiently and the title of the Work and its authorship have been acknowledged in this Work;
(4) I do not have any actual knowledge nor do I ought reasonably to know that the making of this work constitutes an infringement of any copyright work;
(5) I hereby assign all and every rights in the copyright to this Work to the University of Malaya ("UM"), who henceforth shall be owner of the copyright in this Work and that any reproduction or use in any form or by any means whatsoever is prohibited without the written consent of UM having been first had and obtained;
(6) I am fully aware that if in the course of making this Work I have infringed any copyright whether intentionally or otherwise, I may be subject to legal action or any other action as may be determined by UM.

Candidate's Signature Date:

Subscribed and solemnly declared before,

Witness's Signature Date:

Name:

Designation:

ABSTRACT

Nucleic acid testing (NAT), a molecular diagnostic technique that involves nucleic acid extraction, amplification and detection, conventionally relies on well-established laboratories, high-end instrumentation and highly trained operators, limiting its use in resource-poor settings, where most diseases exist. With advances in point-of-care testing (POCT), lateral flow assays (LFA) have been explored for nucleic acid detection. However, as biological samples are generally complex and contain low amounts of target nucleic acids, a substantial off-chip extraction and amplification process (*e.g.*, tube-based extraction and polymerase chain reaction (PCR)) is normally required prior to lateral flow detection. Additionally, the applications of LFA have been currently limited by their low sensitivity and poor functionality. Herein, it was demonstrated for the first time a novel fully integrated paper-based sample-to-answer biosensor incorporating nucleic acid extraction, amplification and sensitive lateral flow detection. The optimum concentration of reagent and environmental conditions (*i.e.,* temperature and relative humidity) for LFA were determined. Paper-based LAMP was integrated into LFA, coupled with a handheld battery-powered heating device for nucleic acid amplification in POC settings, which showed a comparable result to that of conventional tube-based platform. A fully integrated paper-based sample-to-answer biosensor was then developed, which could successfully detect *Escherichia coli* in spiked drinking water, milk, blood, and spinach with a detection limit of as low as 10-1000 CFU/mL, and Hepatitis B virus (HBV) in clinical blood sample, highlighting its potential use in medical diagnostics, food safety analyses and environmental monitoring. The sensitivity of biosensor was further enhanced by incorporating a piece of paper-based shunt and a polydimethylsiloxane (PDMS) barrier into the strip to achieve optimum fluidic delays for LFA signal enhancement, resulting in 10-fold signal

enhancement over unmodified LFA. This strategy could successfully detect HBV with concentrations of as low as ~10^2 IU/mL in clinical blood samples, which was comparable to that of conventional detection strategy and even more sensitive than the existing biosensors, demonstrating its ability to detect acute HBV infections. The phenomena of fluidic delay were also evaluated by mathematical simulation, through which the fluid movement throughout the shunt and the tortuosity effects in the presence of PDMS barrier were revealed, which significantly affect the detection sensitivity. The proposed fully integrated biosensor offers great potential for highly sensitive detection of various targets for wide applications in the near future.

ABSTRAK

Ujian asid nukleik ialah satu teknik diagnotik molekul yang melibatkan pengekstrakan, amplifikasi dan pengesanan asid nukleik yang secara konvensionalnya bergantung kepada makmal yang mantap, peralatan yang mewah dan pekerja yang terlatih. Oleh itu, ini mengehadkan penggunaannya di kawasan yang mempunyai sumber yang amat terhad, di mana terwujudnya pelbagai penyakit. Dengan kemajuan dalam ujian *point-of-care* (POCT), *lateral flow assays* (LFAs) telah dieksploitasikan untuk ujian asid nukleik. Akan tetapi, disebabkan kekompleksan sampel biologi dan kepekatan asid nukleik sasaran yang rendah, proses pengekstrakan dan amplifikasi secara *off chip* (*e.g.*, pengekstrakan dengan menggunakan tiub dan amplifikasi melalui *polymerase chain reaction* (PCR)) amat diperlukan sebelum asid nukleik sasaran dapat dikesan dengan ujian *LFA*. Tambahan pula, aplikasi LFAs telah dihadkan oleh sensitivitinya yang rendah dan fungsinya yang terhad. Walaupun integrasi pengekstrakan DNA dan amplifikasi DNA ke dalam *paper-based biosensor* telah dilaporkan sebelum ini, tetapi pergabungan LFA dengan semua langkah ujian asid nukleik di dalam satu peranti belum dilaporkan. Dalam kajian ini, *novel fully integrated paper-based sample-to-answer biosensor* yang menggabungkan pengekstrakan, amplifikasi dan pengesanan asid nukleik dengan LFA telah berjaya dihasilkan. Kepekatan optimum *reagen* dan faktor persekitaran (*i.e.,* suhu dan kelembapan relatif) untuk LFA telah dikenalpasti. *Paper-based LAMP* dan LFA telah digabungkan dengan alat pemanas mudah alih yang berbateri untuk proses amplifikasi asid nukleik di *POC settings* bagi pengesanan DNA, di mana hasilnya adalah setanding dengan strategi konvensional. Selepas itu, *Fully integrated sample-to-answer biosensor* telah dihasilkan, di mana ia dapat mengesan *Escherichia coli* dalam air, susu, darah dan bayam dengan had pengesanan sebanyak 10-1000 CFU/mL, dan virus Hepatitis B (HBV) dalam sampel darah klinikal, maka

menunjukkan potensi penggunaannya dalam bidang diagnosis perubatan, analisis keselamatan makanan dan pemantauan alam sekitar. Sensitiviti biosensor telah dipertingkatkan dengan menggunakan cara pergabungan *shunt* dan *polydimethylsiloxane (PDMS) barrier* dengan LFA untuk mencapai kadar pengaliran yang optimum untuk peningkatan isyarat LFA. Dengan pengubahsuaian ini, isyarat LFA dapat dipertingkatkan sebanyak 10 kali ganda berbanding dengan LFA yang tidak diubahsuai. Cara ini telah berjaya mengesan HBV dengan kepekatan sebanyak ~10^2 IU/mL seperti yang dikesan dengan menggunakan cara konvensional dan lebih sensitif daripada biosensor lain, maka ini menunjukkan keupayaannya untuk mengesan jangkitan HBV akut. Fenomena pengurangan kadar pengaliran juga telah dinilai dengan simulasi matematik dengan pemerhatian pergerakan cecair melalui *shunt* dan kesan *tortuosity* dengan kehadiran *PDMS barrier*, di mana fenomena ini dikenalpasti dapat menyebabkan peningkatan sensitiviti pengesanan. *Integrated biosensor* ini berpotensi untuk mengesan pelbagai analit bagi pelbagai aplikasi pada masa hadapan.

ACKNOWLEDGEMENTS

First, I would like to express my sincere appreciation to my supervisor at University of Malaya, Associate Prof. Ir. Dr. Belinda Murphy for her encouragement, support and guidance throughout my studies.

I would like to extend my deepest gratitude to my supervisor at Xi'an Jiaotong University, Prof. Xu Feng for giving me the opportunity to join his research group, Bioinspired Enginering and Biomechanics Center (BEBC). His endless support and valuable guidance has truly given me confidence in my research. I am always impressed by his vast knowledge and open mind for scientific discussion. Thank you for providing such a wonderful research environment that makes me a better researcher today.

I am very thankful to all the BEBC Point-of-Care teammates, especially Hu Jie, Tang Ruihua, and Gong Yan for their valuable suggestions and assistance. Special thanks go to Liu Zhi and Dr. Feng Shangsheng for their guidance in the mathematical simulation part of my thesis.

I would also like to express my appreciation to all other students at BEBC and Tissue Engineering Laboratory for all the help and support. I am very fortunate to be surrounded by these excellent students. They have contributed in expanding my knowledge and aiding me in bringing my research goals to fruition.

Finally, million thanks to my family for their encouragement and support throughout my life, and Yong Kar Wey for his endless care and love. Thank you very much to all of you.

TABLE OF CONTENTS

Page

LIST OF FIGURES

LIST OF TABLES

LIST OF ABBREVIATIONS

2D	Two dimensional
3D	Three dimensional
Ab	Antibody
Ag	Antigen
ASSURED	Affordable, Sensitive, Specific, User-friendly, Rapid and Robust, Equipment-free, and Deliverable to end-users
AuNP	Gold nanoparticle
CFU	Colony forming unit
CT	Cycle threshold
DNA	Deoxyribonucleic acid
DP	Detector probe
E. coli	*Escherichia coli*
ELISA	Enzyme-linked immunosorbent assay
FINA	Filtration isolation of nucleic acid
FITC	Fluorescein isothiocyanate
FTA	Fast technology analysis
H_2O_2	Hydrogen peroxide
HBV	Hepatitis B virus
hCG	Human chrorionic gonadotropin
HDA	Helicase-dependent amplification
HIV	Human immunodeficiency virus
HRP	Horseradish peroxidase
IgG	Immunoglobulin G
IgM	Immunoglobulin M
IPP	Image Pro Plus

LAMP	Loop mediated isothermal amplification
LB	Luria-Bertani
LFA	Lateral flow assay
Na_3PO_4	Sodium phosphate
NaCl	Sodium chloride
NASBA	Nucleic acid sequence-based amplification
NAT	Nucleic acid testing
NS1	Non-structural 1
OD	Optical density
PBS	Phosphate buffered saline
PCR	Polymerase chain reaction
PDMS	Polydimethysiloxane
PMMA	Poly(methyl methacrylate)
POC	Point-of-care
POCT	Point-of-care testing
PVC	Polyvinyl chloride
qPCR	Quantitative polymerase chain reaction
RH	Relative humidity
RNA	Ribonucleic acid
RPA	Recombinase polymerase amplification
SAMBA	Simple amplification based assay
SDA	Strand displacement amplification
SDS	Sodium dodecyl sulfate
SEM	Scanning electron microscopy
SSC	Saline sodium citrate
TCEP	Tris(2-carboxyethyl)phosphine

TE	Tris-EDTA
TEM	Transmission electron microscopy
UV/Vis	Ultraviolet-visible
WHO	World Health Organization
μPAD	Microfluidic paper-based analytical devices

CHAPTER 1: INTRODUCTION

1.1 Background

Today, molecular diagnostics is essential for widespread applications, including in medical diagnostics (*e.g.,* human immunodeficiency virus (HIV), dengue, cardiovascular diseases, and stroke), food safety analysis and environmental monitoring. A key aspect of much molecular diagnostics is the use of nucleic acid testing (NAT), which consists of three main steps: nucleic acid extraction, amplification and detection (Liu et al., 2014; Toumazou et al., 2013; Venkatesan & Bashir, 2011; Wanunu et al., 2010). This presents a substantially higher specificity and sensitivity than antigen (Ag)-antibody (Ab)-based assays (Craw & Balachandran, 2012; Peeling & McNerney, 2014; Yu et al., 2012b). Conventional NAT involves high-end instrumentation, labour-intensive procedures, and is time-consuming (*e.g.,* involving phenol-chloroform extraction, polymerase chain reaction (PCR) or electrophoresis), which means that its application is limited in resource-poor point-of-care (POC) settings (Martinez et al., 2010; Wang et al., 2012). With increasing spread of infections with no specific medication for treatment (*e.g.,* dengue infections, *E. coli* O157:H7 infection), rapid diagnosis is imperative to prevent a life-threatening complication (Blažková et al., 2009). Therefore, there is an urgent need to develop a portable, fast and accurate NAT diagnostic tool, which can be readily implemented in disease-endemic, low resource settings to overcome the shortcomings of conventional NAT (Niemz et al., 2011).

With advances in microfluidic technologies, integrated chip-based biosensors have emerged with great potential to address the limitations of conventional equipment for POC NAT. These microfluidic devices can process a small volume of liquid, significantly reducing the consumption of samples and reagents, and thus the cost.

However, most chip-based devices are made of glass (Kumbhat et al., 2010b; Ngo et al., 2014), silicon (Huang et al., 2013) or polymer (*e.g.,* polydimethylsiloxane (PDMS)) (Lien et al., 2006) with integrated functional units (*e.g.,* pumps and valves) (Hawkins & Weigl, 2010) which require complicated fabrication processes, hence reducing their suitability for POC testing.

Recently, paper has been unitized as a feasible and high potential platform for NAT, gaining increasing interest as a platform in the diagnostic field, especially for low-resource settings due to its simplicity, cost-efficiency, biodegradability, and biocompatibility (Hu et al., 2014). It is predominantly composed of cellulose fibers with a porous structure, allowing fluids to wick through via capillary force (Chen et al., 2015). The utilization of paper to fabricate paper-based biosensors, particularly lateral flow assays (LFAs), has currently attracted significant interest. As compared to chip-based biosensors, paper-based biosensors are simple, portable, cost-effective and user friendly, offering a promising choice for NAT at the POC (Blacksell et al., 2007). Recent studies have focused on the use of nucleic acid-based LFA for accurate POC diagnostics (Blažková et al., 2009; Hu et al., 2013; Wang et al., 2013a). However, the main limitations of nucleic acid-based LFA are difficulties in quantification, low sensitivity and poor functionality.

Several approaches have been investigated to address these limitations. To achieve quantification, researchers have developed a variety of handheld or smartphone-based readers to quantify LFA results (Mudanyali et al., 2012; Xu et al.). As for the analytical sensitivity improvement, even though there have been several attempts to develop multiple techniques for sensitivity improvement (*e.g.,* through probe-based signal enhancement (Hu et al., 2013), enzyme-based signal enhancement

(He et al., 2011), thermal contrast (Qin et al., 2012), or fluidic control (Parolo et al., 2013; Rivas et al., 2014), most of them involve high cost equipment, complex modifications and multistep operations. Therefore, a simple and low cost method is essential for LFA sensitivity enhancement.

In fact, the main challenge in developing an ideal nucleic acid-based LFA is to produce a nucleic acid-based LFA with integrated nucleic acid extraction and amplification. Recent studies have reported the use of commercial Fast Technology Analysis (FTA) card to perform nucleic acid extraction (Lange et al., 2014; Liang et al., 2014), the use of glass fiber for nucleic acid amplification (De Paula & Fonseca, 2004), and the use of LFAs or paper-based microfluidic devices (He et al., 2010; Hu et al., 2013) for amplicon detection. However, the paper-based extraction, amplification and LFA were separately performed, which entails multiple processing steps, limiting their usability in POC settings. The integration of the three key steps of NAT into integrated paper-based biosensors may pave the way for rapid POC testing.

This study aims to significantly improve the analytical sensitivity and functionality of LFAs, to yield a fully integrated paper-based sample-to-answer diagnostic platform for cost-effective, sensitive, specific, user-friendly and rapid target detection. The pathogenic agents such as dengue virus, hepatitis B virus (HBV) and *Escherichia coli*, which commonly lead to severe clinical outcomes, are selected as model analytes in the study. The fully integrated paper-based sample-to-answer biosensor can be widely used to accurately detect a broad range of nucleic acid in resource-poor settings.

1.2 Aim and objectives

The aim of this study is to develop a fully integrated paper-based sample-to-answer biosensor for POC NAT. The specific objectives include:

i. To optimize the concentration of reagent (*i.e.,* gold nanoparticle-detector probe (AuNP-DP), saline sodium citrate (SSC) buffer and streptavidin) and environmental factors (*i.e.,* temperature and relative humidity (RH)) in LFA.

ii. To improve the functionality of LFA by integrating paper-based nucleic acid extraction and amplification into the test strip, creating a fully integrated paper-based biosensor.

iii. To enhance the sensitivity of LFA by incorporating simple fluidic control method into the test strip.

iv. To evaluate the potential of a fully integrated biosensor for sensitive clinical sample testing.

1.3 Research question

How to improve the performance of existing LFA in terms of detection sensitivity and functionality for rapid POC NAT in resource-poor settings?

1.4 Thesis outline

The thesis is written in the article style format, which consists of seven chapters briefly described in the following:

Chapter 1 provides an overview of the research background, the aim and objectives of the study, the research questions addressed and the content of each chapter.

Chapter 2 presents a critical review relevant to the study. The current global health status, the conventional diagnostic method and the development of POC biosensors are discussed. In view of the escalating demand for the low cost diagnostic devices, the advantages of developing paper-based biosensors, particularly LFA are highlighted especially in nucleic acid detection. The advances in development of nucleic acid-based LFA, particularly in sensitivity enhancement and functionality improvement are also comprehensively discussed. This chapter contains selected text reprinted in part with permission from one of my review articles: Choi, J. R., Tang, R., Wang, S., Wan Abas, W. A. B., Pingguan-Murphy, B*. & Xu F.* (2015). Paper-based Sample-to-Answer Molecular Diagnostic Platform for Point-of-Care Diagnostics. *Biosensors and Bioelectronics, 74*, 427-439. Copyright (2016) Elsevier.

Chapter 3 presents the evaluation of the optimum reagent and environmental conditions for the commonly used nucleic-acid based LFA. This chapter contains selected text reprinted in part with permission from one of my research articles: Choi, J. R., Hu, J., Feng, S., Wan Abas, W. A. B., Pingguan-Murphy, B.* & Xu, F.* (2016). Sensitive Biomolecule Detection in Lateral Flow Assay with A Portable Temperature-Humidity Control Device. *Biosensors and Bioelectronics, 79,* 98-107. Copyright (2016) Elsevier.

Chapter 4 presents the study of integrating paper-based amplification into LFA to create an integrated LAMP-LFA biosensor. This chapter contains selected text reprinted in part with permission from one of my research articles: Choi, J. R., Hu, J., Gong, Y., Feng, S., Wan Abas, W. A. B., Pingguan-Murphy*, B. & Xu, F* (2016). An Integrated Lateral Flow Assay for Effective DNA Amplification and Detection at the Point of Care. *Analyst,* doi: 10.1039/C5AN02532J. Copyright (2016) Royal Society of Chemistry.

Chapter 5 presents the study of integrating paper-based extraction and amplification into LFA to create a fully integrated paper-based sample-to-answer biosensor for potential use in biological testing. This chapter contains selected text reprinted in part with permission from one of my research articles: Choi, J. R., Hu, J., Tang, R., Gong, Y., Feng, S., Ren, H.,… Xu, F.* (2016). An Integrated Paper-based Sample-to-Answer Biosensor for Nucleic Acid Testing at the Point of Care. *Lab on a Chip, 16,* 611-621. Copyright (2016) Royal Society of Chemistry.

Chapter 6 presents the approach of incorporating simple fluidic control method into a fully integrated paper-based sample-to-answer biosensor for sensitivity enhancement with clinical sample testing. This chapter contains selected text reprinted in part with permission from one of my research articles: Choi, J. R., Liu, Z., Hu, J., Tang, R., Gong, Y., Feng, S., . . . Xu, F*.(2016). Polydimethylsiloxane-Paper Hybrid Lateral Flow Assay for Highly Sensitive Point-of-Care Nucleic Acid Testing. *Analytical Chemistry,* doi: 10.1021/acs.analchem.6b00195. Copyright (2016) American Chemical Society.

Chapter 7 includes the conclusion drawn from the findings of the thesis, the existing challenges, and suggestions for possible future work.

CHAPTER 2: LITERATURE REVIEW

2.1 Global health

Worldwide, infectious diseases impose a great health burden. Pathogenic infections commonly arise as a result of disease transmission among humans. Where diseases are able to spread over long distances, there is the potential for them to become pandemics. Unlike the onset of non-infectious types of disease (*e.g.*, some chronic diseases), the onset of an infectious illness can be abrupt and unmistakable. Annually, approximately 4.3 million die from acute respiratory infections, 1.8 million from AIDS, 0.8 million people from malaria, 0.1 million people from Hepatitis B and 0.05 million from dengue infection (Pyrek, 2014). Sexually transmitted infections and tropical parasitic infections are responsible for hundreds or thousands of deaths and an enormous burden of morbidity (Ortayli et al., 2014; Pyrek, 2014). In resource limited settings, particularly in underdeveloped and developed countries, lack access to medical diagnostics due to the limited infrastructure, trained personnel and healthcare management have become the major challenges. The diagnostic facilities in these areas are very frequently ineffective and out of date. Therefore, more than 95% of these deaths occur in underdeveloped and developing countries, including Southeast Asia, the Western Pacific, and South America (Bhatt et al., 2013; Fauci & Morens, 2012).

Food safety issues have also attracted public concern in recent years. Foodborne illnesses are the direct consequence of ingesting food that contains toxic or infectious agents. In the United States, there are an estimated 7.6 million illnesses contracted, over 325,000 hospitalizations and 5,000 deaths (Nyachuba, 2010; Scallan et al., 2011a; Scallan et al., 2011b) attributed to foodborne diseases each year with an annual economic cost of US$10–83 billion (Scharff, 2012). In 2010, *Escherichia coli* (*E. coli*)

O157:H7 and *Salmonella spp.* caused about 1.4 million incidents of foodborne illness in the US alone. In the developing countries, especially in China and Brazil, the incidence of food poisoning has increased over the past few years mainly due to the presence of illegal additives or bacterial pathogens in food (*e.g.,* melamine in milk powder, clenbuterol in pork, Sudan dyes in duck eggs and plasticizer in beverages) (Gomes et al., 2013; Liu et al., 2013).

In addition, water safety represents another public health concern. Waterborne diseases due to contaminated water remain a major issue, and cause diarrheal diseases. Today, about 600 million people have no access to the safe drinking water. Drinking water contaminated with industrial sources (*e.g.,* lead and mercury), human and animal faeces and chemicals from agriculture have affected approximately 40% of the global population, especially in rural areas (Nations, 2015; WHO/UNICEF, 2015). Ingestion of water that is contaminated with human or animal faeces can cause pathogenic infections, including bacteria, viruses and protozoa infections. To date, more than 250 infectious diseases are known to be caused by food- and water-borne pathogens, including pathogenic bacteria, viruses, fungi, parasites, marine phytoplankton, and cyanobacteria. Salmonella typhimurium, Staphylococcus aureus, Legionella pneumophila, and *E. coli* O157:H7, together making up the major class of pathogenic bacteria that causes large-scale outbreaks of infection worldwide (Park et al., 2010).

Currently, in the absence of suitable vaccine and therapies for most diseases, early and rapid detection of the harmful target analytes is essential (Peeling et al., 2010). Development of a rapid, affordable, portable and simple diagnostic technology that can improve healthcare, environmental safety and food quality, especially in developing or

underdeveloped countries plays a significant role in controlling and monitoring diseases to achieve the goal of "touching life, impacting society".

2.2 Conventional diagnostic assays

Current laboratory tests such as culture, enzyme-linked immunosorbent assay (ELISA), and quantitative polymerase chain reaction (qPCR) are commonly used for medical diagnostics, food safety analyses and environmental monitoring (Peeling et al., 2010) **(Fig. 2.1)**. Culture or target isolation represents the gold standard for most diagnosis. For instance, the detection of foodborne pathogens (*e.g., E. coli, Shigella* and *Salmonella*) normally involves bacteria culture on an agar plate (Venkatesan & Bashir, 2011). This diagnostic procedure is expensive, time-consuming (*i.e.,* several days to a week), requires expertise and necessitates a high-level biosafety laboratory (Peeling et al., 2010).

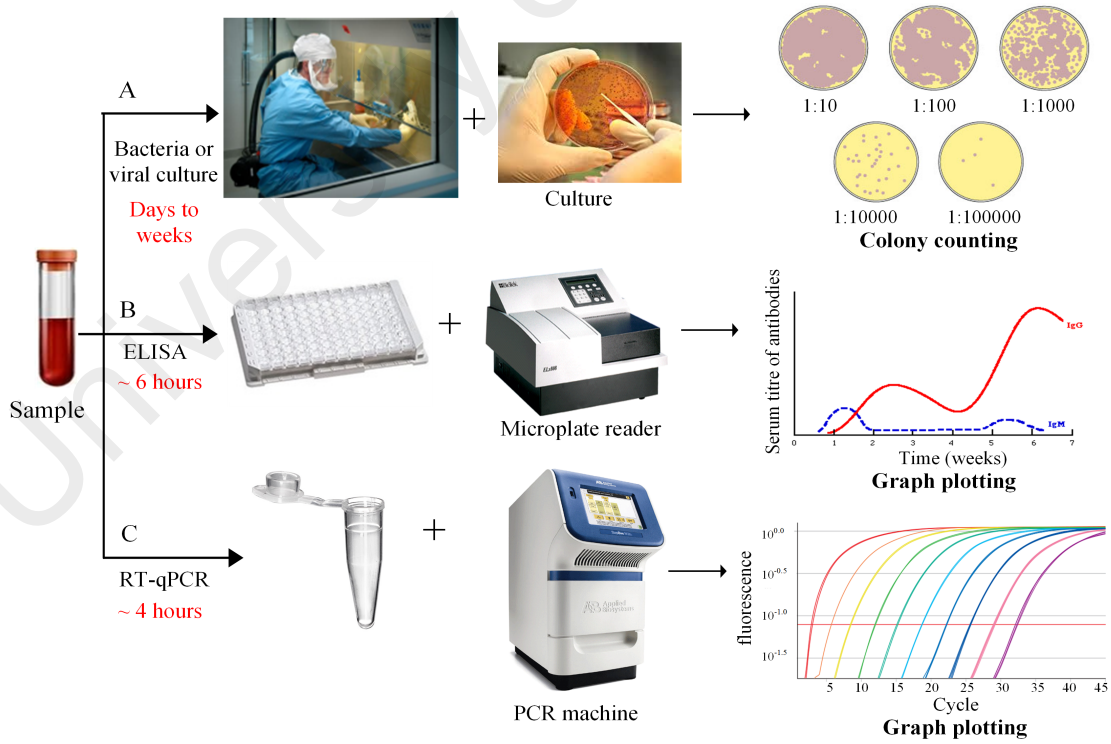

Figure 2.1: Conventional diagnostic assays. Laboratory tests include (A) Culturing, (B) ELISA and qPCR, which are generally time-consuming and expensive.

Serological tests such as ELISA have been widely used for diagnosis of infectious diseases (Guzman et al., 2007). This assay uses the basic immunological concept of an antigen binding to its specific antibody, which allows detection of very small quantities of antigens such as proteins, peptides, hormones, or antibodies in a fluid sample. The enzyme-labeled antigens and antibodies are normally used to detect the biological molecules. The most commonly used enzymes are alkaline phosphatase and glucose oxidase. The antigen is allowed to bind to a specific antibody, which is itself subsequently detected by a secondary, enzyme-coupled antibody. A chromogenic substrate for the enzyme yields a visible color change or generates fluorescence, indicating the presence of the antigen (Perumal & Hashim, 2014). Quantitative or qualitative measures can be assessed based on such a colorimetric reading. An external reader is normally required for an assay read out. To date, ELISA represents the gold standard for diagnosis of various infections (e.g., dengue infections). However, in dengue infections, the persistence of specific Ab for a specific period of time may complicate the diagnosis of the disease. A false-positive result may occur from other infections because of cross-reaction when using antibody-based ELISA (Hunsperger et al., 2009). Additionally, ELISA is unable to distinguish between infection by different viral serotypes.

Currently, qPCR, represents the most common NAT used to detect target DNA, especially in viruses. This assay is able to identify a particular viral serotype and allows quantification of viral titre, making it more sensitive and specific than other diagnostics assays. In addition to singleplex assays, multiplex assays have now been developed to detect all viral serotypes in a single sample (Chien et al., 2006; Johnson et al., 2005; Kong et al., 2006). However, this assay is expensive, dependent on high-end equipment and labor-intensive (Peeling et al., 2010).

Whilst these laboratory tests have been introduced to provide early diagnosis of various diseases, access to these tests is limited in underdeveloped and developing countries. Therefore, there is still an unmet need to develop simple, portable and low-cost biosensors to detect early infections in resource-limited settings.

2.3 Point-of-care biosensors

Biosensors are currently available at the POC for various applications (Blacksell et al., 2007). Biosensors can serve as substitutes for conventional laboratory-based assays, especially in resource-limited settings, due to their simplicity, portability and cost-effectiveness (Kahn & Plaxco, 2010; Lowe, 2007). The difference between the laboratory-based assays and biosensor-based assay are summarized in **Table 2.1**. Biosensors have significantly reduced sample and reagent consumption, the complexity of the operational steps and the entire assay cost and time, without compromising sensitivity and specificity. These rapid and cost-effective diagnostic assays are particularly important for disease management, surveillance, epidemiologic investigation and supportive treatment (Guzman & Kouri, 2004). There are two main types of biosensors - chip-based and paper-based biosensors.

Table 2.1: Comparison between laboratory-based and biosensor-based assay

	Laboratory-based assay	**Biosensor-based assay**
Well-established laboratory required	Yes	No
Special equipment required	Yes	No
Skilled worker required	Yes	No
Assay time	Long (days to week)	Short (< 30 min)
Assay cost	High cost ($ 15-20 per assay)	Low cost ($ 1-3 per assay)
References	(Hue et al., 2011; Pok et al., 2010; Waggoner et al., 2013)	(Blacksell et al., 2011; Fry et al., 2011; Pan-ngum et al., 2013)

2.3.1 Chip-based biosensors

In recent years, sensitive and specific chip-based biosensors have been used in many applications in which disease-specific biomarkers such as Ag, Ab and nucleic acid are detected (Fang et al., 2010; Kumbhat et al., 2010a). Nowadays, a variety of chip-based biosensors are commercially available for diagnosis of various diseases **(Fig. 2.2)**. Thus far, chip-based biosensors are mainly classified as optical, electrochemical or piezoelectric detection based on their signal transduction mechanism (Teles, 2011).

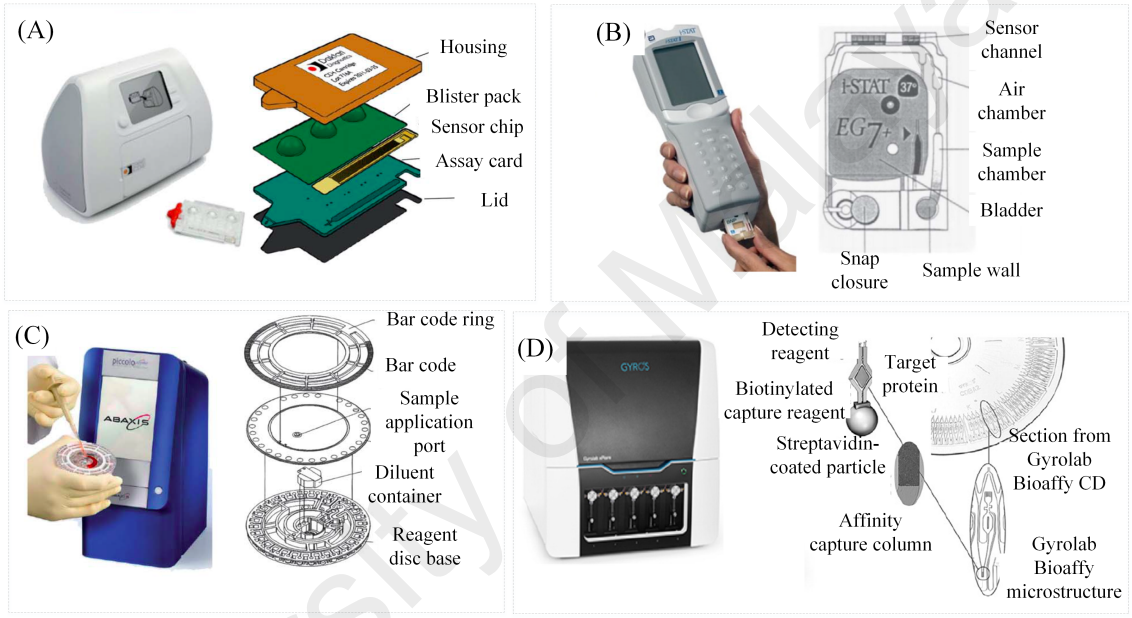

Figure 2.2: Chip-based biosensors. (A) Daktari devices for CD4 counting, (B) Abbott iSTAT device for detection of blood chemistries and cardiac markers, (C) Abaxis microfluidic compact disc to detect renal diseases and (D) Gyrolab xPlore™ microfluidic compact disc for multiple protein analysis. Adapted from (Hu et al., 2016).

Optical detection techniques, the most commonly used methods have been introduced for rapid diagnosis of diseases, with the detection of optical signal, directly proportional to the analyte concentration. For instance, using virus-bound magnetic beads, a microfluidic system has been developed to simultaneously detect Immunoglobulin G (IgG) and Immunoglobulin M (IgM) in dengue viral infections, generating an optically detectable fluorescent signal (Lee et al., 2009). Unfortunately, they suffer from poor long-term stability due to the leaching of immobilized indicators

and low assay sensitivity, especially when coupled with radioimmunoassays (Perumal & Hashim, 2014). Electrochemical-based biosensors have also been used for detection of infectious diseases. These biosensors allow the amplification of the biochemical signal into a detectable electrical signal (Lau et al., 2015). For example, an electrochemical biosensor has been introduced to detect *Mycobacterium tuberculosis* DNA based on a gold nanotube array electrode platform (Teles & Fonseca, 2008). These biosensors have attracted broad interest due to their rapidity and high selectivity. However, their sensitivity has yet to be improved, and they are limited in the adhesion of the material to the patterned electrodes (Teles & Fonseca, 2008). In addition to these optical and electrochemical-based biosensors, the development of piezoelectric-based biosensors has also received a great deal of attention. These biosensors detect the frequency shift of different concentrations of analyte, following the attachment of the analyte to the immobilized sensing material. For instance, a piezoelectric transducer has been developed with two different immobilized monoclonal Abs to detect both non-structural 1(NS1) protein and glycoprotein-E in dengue infections (Wu et al., 2005). The piezoelectric method is simple and sensitive. However, this technique is susceptible to the effect of environmental interferences, thus limiting its applications outside the laboratory (Teles, 2011).

Taken together, even though chip-based biosensors are simpler, cheaper and faster than conventional laboratory techniques, they still require a complicated fabrication process and an expensive signal detector (Teles, 2011), which are not compatible with point-of-care testing (POCT) in developing countries. Therefore, existing chip-based biosensors have to be further simplified to improve their applicability in primary healthcare settings.

2.3.2 Paper-based biosensors

Paper has gained increasing interest as a platform in the diagnostic field (Webster et al., 2009). Nowadays, paper-based assays have become an alternative to conventional laboratory-based and chip-based assays. The comparison between chip-based and paper-based biosensors is summarized in **Table 2.2**. In general, paper is a thin sheet of material normally made up of raw sources including cotton (filter paper and chromatography papers), wood (printing paper), jute, flax and so forth. As a high amount of lignin, which consists of chromophores, is present in wood, paper made of a high percentage of cotton is more desirable in diagnostic applications. The grade of paper is normally selected based on the application of the assay. Commercially available paper grades usually differ in various characteristics such as pore size, porosity, and absorbence capacity and flow rate. Both filter paper and chromatography paper are normally made of high-quality cotton linters with about 98% cellulose content.

In the field of paper-based microfluidics, two main kinds of material have been widely utilized in fabrication of paper-based biosensors: cellulose (including chromatography papers and filter papers, which represent the main substrates of dipsticks and microfluidic paper-based analytical devices (μPADs)) and nitrocellulose (the key component of a lateral flow strip). Cellulose is composed of an abundance of glucose units, which is fibrous, biodegradable, hydrophilic and insoluble in water. Nitrocellulose, another main component of a lateral flow strip is produced by nitration of cellulose, which strengthens the porous properties of cellulose. These paper substrates have been widely explored to develop paper-based biosensors (*e.g.,* dipsticks, lateral flow strips and μPADs).

Table 2.2: Comparison between chip-based and paper-based biosensors

	Chip-based biosensors	**Paper-based biosensors**
Components	Polymer (polydimethysiloxane (PDMS) or Poly(methyl methacrylate)(PMMA), glass, silicon	Paper and membrane
Fabrication technique	Photolithography, wet chemical etching or high precision laser cutting technique	Hydrophilic-hydrophobic patterning, paper stacking and folding
Driving force	Pump	Capillary force
Result analysis	Reader	Visual detection
Advantages	Normally are fully enclosed which reduces the risk of contamination	Low cost, simple fabrication process, allows reagent storage
Limitations	Risk of gas bubbles formation, potential adsorption of the reagent to the chip surface	Improvement needed in tems of sensitivity, quantification and functionality

Paper-based biosensors have been unitized as a feasible and high potential platform for POC testing, especially for use in low-resource settings due to their simplicity, cost-efficiency, biodegradability, and biocompatibility (Hu et al., 2014). They are predominantly composed of cellulose fibers with a porous structure, allowing fluids to wick through via capillary force (Chen et al., 2015), eliminating the need for an external pumping force normally required in chip-based biosensors. Paper can be readily manufactured on a large scale via standardized coating or inkjet printing techniques. The desired biomolecules can be incorporated into paper substrates (Zhao & van der Berg, 2008). Additionally, the white colour of paper is particularly suited for implementing colorimetric tests with visually detectable colorimetric changes. As compared to chip-based assays, the ability to use naked eye detection with a paper-based assay has simplified the assay readout, and eradicated the need for external readers. The strong correlation between the colour intensity and the concentration of analyte allows semi-quantitative or even quantitative measurements to take place in a

simple manner (Zimmermann et al., 2007). There are three main types of paper-based biosensors - dipsticks, lateral flow strips and μPADs **(Fig. 2.3)**. A comparison of these biosensors is presented in **Table 2.3.**

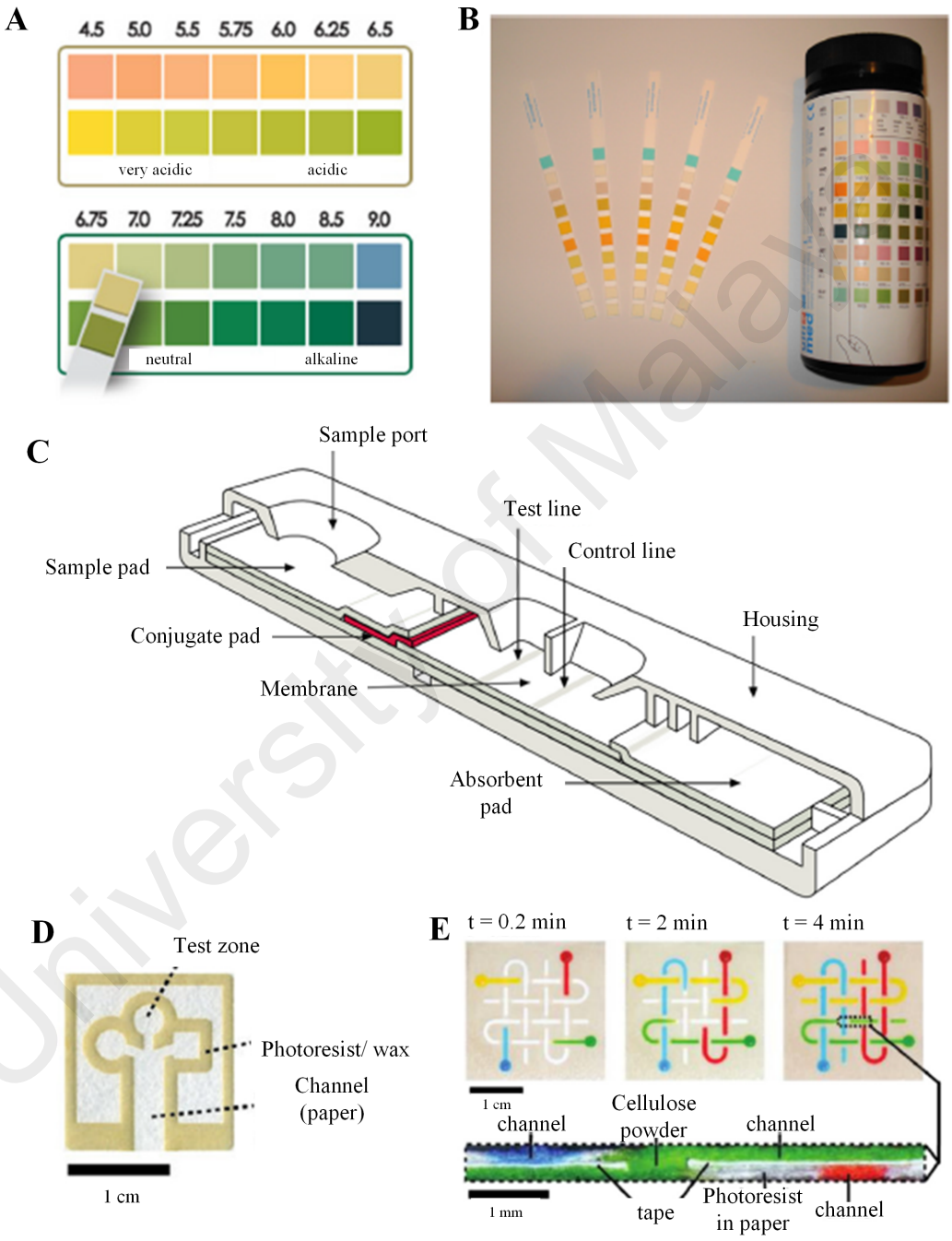

Figure 2.3: Paper-based biosensors. There are three main types of paper-based biosensors – (A-B) pH and urine dipsticks, (C) lateral flow strips and (D-E) μPADs. Adapted from (Hu et al., 2014).

Table 2.3: A summary of dipstick, lateral flow test strip and μPAD

Platform	Fabrication method	Reaction	Example
Dipstick	Soaking	Chemical reaction (acid-alkali reaction)	pH test strip Urine test strip
Lateral flow test strip	Dispensing, drying, assembling, cutting	Biological reaction (antigen-antibody reaction, nucleic acid hybridization)	Pregnancy test strip, nucleic acid-based test strip
μPAD	Hydrophilic-hydrophobic patterning, stacking layers of patterned paper	Biological reaction	ELISA test paper Liver function test paper

The first dipstick was proposed in the 1950s. Dipsticks, such as urine test strip or pH test strip, involves a simple manufacturing and operation process (Dossi et al., 2013; Luong et al., 2008). In general, pH test strips are manufactured by soaking a piece of filter paper into a mixture of acid–alkali indicators at certain concentration ratios. After drying, the paper is then impregnated with detection reagent. When the strip is immersed into a sample, the analyte (H^+) reacts with the detection reagent, resulting in colour formation. The pH value of the solution can be determined and the H^+ concentration can be semi-quantified based on the manufacturer's colour scale. These test strips have been widely used in medical diagnostics for monitoring diet intake by determining the pH level in saliva or urine. Similarly, urine test strips have been developed to detect various analytes in urine, including protein, glucose, ketone, haemoglobin, bilirubin, urobilinogen, acetone, nitrite and leokocyte to indicate pathological changes (Luong et al., 2008). For instance, nephritic or diabetic diseases can be detected via determining the level of the main urinary metabolic products (*e.g.,* protein and glucose) from patients using a standard urine test strip.

In the 1980s, lateral flow tests were developed particularly the human pregnancy test, derived from the development of the human chrorionic gonadotropin (hCG) beta-subunit radioimmunoassay, which has been widely available in the market. Since then, commercial rapid lateral flow tests were expanded beyond clinical diagnostics to environmental monitoring, food safety, veterinary, biodefense and drug abuse applications. Currently, multiplexing of rapid tests is becoming common. There exist some lateral-flow tests, which separate each single lateral flow test strip into multiple channels, enabling the detection of more than one target simultaneously. Details of the most commonly used lateral flow assay are briefly discussed in the following section (**Section 2.4**).

More recently, development in this field has been extended towards the μPADs. μPADs were pioneered by Whitesides's group in 2007 (Wang et al., 2013b). Both two-dimensional (2D) and three-dimensional (3D) μPADs were developed by patterning paper with a variety of assay designs (Park et al., 2011). 2D μPADs are made by patterning hydrophobic boundaries to form microchannels on paper (Han et al., 2014). Recent advances in fabrication of paper, including cutting, photolithography, plotting, injet etching, plasma etching and wax printing, make it possible to create channels and barriers in paper (Zhang et al., 2006). The capturing molecules required for biochemical reactions can be immobilized on paper with different patterns by hand dispensing or inkjet printing (Zhang et al., 2006). Functional chemical or biological molecules can be immobilized on paper by physical absorption, chemical coupling and carrier-mediated (*e.g.,* gold nanoparticles) deposition. 3D μPADs are normally formed by stacking layers of patterned paper in such a way that channels in adjacent layers of paper connect to each other. Compared with 2D μPADs, 3D μPADs offer several advantages due to their ability to incorporate a complex network of channels, hence providing multiple

functionalities. Among the various main forms of paper-based biosensors (*i.e.,* dipstick assays, LFAs and paper-based microfluidics devices), LFAs represent the most widely used paper-based biosensors in the diagnostic field to date.

2.4 Lateral flow assay (LFA)

Today, LFAs have received significant interest for detection of various target analytes (Dineva et al., 2005; Mao et al., 2009; Zhu et al., 2011). A variety of lateral flow strips are commercially available for rapid testing of diseases, such as Human Immunodeficiency Virus (HIV), Hepatitis C Virus (HCV), dengue, malaria and chikungunya (Wang et al., 2010).

Lateral flow test strips are typically composed of a sample pad, a conjugate pad, a reaction membrane, an absorbent pad and a backing pad. **Table 2.4** summarizes all the components of a typical lateral flow strip. The sample pad is usually pretreated with a buffer (*e.g.,* to adjust pH) to treat the raw sample and modulate the chemical variability in the sample, to improve the performance of the assay. The conjugate pad is normally overlapped with the sample pad, and carries the conjugated particles (normally the gold nanoparticles (AuNPs)), that would be coupled with the target analyte before wicking through the reaction membrane. The reaction membrane (normally nitrocellulose membrane) is an essential material in LFAs as it provides a platform for reaction and allows the forming of visible bands at the control and/or test zone. Capturing molecules, *e.g.*, antibodies or DNA, can be deposited on the nitrocellulose membranes to form test and control zones by electrostatic interaction, hydrogen bonds and/or hydrophobic forces. The absorbent pad provides a driving force based on capillary effect once the fluid reaches it, and serves as a sink for waste or excessive sample absorption, whereas

the backing pad provides a certain mechanical support to the device (Tamama et al., 2011).

Table 2.4: Components of a lateral flow strip

Component	Material	Function
Sample pad	100% cotton linter, rayon, glass fiber, and filtration materials	Modulate any chemical variability in the sample, treat the crude sample and release the assay adjusted sample
Conjugate pad	Glass fibers, polyesters, and rayon	Couple the analyte in the sample with the conjugate and release the sample
Reaction membrane	Nitrocellulose, nylon and polyvinylidene fluoride	Provides a platform for target detection and form visible bands at the control and/or test zone
Absorbent pad	100% cotton linter, high-density cellulose	Serve as a sink for waste or excessive sample and provides a driving force based on capillary effect once the fluid reach it
Backing pad	Vinyl (polyvinyl chloride or PVC), polystyrene and polyester	Provides a mechanical support to all the components of the strip

Most LFAs involve in diverse detection approaches including optical (e.g, colorimetry, fluorescence and chemiluminescence) and electrochemical detection (Cate et al., 2014; Martinez, 2011). The optical signal detection method is commonly used in LFAs, which can be classified as colorimetric, fluorescence or chemiluminescence detection. Colorimetric signal detection is particularly attractive due to its facilitation of simple naked eye detection without the need for an external reader. Today, colorimetric-based lateral flow strips **(Fig. 2.4)** have been widely used in colorimetric detection of target proteins (Ag or Ab) or nucleic acids using the gold nanoparticle as an indicator (Blacksell et al., 2007).

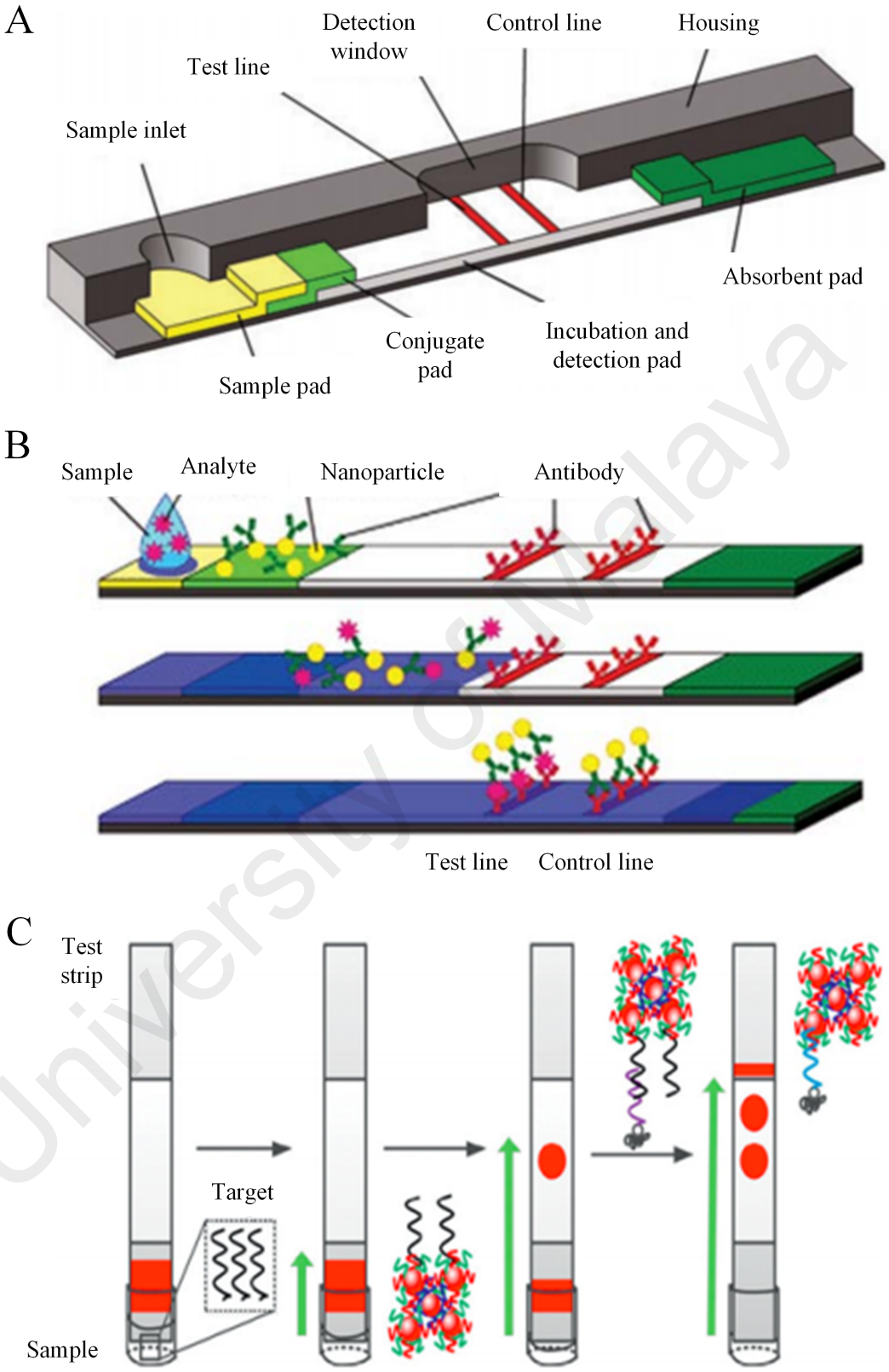

Figure 2.4: Lateral flow assay. (A) Schematic view of LFA. LFA for (B) antigen and (C) nucleic acid detection. Reproduced from (Feng et al., 2015).

Gold nanoparticles have been frequently used in paper strips due to their monodispersity properties, ease of preparation of the desired particle size, and ability to present a stable optical signal (Li et al., 2012). Stability of gold nanoparticles can be achieved by tagging them with biomolecules (*e.g.,* Ab or Ag or nucleic acid), which can then be specifically bound to the target analyte. These biomolecules are attached to the gold nanoparticle by non-covalent interactions, namely hydrophobic interaction and van der Waals forces (Eichmann & Bevan, 2010). Nanoparticles eventually create a visually detectable colour intensity based on the amount of analyte (Dungchai et al., 2010).

2.4.1 Antigen or antibody detection

Protein-based LFAs (*i.e.* immunochromatographic techniques based on Ag-Ab interactions) are available in the market to detect the target Ag or Ab for diagnosis of several diseases **(Fig. 2.5)** (Yetisen et al., 2013). There are two formats of LFAs based on the principle of Ag-Ab interactions, first, the sandwich format and second, the competitive format. In the more commonly used sandwich format, the presence of analyte (*e.g.,* Ab or Ag) leads to the formation of an analyte-gold conjugate, which migrates along the paper strip via capillary force and forms a visible red-purple band at the test zone after binding to the corresponding capturing molecule. The analyte-free gold conjugates can be captured by another capturing molecule at the control zone, creating another visible red band. The control band must appear to confirm the validity of the assay. Thus, the appearance of red band in both control and test regions indicates a positive result whereas the appearance of red band only in the control region shows a negative result. For example, a rapid immunochromatographic test strip based on the sandwich format has been developed for detecting dengue virus Ab (Cuzzubbo et al., 2001). The target Ab reacts with the colloidal gold-NS1 to form a complex, which diffuses across the nitrocellulose membrane to bind to the highly specific anti-IgG

and/or anti-IgM at the test zone. The unreacted gold-NS1 complex further reacts with the IgG or IgM and forms a visible control zone. A positive IgM and a negative IgG indicates a primary infection, whereas a positive IgG with negative IgM shows a secondary infection. A negative result is indicated by no visible line formation in both test zones (Cuzzubbo et al., 2001).

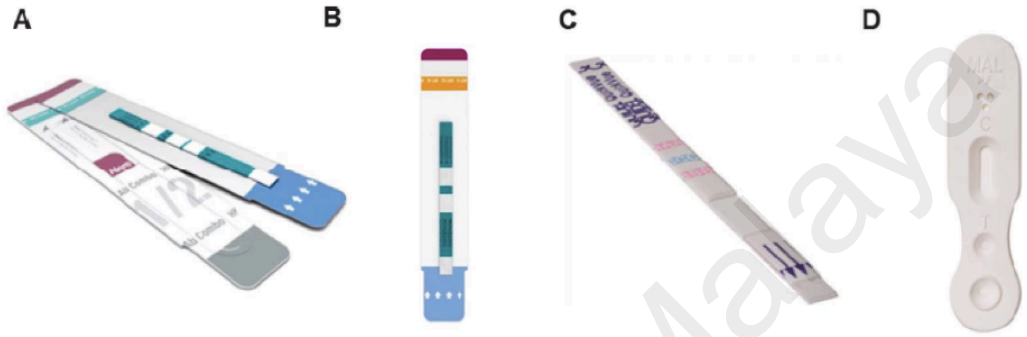

Figure 2.5: The commercial lateral flow test strips. The example of commercially available test strips include (A) DetermineTM HIV 1/2 Ag/Ab Combo for HIV diagnosis, (B) DetermineTM TB LAM Ag test for tuberculosis diagnosis, (C) QuickVue Influenza A + B test for the detection of influenza and (D) Clearview Malaria P.f. Test to detect Malaria. Adapted from (Yetisen et al., 2013).

In the competitive format, the conjugated particles (*e.g.,* gold-labeled Ab) are able to bind to the capturing molecules deposited at both test and control zones. The analyte competes for the binding sites of the capturing molecules deposited on both test and control zones. In contrast to the outcome of the sandwich format, a positive result is indicated by red colour formation in the control zone whereas a negative result is indicated by red colour formation in both control and test zones. In general, sandwich format assays are utilized for an analyte with multiple Ag epitopes, while competitive format assays are designed to detect an analyte with a single Ag epitope (Posthuma-Trumpie et al., 2009).

2.4.2 Nucleic acid detection

As compared to antigen or antibody detection, NAT is more suitable to detect the presence of the target at an early stage of infection (Wang et al., 2014), displaying a higher sensitivity and specificity for the diagnosis of infectious diseases than Ag-Ab interactions (Wang et al., 2014; Yu et al., 2012a). Commonly, a NAT assay involves nucleic acid hybridization or streptavidin-biotin interaction. In the detection method involving nucleic acid hybridization, two types of oligonucleotide probes, *i.e.,* detector probe and capture probe are typically used. Detector and capture probes are both complementary with the target nucleic acid sequence, while the detector probe is used to combine with a tag (*e.g.,* AuNPs) to make the reaction visible or measurable. In fact, detection of single-stranded amplicons normally involves nucleic acid hybridization at the test zone. For instance, as NASBA produces single-stranded RNA, the amplicons can hybridize with the control probe. The target RNA would bind to the AuNP labeled detector probe (AuNP-DP) to form complexes, which in turn bind to the control probe at the test zone to produce an observable signal (Rohrman et al., 2012).

In another case, detection of double-stranded amplicons (*e.g.*, PCR, RPA or LAMP products) (De Paula & Fonseca, 2004; Kersting et al., 2014; Kim et al., 2014), which cannot hybridize with the single-stranded probe, normally involve streptavidin-biotin interaction at the test zone. Streptavidin-coated commercial lateral flow strip are available which are able to detect biotinylated double-stranded amplicons (Rigano et al., 2014; Siah & McKenna, 2013; Song et al., 2013b; Thongkao et al., 2013). As most amplicons are double-stranded, denaturation at high temperature (95°C) is required to separate double-stranded DNAs into single strands, allowing the single-stranded DNA to bind with the complementary DNA probe. For example, LAMP product could be detected via a streptavidin-biotin interaction. At the initial stage of LAMP product

detection, biotinylated LAMP amplicons produced from biotinylated primers are denatured. These single-stranded biotinylated amplicons are then allowed to bind to the fluorescein isothiocyanate (FITC)-labeled DNA probe, which in turn forms complexes with the gold-labeled anti-FITC antibodies and further interacts with streptavidin at the test zone, producing a red signal observable by the naked eye (Kersting et al., 2014). The excess products in turn bind to a protein (*i.e.*, FITC) to give a red signal at the control zone for assay validation (Khunthong et al., 2013).

2.5 Advances in development of nucleic acid-based LFA

As mentioned above, numerous studies have demonstrated nucleic acid-based LFA. However, the existing LFAs suffer from poor quantification, low sensitivity and limited functionality. Quantification of LFAs has been currently achieved by the development of handheld or smartphone-based readers (LaBarre et al., 2011; Wu et al., 2014). However, the simple sensitivity enhancement method and functionality improvement (in particular, the integration of extraction and amplification into LFA) have not yet been demonstrated. Therefore, these limitations have to be addressed to create an ideal nucleic acid-based LFA for a wide range of applications.

2.5.1 Sensitivity enhancement in LFA

As these LFAs usually suffer from low sensitivity, which fails to meet the detection sensitivity requirement for clinical applications, there have been several attempts to develop new techniques for enhancing sensitivity. Common signal enhancement techniques include probe-based signal enhancement (Hu et al., 2013), enzyme-based signal enhancement technique (He et al., 2011), thermal contrast (Qin et al., 2012), or fluidic control techniques (Parolo et al., 2013; Rivas et al., 2014) **(Fig. 2.6)**. It has been reported that the sensitivity of LFA could be enhanced by using particles such as

liposomes (Connelly et al., 2008; Kumanan et al., 2009) or the aggregation of AuNP aggregates to achieve an almost 3-fold signal amplification (Hu et al., 2013). Besides that, the potential of enzymatic amplification has been demonstrated for signal enhancement. For instance, horseradish peroxidase (HRP) has been used to catalyze luminol in the presence of hydrogen peroxide (H_2O_2), and generate a chemiluminescent signal with improved sensitivity (Kim et al., 2010).

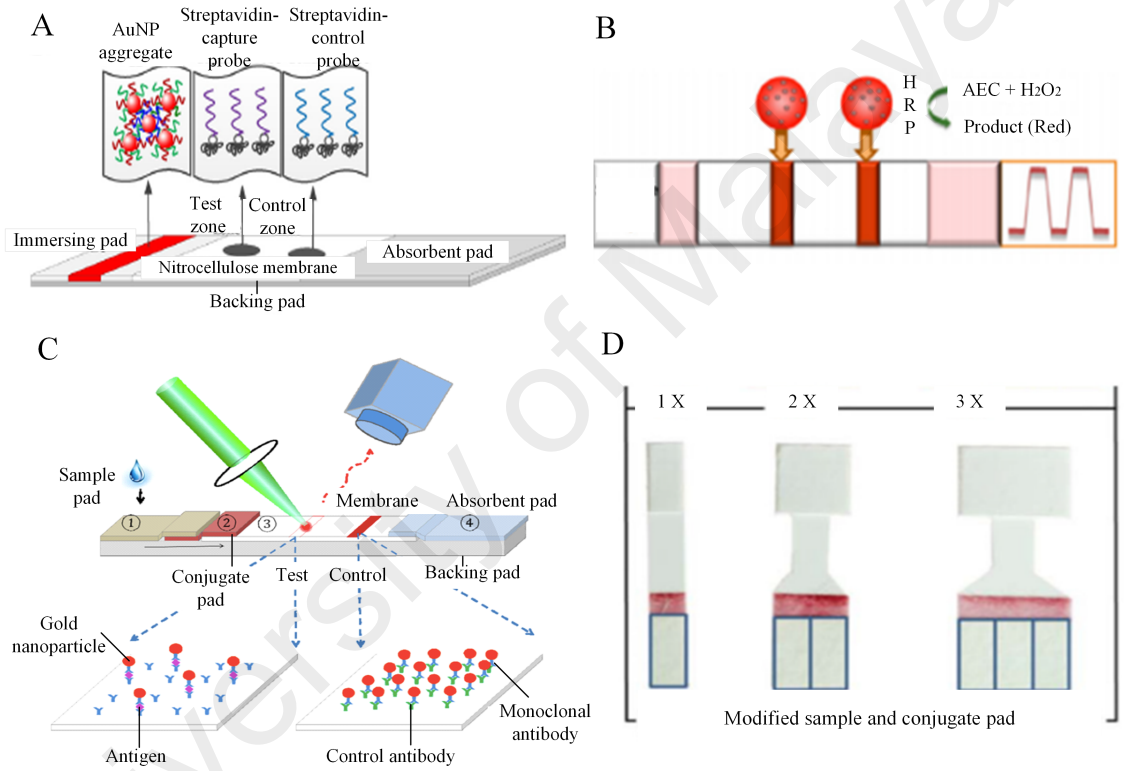

Figure 2.6: Sensitivity improvement in LFA. (A) probe-based signal enhancement, (B) enzyme-based signal enhancement technique, (C) thermal contrast and (D) fluidic control technique. Adapted from (Tamama et al., 2011).

In addition, a hairpin oligonucleotide-AuNP has been proven to be successful in enhancing the sensitivity of single-nucleotide polymorphism detection. The unique recognition characteristic of HO to specific DNA and single-base mismatched DNA lowers the detection limit (He et al., 2010). An ultrasensitive nucleic acid-based LFA has been further developed using HRP-AuNP dual labels. In the presence of H_2O_2, the enzymatic reaction between HRP and 3-amino-9-ethyl-carbazole produces insoluble red

products, which are deposited on the AuNP. This technique enables the detection of as low as 0.01pM without using instrumentation, showing a great promise for POC diagnosis (He et al., 2011).

Additionally, several fluidic control techniques have also been reported to improve the sensitivity of LFA, including paper architecture modifications to increase the amount of collected sample being collected (Parolo et al., 2013) and the use of wax-printed pillars as delay hydrophobic barriers to slightly reduce flow rate and allow the sufficient mixing of biomolecules and gold nanoparticle-detector probe prior to the detection (Rivas et al., 2014).

2.5.2 Multi-functionalization in LFA

As mentioned earlier, NAT, which generally consists of three key steps, *i.e.*, nucleic acid extraction, amplification and detection, currently involves labour-intensive, high-cost, and time-consuming processes, significantly limiting its applications in diagnostics at the POC (Martinez et al., 2010; Wang et al., 2012). Therefore, the main approach for multi-functionalization is to integrate paper-based nucleic acid extraction and amplification into LFA.

2.5.2.1 Paper as a platform for nucleic acid extraction

In a molecular assay, the nucleic acid extraction step plays a significant role in isolating DNA or RNA from a complicated biological sample (*e.g.*, blood sample) (Niemz et al., 2011). This process is important to eradicate undesirable substances, which may interfere with the subsequent amplification process (*e.g.*, haem from red blood cells). Without sample preparation, LFAs are unable to detect the nucleic acid in raw

biological samples. Therefore, integrating paper-based extraction into LFA is in highly desirable for POC testing.

A variety of commercial paper-based extraction devices are currently used in sample collection and nucleic acid extraction. Guthrie card or dried blood spot (DBS) filter paper, consisting of 903 filter paper, made of > 90% cellulose, has been used for blood collection from a pricked finger for subsequent analysis (de Vries et al., 2012). As an alternative, 903 protein saver card or Whatman™ 903 filter paper has been introduced for sample collection and nucleic acid extraction (Kudo et al., 2004). These cards have no stabilizing properties, thus requiring a low temperature (-80 to -20℃) for storage. To improve the extraction efficiency and facilitate high throughput, FTA cards (FTA classic and elute cards) have been introduced. Unlike the 903 protein saver card, FTA cards (Lange et al., 2014; Liang et al., 2014) are chemically-treated for DNA storage and extraction. The FTA classic card, in particular, has been commonly used for routine production of nucleic acid samples from a broad range of biological specimens, such as whole blood, plant cells, tissue culture cells and microorganisms **(Fig. 2.7A)**. FTA classic card consists of filter matrices impregnated with a patented chemical formula that lyses cell membranes and denatures proteins (Aye et al., 2011). It immobilizes the DNA to produce a web-like structure around the filter matrices and protects the DNA from oxidation, nucleases, UV radiation damage or microbial contamination (Beckett et al., 2008). The cellular debris, inhibitors and stabilizing chemicals can be readily washed off with washing buffer (Goldsborough & Fox, 2006). The DNA can be stored in the form of dried whole blood spots for at least 7.5 years at room temperature, and the extracted DNA can remain stable in the card, circumventing the need for centrifugation and refrigeration equipment (Pezzoli et al., 2007). A study has demonstrated the use of the FTA Classic Card in a microcapillary for sample-to-

answer NAT (Christopher et al., 2005) **(Fig. 2.7B)**. Recently, another type of FTA card for DNA extraction purposes, namely FTA Elute Cards, has been made commercially available. Instead of keeping the DNA attached to the paper matrix for analysis, these cards release the DNA upon the addition of sterile water, hence making the extraction much easier (de Vargas Wolfgramm et al., 2009). However, punching these commercial extraction devices into a tube with a single punch for downstream analysis (*e.g.*, PCR) could easily lead to cross-contamination between blood spots, and the manual process fails to meet the needs of large-scale samplings.

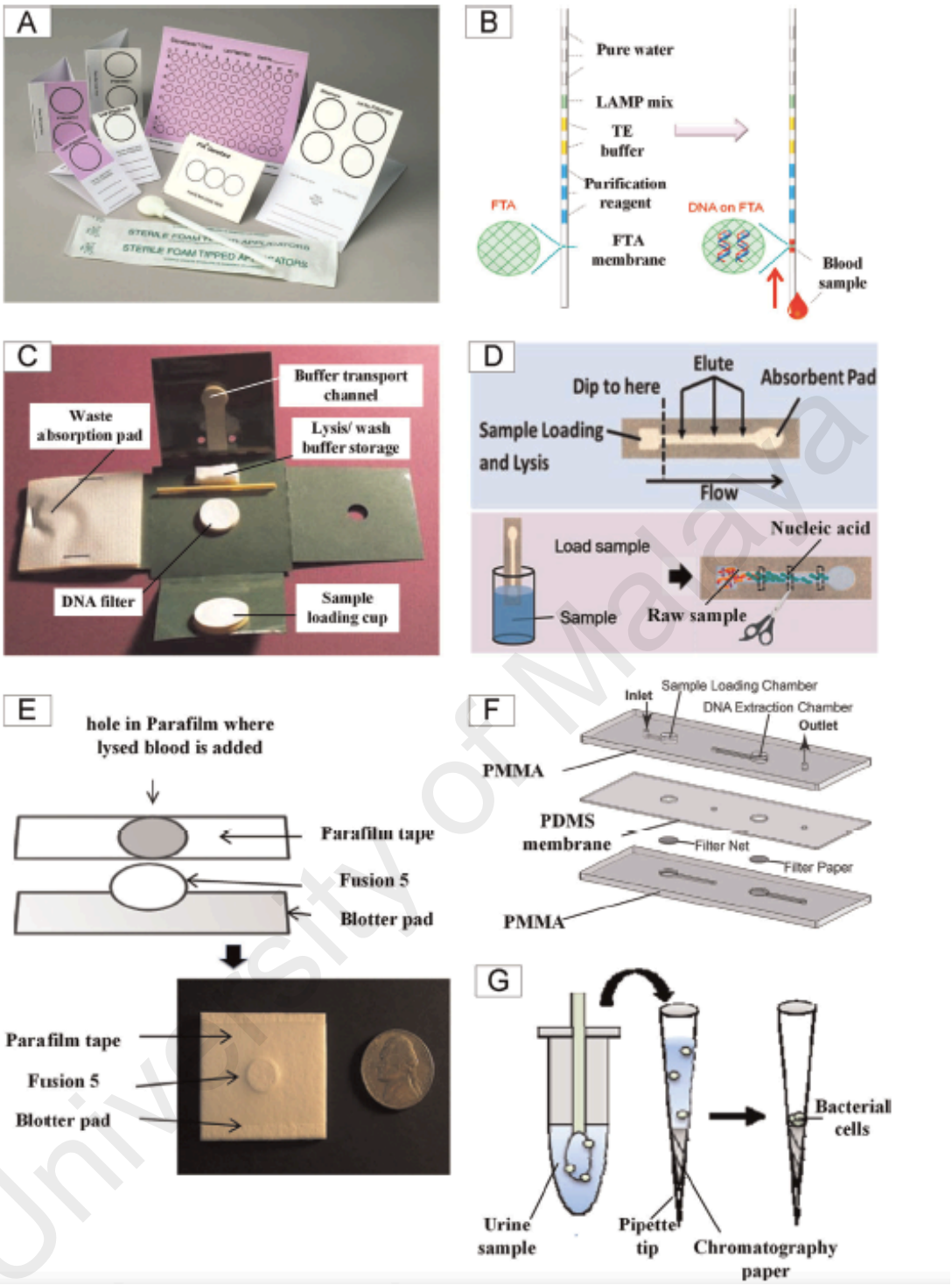

Figure 2.7: Paper as a platform for nucleic acid extraction. (A) commercial FTA cards , (B) integration of FTA card into microcapillary, (C) paper-based microfluidic origami fabricated by paper folding technique, (D) paper-based microfluidic device for DNA extraction from the real sample, (E) DNA extraction by FINA, (F) paper-based extraction device coupled with PMMA and PDMS, and (G) an extraction model consisting of a chromatography paper and a pipette tip. Reproduced from (Choi et al., 2015b)

With advances in fabrication technologies for paper, such as printing (Rosenfeld & Bercovici, 2014; Yang et al., 2012), stacking (Liu & Crooks, 2011), and folding (Luo et al., 2014; Martinez et al., 2008), several studies have demonstrated the fabrication of simpler and lower-cost paper-based microfluidic devices for the storage and extraction of nucleic acid (McFall et al., 2015; Shu et al., 2003). For instance, paper-based microfluidic origami consisting of a stack of polymer sheets and papers has been fabricated by a simple paper-folding technique in fewer than 30 mins (Shu et al., 2003) **(Fig. 2.7C)**. In addition, an easy-to-use paper microfluidic chip has been developed to extract the DNA via cellulose from a real sample in conjunction with direct detection of nucleic acid by a smartphone (Fronczek et al., 2014) **(Fig. 2.7D)**.

Further, fusion 5, a single layer matrix membrane, has been used in a DNA extraction technique, termed filtration isolation of nucleic acid (FINA) (McFall et al., 2015) **(Fig. 2.7E)**. This technique has been introduced for DNA extraction at the POC, and takes fewer than 2 mins. Additionally, another study has also demonstrated the use of fusion 5 membrane for DNA extraction in a microfluidic device that consists of PMMA and PDMS (Gan et al., 2014) **(Fig. 2.7F)**. As compared to the commercial QIAamp® DNA Micro kits, this device has been proven to yield a high volume of DNA from a variety of raw samples in 8 mins, including whole blood, dried blood stains from both FTA cards and Whatman 903 filter paper, buccal swabs, cigarette butts and saliva (Gan et al., 2014). In another study, a model consisting of a piece of 3MM filter paper and a pipette tip has been used for DNA extraction (Linnes et al., 2014). This model was fabricated by cutting and folding the paper, followed by the insertion of the paper into the pipette tip **(Fig. 2.7G)**. In short, the use of paper as a platform for nucleic acid extraction can fulfill the criteria of being low-cost, automated, rapid, portable, user-

friendly, having the capability to process a broad range of raw samples, and being flexible enough to be integrated into a sample-to-answer analytical system.

2.5.2.2 Paper as a platform for nucleic acid amplification

In the absence of an amplification step, the extracted nucleic acid is usually undetectable by existing technologies due to the low concentration of target nucleic acid in the body (Wang et al., 2014). Therefore, nucleic acid amplification is mandatory in NAT (Niemz et al., 2011). Apart from the various cost-effective paper-based sample preparation techniques, a low-cost nucleic acid amplification technique is also required for downstream nucleic acid detection at POC.

Various isothermal nucleic acid amplification techniques have been developed, such as loop-mediated isothermal amplification (LAMP), nucleic acid sequence-based amplification (NASBA), strand displacement amplification (SDA), helicase-dependent amplification (HDA), recombinase polymerase amplification (RPA) and simple amplification based assay (SAMBA) (de Paz et al., 2014). Since only a fixed temperature is required in an isothermal amplification process, the assay cost can be significantly reduced.

A study has reported the use of glass fiber as a platform for nucleic acid amplification (De Paula & Fonseca, 2004) **(Fig. 2.8A)**. This study integrates the RPA technique with a paper-based device, coupled with reagent storage and mixing both in the device. Another study has demonstrated a paper-based amplification technique by HDA (Linnes et al., 2014) **(Fig. 2.8B)**. Isothermal amplification was performed in the cellulose chromatography paper supported by a pipette tip, which was sealed with waterproof adhesive tape. Taken together, the introduction of a paper-based

amplification device would accelerate progress towards an ideal molecular diagnostic device for low-resource settings (Pai et al., 2012).

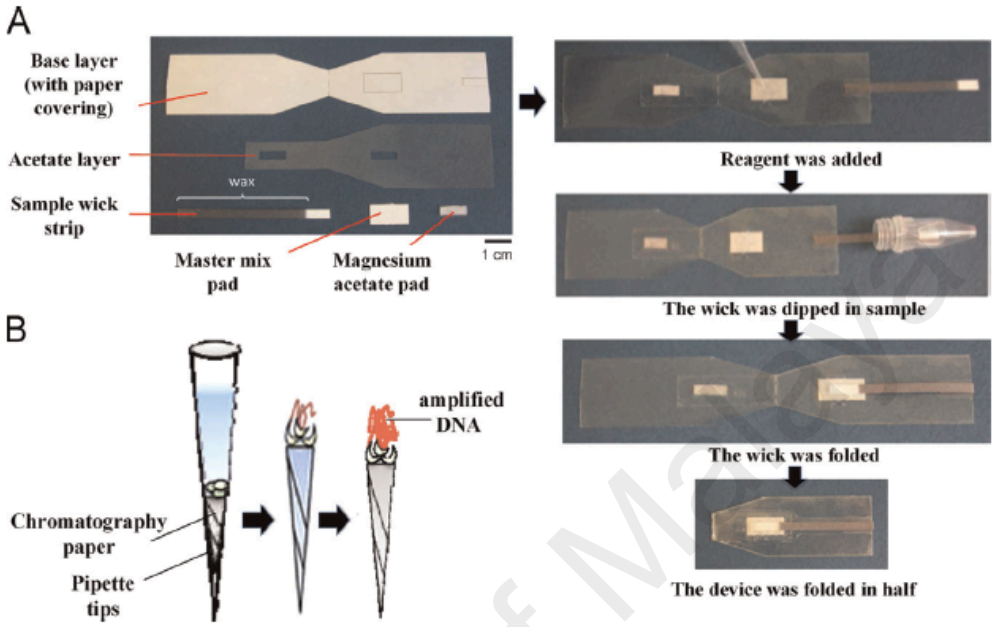

Figure 2.8: Paper-based as a platform for nucleic acid amplification. Paper as a platform for (A) RPA and (B) HDA. Adapted from (Webster et al., 2009).

2.6 A fully integrated sample-to-answer LFA

Although each step of paper-based NAT has been briefly discussed earlier, a key challenge for the development of an ideal POC nucleic acid detection technique is integrating all these steps into a single diagnostic biosensor. The advantages of developing a fully integrated paper-based system for NAT include cost reduction (Carrilho et al., 2009), simplification of device fabrication and operation process, increased portability of the device, simplicity of data read out, and suitability for POC applications. In fact, even though the integration of DNA extraction and amplification into a paper-based biosensor has been reported, a combination of LFA with the aforementioned steps for simple colorimetric readout has not yet been demonstrated.

Without nucleic acid extraction and amplification, a LFA is unable to detect DNA from raw blood samples, making them impractical in resource-limited settings. Therefore, the integration of the three main NAT steps into a single paper-based biosensor is suggested, termed a "sample-to-answer" biosensor for POC settings. The need for no more than a single drop of blood obtained by a finger prick for analysis would bring this simple molecular diagnostic technology to the next level. Owing to the excellent capability of the paper-based platform when used with advanced paper-based fabrication and modification technologies, it is anticipated that in the near future, more paper-based sample-to-answer molecular diagnostic biosensors will be developed to overcome the financial barriers and improve public health in the underdeveloped and developing countries.

CHAPTER 3: OPTIMUM BIOMOLECULE REACTION IN LATERAL FLOW ASSAY UNDER OPTIMUM ENVIRONMENTAL CONDITIONS

3.1 Introduction

NAT has found widespread applications in medical diagnosis, food safety analyses and environmental monitoring. Conventional NAT (e.g., PCR, qPCR or electrophoresis) is normally performed in well-established laboratories with high-end facilities [2]. To eliminate the need for expensive equipment and well-trained personnel, a robust device is required to bring accurate diagnostic assays to the POC. Today, the use of a paper-based platform represents a promise of a simple, portable, cost-effective, and user-friendly POC diagnostic tool, which holds a great potential as an alternative to the conventional laboratory techniques (Choi et al., 2015b; Chun, 2014; Dungchai et al., 2010). Nucleic acid-based assays, in particular, have been studied extensively in paper-based diagnostics (Liu et al., 2014; Toumazou et al., 2013; Venkatesan & Bashir, 2011; Wanunu et al., 2010), presenting a substantially higher specificity and sensitivity than Ag-Ab-based assays (Craw & Balachandran, 2012; Peeling & McNerney, 2014; Yu et al., 2012b). Recent studies have focused on the use of nucleic acid-based LFA for accurate POC diagnostics (Blažková et al., 2009; Hu et al., 2013; Wang et al., 2013a). These assays normally involve hybridization of a single stranded-target analyte (RNA or DNA) with a complementary probe to form a double-stranded nucleic acid, or binding between streptavidin and biotinylated target DNA to form streptavidin-biotinylated target DNA complex at the test zone and produce a colorimetric signal.

Accumulating evidence has shown that environmental factors (*e.g.,* temperature and RH) may have a significant influence on biomolecule reactions (Barry & DeMille, 2012; Chun, 2014; De Roy et al., 2013; Wu et al., 2014), which have been overlooked

in most LFA studies. Further, RH may also influence the assay readout by affecting the fluid wicking rate in the paper, which may in turn affect the sensitivity of several paper-based assays (Giokas et al., 2014; Lutz et al., 2013; Renault et al., 2013; Rivas et al., 2014). As LFAs are intended for field application, they may be affected by user's environmental conditions (*e.g.,* extremely hot or cold, and dry or wet environments) more than in a typical controlled laboratory. Therefore, besides optimizing the concentration of reagent required in LFA, investigating the optimum environmental conditions is also important to ensure optimum biomolecule reactions in LFA. Several studies have investigated the stability of LFA in different environmental conditions (Chien et al., 2006; Johnson et al., 2005). However, the optimum environmental requirement in nucleic acid-based LFA has not yet been explored.

The present study reports the use of a portable temperature-humidity control device to provide an optimum environmental requirement for LFAs, followed by target quantification. As most amplicons are double-stranded and are biotinylated, the proof-of-principle investigation of environmental temperature and RH on streptavidin and biotinylated target interaction on the test strip was conducted, using dengue viral DNA and HBV DNA as model analytes. Given that precise temperature and humidity control is technically challenging outside the laboratory, a portable temperature-humidity control device was developed to maintain both environmental factors to achieve optimum streptavidin-biotin interactions and optimum LFA performance in the POC setting. In the future the device could be upgraded to facilitate rapid onsite NAT, from sample pretreatment to detection, especially in resource-poor settings.

3.2 Materials and methods

3.2.1 Preparation and characterization of gold nanoparticles (AuNP) and AuNP-DP (detector probes) conjugates

AuNP with diameter of 13 ± 3 nm were prepared according to the previously published protocol (Hu et al., 2013). Briefly, in a 250 mL round-bottom flask, 4.5 mL of 1% tri-sodium citrate and 1.2 mL of 0.825% chloroauric acid was added to 100 mL-boiled ultrapure water. The solution turned from yellow to purple and finally turned wine-red in 2 min. The solution was used to prepare AuNP-DP conjugates. Both AuNP and AuNP-DP conjugates were characterized by UV/Vis spectrophotometry and transmission electron microscopy (TEM) (TEM, JEM-2100F).

About 100 μM of thiolated oligonucleotide (DP) was used to conjugate with AuNPs, with the ratio of the volume of gold nanoparticle to oligonucleotide 160:1. The 24.1 nmol oligonucleotide was activated before the conjugation, by mixing with 39 μL of 500 mM acetate buffer (pH 4.76), 8 μL of 10 nM tris(2-carboxyethyl)phosphine (TCEP) and 194 μL of distilled water to achieve a final concentration of 100 μM. After 24 hr, 1% sodium dodecyl sulfate (SDS) and 2M NaCl were added to the solution to reach a final concentration of 0.01% SDS and 0.16M NaCl, respectively. Following the centrifugation at 10000 rpm, the pellet was suspended in 1 mL eluent buffer, consisting of 5% BSA, 0.25% Tween 20, 10% sucrose and 20 nM Na_3PO_4. The AuNP-DP with the concentration of 3 nM were characterized by observation of colour changes, determination of the absorbance value in ultraviolet-visible (UV/Vis) spectrophotometry and aggregates formation in TEM.

3.2.2 Fabrication of lateral flow test strips

The process of lateral flow test strip fabrication is depicted in **Fig 3.1**. Briefly, a lateral flow test strip is made up of a nitrocellulose membrane (30 cm × 2.0 cm × 0.01 cm) (HFB 18002, Millipore, USA), a sample pad (30 cm × 1.2 cm × 0.05 cm) (H-8, Jiening, China), a conjugate pad (30 cm × 1.0 cm × 0.05 cm) (Pall 8964, Saint Germain-en-Laye, France) and an absorbent pad (30 cm × 2.5 cm × 0.1 cm) (H-1, Jiening, China), mounted on a PVC backing pad (30 cm × 6.0 cm × 0.02 cm) (J-B6, Jiening, China). All the components were first assembled to produce a large piece of test strip. By using Matrix^{TM} 2360 Programmable Shear, the assembled pads were then cut into a large number of strips with 6 cm length and 0.25 cm width. About 0.5 µL of 100 µM control probe was then dispensed onto the control zone. As for the test zone, about 0.5 µL of 2 mg/ml streptavidin was dispensed onto it. After adding 10 µL of AuNP-DNA conjugates to each test strip, they were dried at 37 °C for 2 hr prior to the assay.

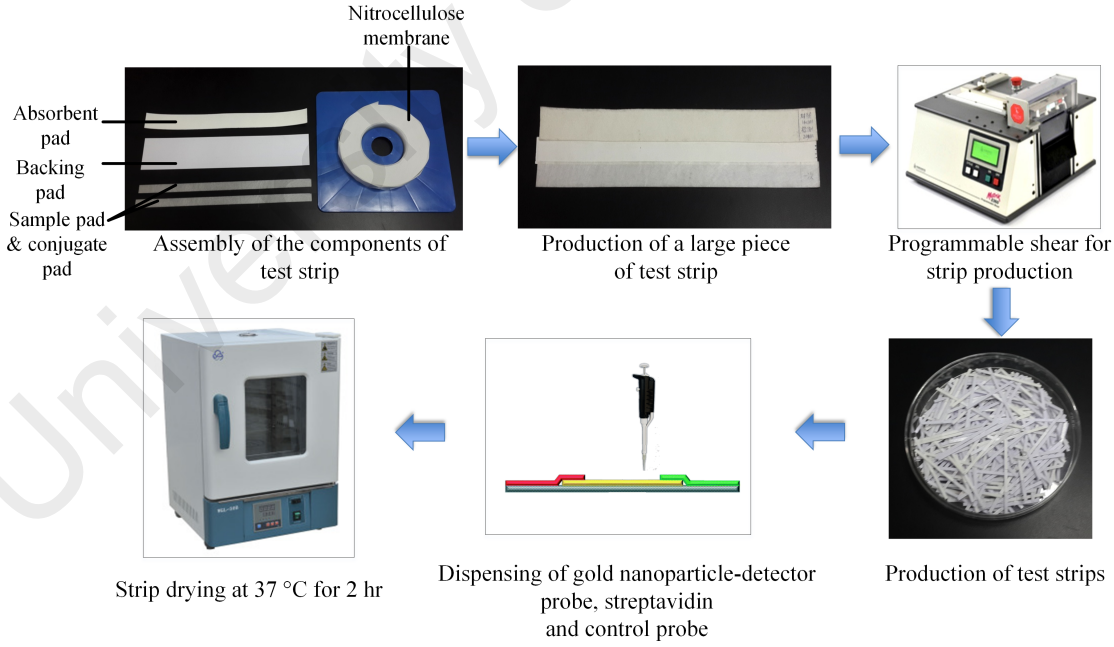

Figure 3.1: Fabrication of lateral flow strip. All the components of test strip were assembled, including the absorbent pad, sample pad, conjugate pad, backing pad and nitrocellulose membrane. A large piece of test strip was then produced, and was cut into smaller pieces using a programmable shear. The reagents, including gold nanoparticle-detector probe, streptavidin and control probe were dispensed onto the strip. The strips were then dried at 37 °C for 2 hr prior to the assay.

3.2.3 Assay optimization

As DNA is normally the final analyte in NAT, synthetic Dengue viral DNAs were used as model analytes for proof-of-principle investigation of the effects of environmental condition on LFA. All sequences used in the study were obtained from Sangon Biotechnology Co., Ltd. (Shanghai, China) (**Table 3.1**). The highly conserved regions of the dengue virus genome were selected as detector probe (Stubbs et al., 2011). Various concentration of streptavidin (0.5, 1, 2, 4, 6 and 8 mg/mL), AuNP-DP (3 nM , 6 nM and 9 nM) and SSC buffer (2×, 4×, 6× and 8×) were prepared to study their effects on the test strip at ambient condition (25°C, 60 % RH). At the end of each assay, images of all the test zones were captured with a smartphone, and the colour intensities were converted to optical density (OD) using the software of *Image Pro Plus* (IPP). The OD presented in the graph represents the difference between the OD of a certain target concentration and OD of negative control (without target).

Table 3.1: DNA sequences used in the study

Name	**Sequence (5'-3')**
DENV detector probe	5'-tagaggttagaggaga-$(CH_2)_6$-SH-3'
DENV control probe	5'-tctcctctaacctcta/Biotin-3'
DENV target DNA	5'-tctcctctaacctcta-3'
HBV detector probe	5'-atgaatctggccacctgggt -$(CH_2)_6$-SH-3'
HBV control probe	5'-acccaggtggccagattcat/Biotin-3'
HBV target DNA	5'-acccaggtggccagattcat -3'

3.2.4 LFA at various temperature and relative humidity

To study the effect of RH on the LFA, the assay was performed at 30, 40, 50, 60, 70, 80 and 90% RH at 25 °C. With the optimum RH, the assay was performed at different temperatures, 10, 20, 25, 30, 40, 50, 55, 60, 65 and 70 °C. All data was collected in 10 min per condition. The SSC buffer used in this study was diluted from the commercial SSC buffer 20× (Sigma-Aldrich). The desired concentration of target DNA was prepared by dilution with SSC buffer. Subsequently, 50 µL of target DNA solution was added onto the sample pad. The test strip was then tested and the colour formation in the test zone was observed.

3.2.5 Statistical analysis

Statistical analysis was performed using One-Way ANOVA with Tukey post-hoc test to compare the data among different groups in optimization assays and temperature and humidity assays. Data were expressed as mean ± standard error of the mean of three independent experiments (n=3). $p<0.05$ was reported as statistically significant.

3.3 Results

3.3.1 Characterization of AuNP and AuNP-DP

The AuNP-DP with the concentration of 3 nM were characterized by visible colour changes from wine red to dark red, a slight shift of the absorbance values (6 nm) in UV/Vis spectrophotometry and AuNP-DP aggregates formation in TEM as compared to AuNP, with the particle size of 13 nm **(Fig. 3.2).**

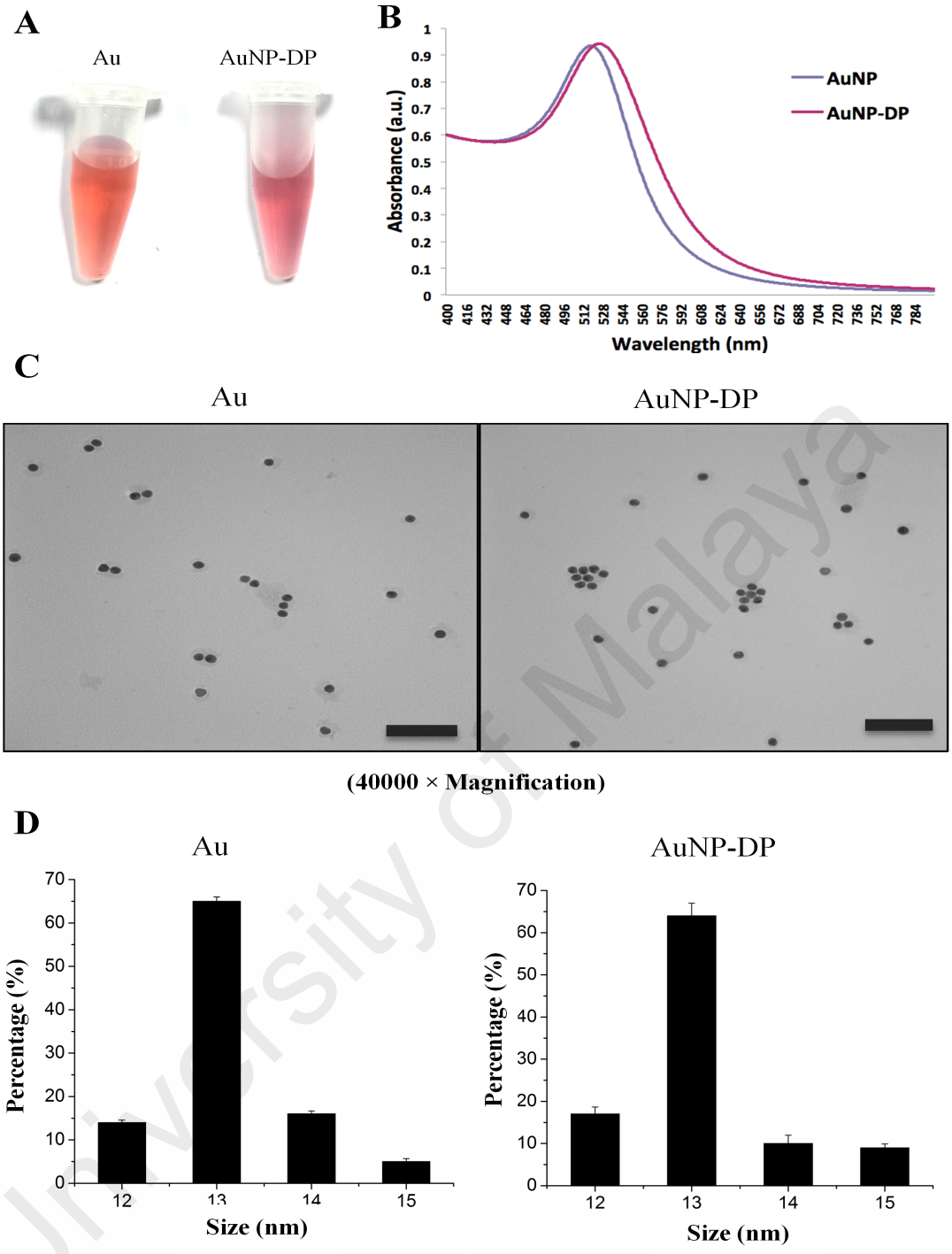

Figure 3.2: Characterization of AuNP and AuNP-DP. AuNP-DP was characterized by (A) the change of colour from wine red to dark red, (B) a slight shift of the absorbance values (6 nm) in ultraviolet-visible spectrophotometry, and (C) AuNP-DP aggregates formation in transmission electron microscopy, as compared to AuNP. (D) The size of most AuNP was shown to be 13 nm.

3.3.2 Assay optimization

Dengue DNA was used as a target analyte in optimization assay. To determine the optimum concentration of the streptavidin at the test zone for optimum amplicon detection, the assay was performed using different concentration of streptavidin (0.5, 1, 2, 4, 6 and 8 mg/mL). It was found that the concentration of 2 mg/mL produced a significantly higher optical density of the test zone over the concentration of 0.5 and 1 mg/mL of streptavidin (p<0.05) and showed no significant difference from 4, 6 and 8 mg/mL. Therefore, the concentration of 2 mg/mL was selected for the subsequent assay **(Fig. 3.3)**.

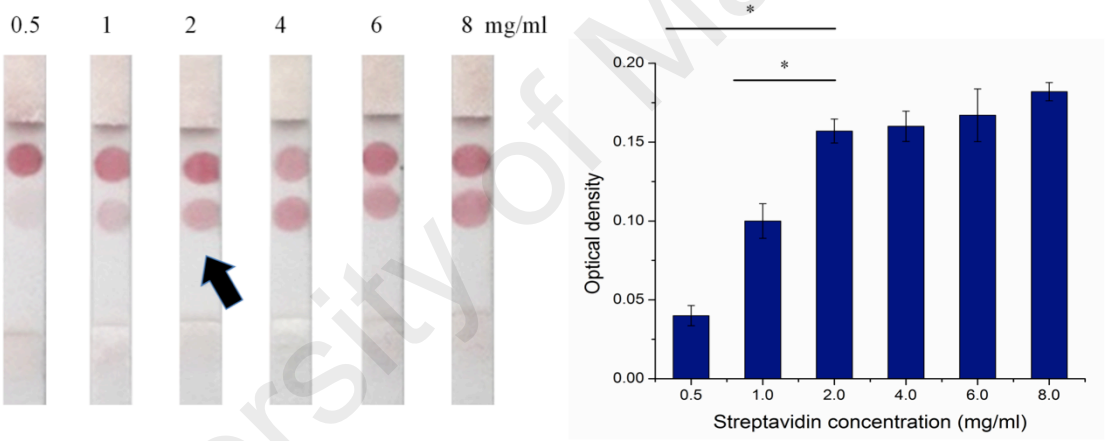

Figure 3.3: Optimization of streptavidin concentration at the test zone. 2 mg/mL was the optimum concentration based on the higher optical densities of test zone (* p<0.05 relative to 2 mg/ml).

To determine the optimum concentration of AuNP-DP in amplicon detection, the assay was performed using 1 nM, 3 nM, 6 nM and 9 nM of AuNP-DP. It was found that the optical density of the test zone in LFA was significantly increased with increase in the concentration of AuNP-DP (p<0.05). 3 nM of AuNP-DP produced less background signal than 6 nM and 9 nM, as indicated by the significant lower optical density of background as compared to that of 6 nM and 9 nM of AuNP-DP (**Fig. 3.4**). The 3 nM concentration also showed a significantly higher optical density of test zone

as compared to 1 nM and showed no significant difference with 1 nM in terms of background signal. Therefore, 3 nM was selected as the optimum concentration of AuNP-DP for the subsequent assays.

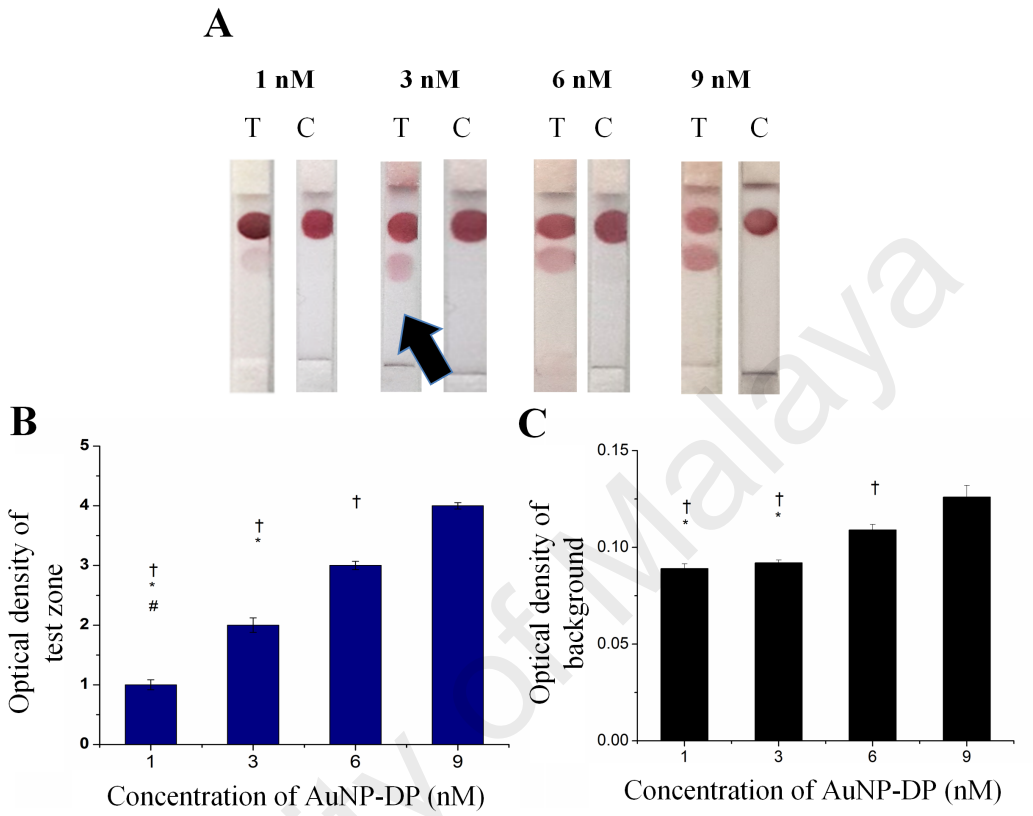

Figure 3.4: Optimization of AuNP-DP concentration. 3 nM of AuNP-DP was chosen due to the clearly visible test zone (A), high optical density of test zone (B) and less background signal produced (C) (# p<0.05 relative to 3 nM, * p<0.05 relative to 6 nM, † p<0.05 relative to 9 nM).

To determine the optimum concentration of SSC buffer, which promotes biomolecule reaction, the assay was performed using 2×, 4×, 6× and 8× SSC buffer. It was found that higher concentrations of SSC buffer significantly increased the optical density of the test zone in LFA (p<0.05). However, 2× and 4× of SSC buffer showed a significantly lower background signal compared to that of 6× and 8×. Therefore, 4× of SSC buffer was selected for subsequent assays, which produced a clearly visible test zone and a low background signal, compared to the other concentrations tested (**Fig. 3.5**).

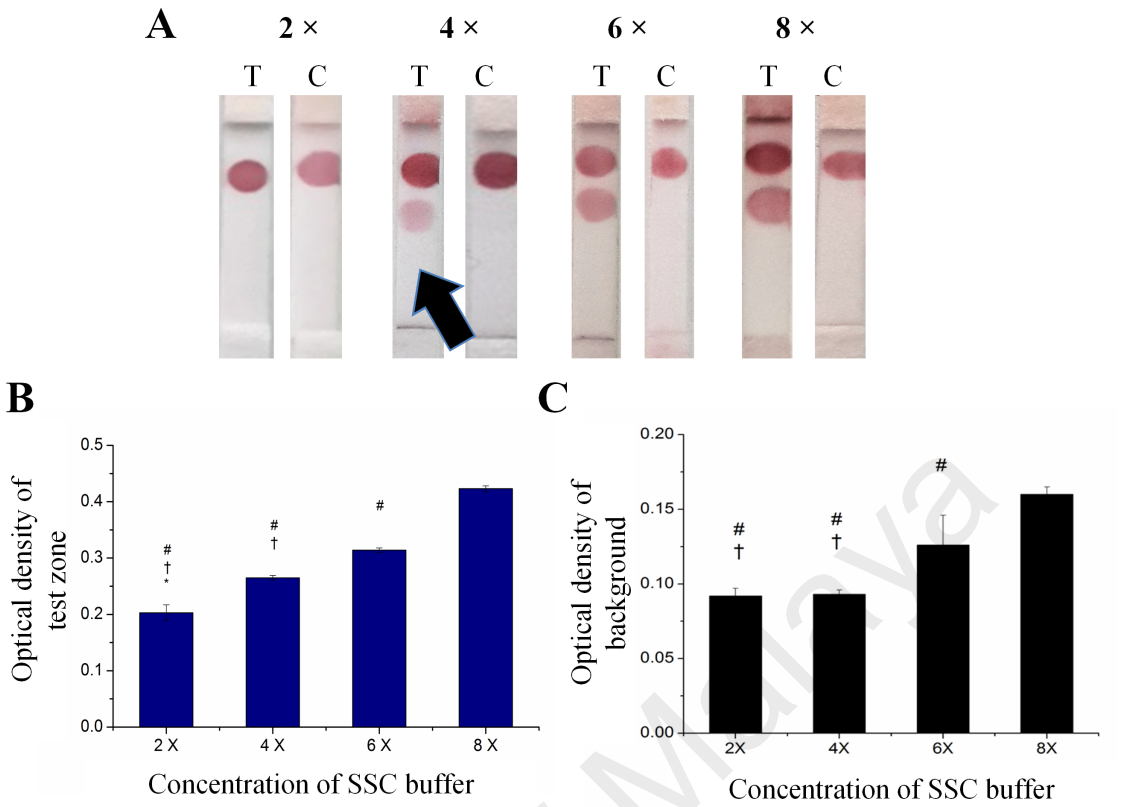

Figure 3.5: Optimization of SSC buffer concentration. 4× SSC buffer was selected based on the more clearly visible test zone (A), high optical density of test zone (B) and lower background signal (C) as compared to other concentrations tested (* p<0.05 relative to 4×, † p<0.05 relative to 6×, # p<0.05 relative to 8×).

3.3.3 Effect of environmental temperature and relative humidity on LFA

To achieve an optimum streptavidin-biotin interaction on the test strip, two main environmental factors (*i.e.,* temperature and RH) in the assay were manipulated with the optimum concentration of streptavidin (2 mg/ml), AuNP-DP (3 nM) and SSC buffer (4×). The test strip was initially tested over a range of 30%-90% RH. RH represents the ratio of the partial pressure of water vapor to its saturation vapor pressure at particular temperature. It was found that at low humidity, particularly at 30% RH, the fluid was unable to completely diffuse across the nitrocellulose membrane, whereas RH >50% enables the fluid to completely diffuse across the nitrocellulose membrane (**Fig. 3.6**). To prove the ability of paper-based assays to support the theory of streptavidin-biotin interaction, with the average optimum RH (80%), using dengue DNA as a target analyte,

the test strip was tested over a range of environmental temperatures (10, 20, 25, 30, 40, 50, 55, 60, 65, 70, 80 and 90 °C). It was observed that among all temperatures, 25-30 °C produced the optimum signal (p<0.05).

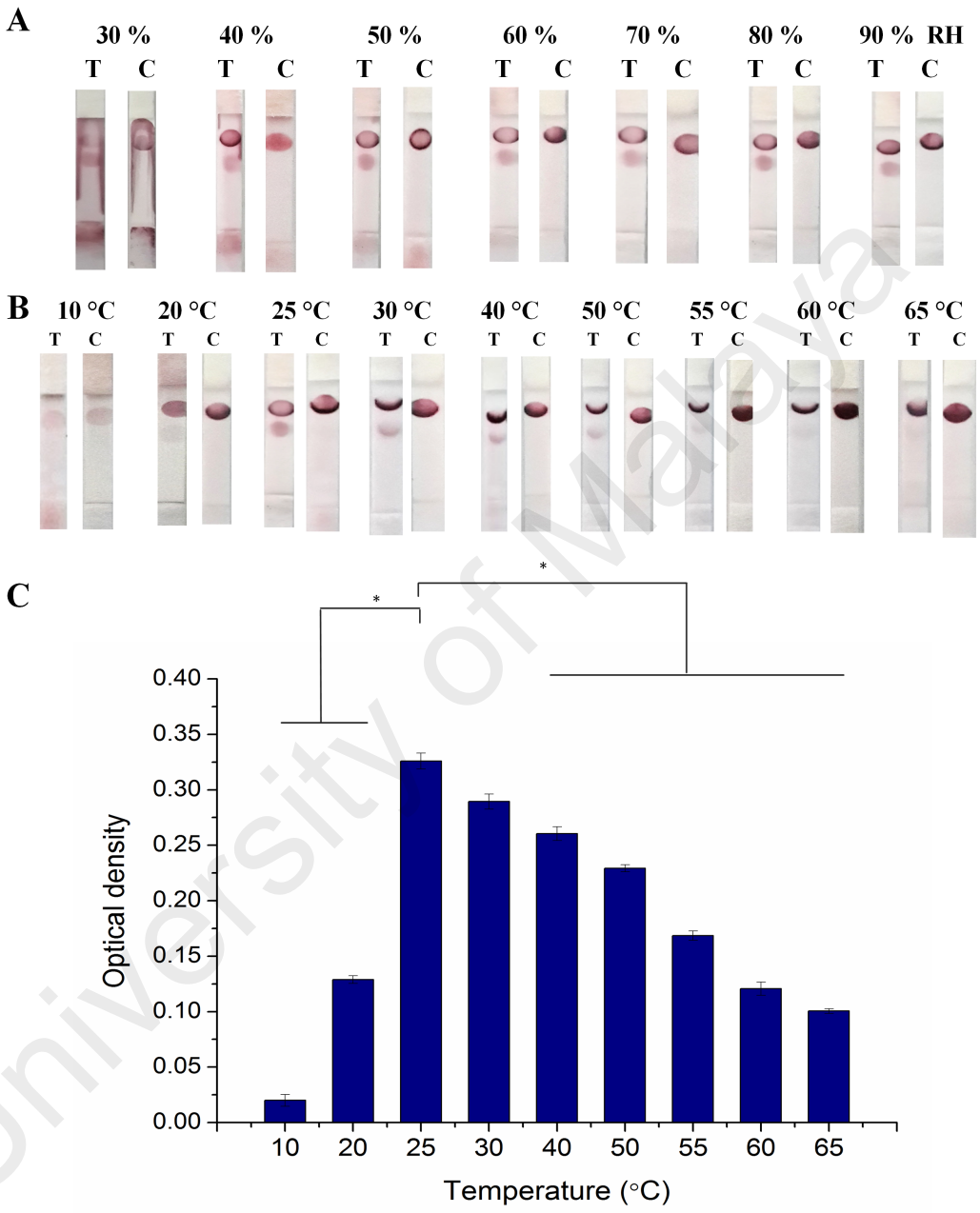

Figure 3.6: Temperature and humidity effects on nucleic acid-based LFA. (A) Humidity affects the fluid flow in LFA. It was found that at low humidity (30% RH), the fluid was unable to completely diffuse across the nitrocellulose membrane, whereas the RH > 50% enabled the complete fluid diffusion across the nitrocellulose membrane. (B & C) 25-30 °C produced the optimum signal of nucleic acid-based LFA (* p<0.05 relative to 25 °C).

To rapidly and accurately detect the target analytes by LFA at optimum conditions (25 °C, >50% RH) in the remote settings, a small and portable temperature-humidity control device was developed, coupled with a smartphone signal detection, to substitute the large and complex commercial temperature-humidity control device **(Fig. 3.7)**. To verify the effect of temperature and humidity on nucleic acid hybridization in LFA, the test strip was further tested with another model analyte, HBV DNA using the portable device. Similar to dengue DNA detection, a temperature of 25-30 °C showed the greatest streptavidin-biotin interaction, as indicated by the highest colour intensity of test zone and the highest optical density value (p<0.05) among all the temperatures tested (**Fig. 3.7**).

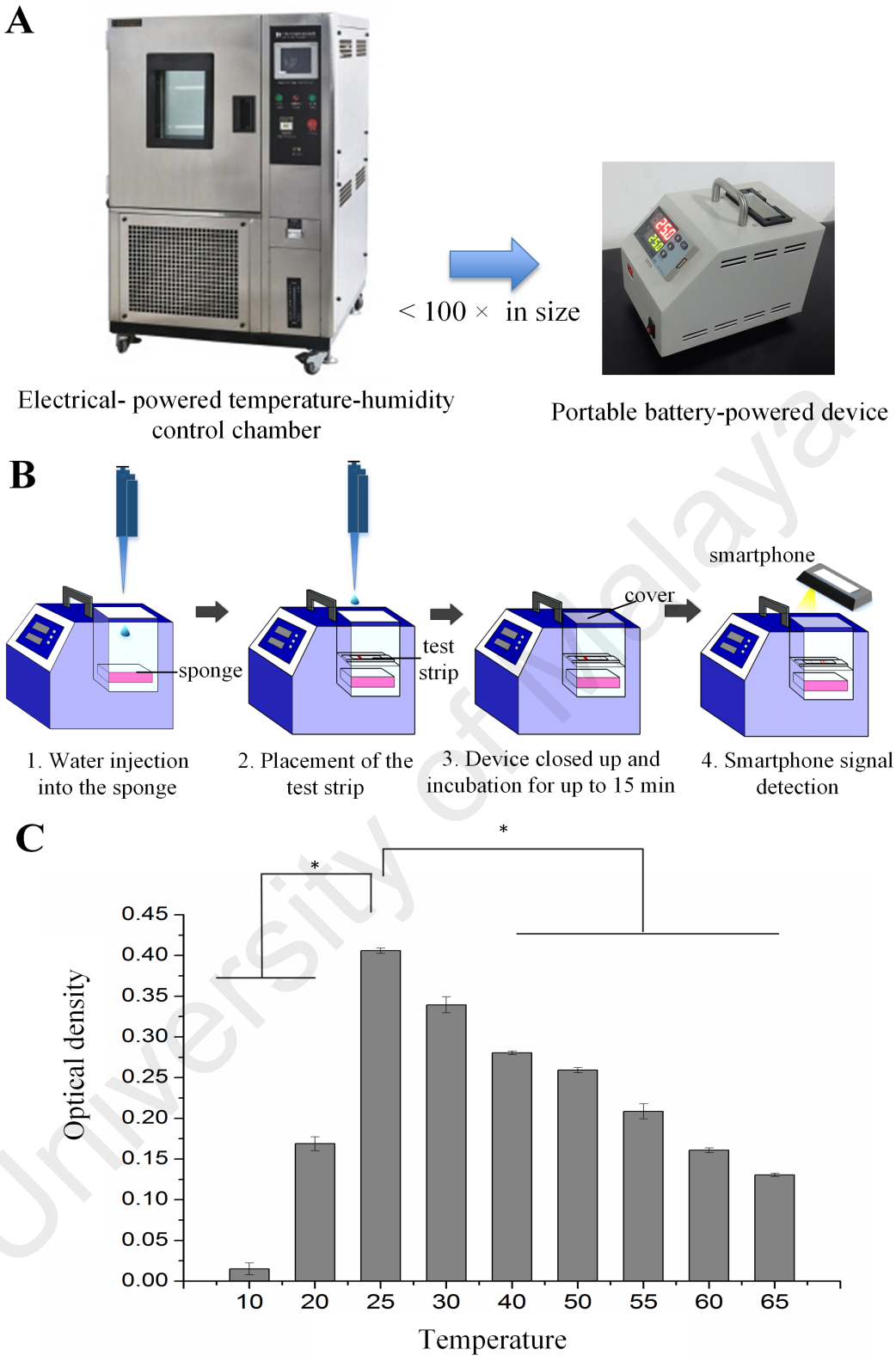

Figure 3.7: Portable temperature-humidity control device for DNA detection. (A) A portable battery-powered device, which could substitute the large and complex electrical-powered temperature-humidity control device. (B) The schematic diagram of experimental procedure. (C) Temperature of 25-30 °C showed the greatest signal of nucleic acid-based LFA in HBV DNA detection (* p<0.05 relative to 25 °C).

3.4 Discussion

In optimization of reagent concentration, the data suggests that 2 mg/ml streptavidin at the test zone, 3 nM AuNP-DP and 4× SSC buffer concentration allow optimum biomolecule reaction in LFA. As LFAs are intended for field application, investigating an optimum environmental condition is very important to lead to the development of a closed system in the future to provide the optimum temperature and RH for optimum biomolecule reactions in LFA even under the extreme environmental conditions. The data showed that low environmental RH (30-40%) led to the water loss from the test strip via evaporation, which ultimately reduced the wicking rate of the fluid. The phenomenon can be explained by the equation, (M_{ev} = (1- RH) × P_w × (0.089 + 0.0782 V_a) / γ), where M_{ev}, P_w, V_a and γ are the evaporation rate, the water saturated pressure, the air flow rate and the latent heat of vaporization of water, respectively. Theoretically, in a closed system, with a fixed temperature, the air flow rate is assumed to be zero, whereas the water saturated pressure and the latent heat of vaporization of water remain constant (Tang et al., 2016). In this case, the evaporation rate is directly proportional to the (1-RH). This equation supports the experimental data, indicating that the higher the RH, the lower the evaporation rate. The reduction of fluid wicking rate resulted in the accumulation of free AuNP-DP and AuNP-DP-target DNA along the nitrocellulose membrane. On the contrary, RH beyond 50% reduced the water evaporation. As a result, the fluid was able to completely diffuse across the nitrocellulose membrane and yielded the desired signal.

In evaluating the temperature effect on LFA, with the average optimum RH (70 %), the optimum signal was observed at 25-30 °C, which strongly suggests that the proof-of-principle of the streptavidin-biotin interaction (most stable at 25-30 °C) (Qu et al., 2013) can be successfully achieved by using a test strip, with dependence on

temperature and RH. Given that precise temperature and humidity control is technically challenging outside the laboratory, a portable temperature-humidity control device was developed to achieve optimum LFA performance in a POC setting. Generally, the device consists of a testing compartment, an integrated battery, an integrated temperature controller, a sponge and a charger. This closed device is internally made of a good thermal conductor, aluminium alloy, with external insulation wall, with a glass window on top for visual signal detection or photo capture by a smartphone for analysis. A range of temperatures (25-100 °C) can be achieved with an accuracy of ±0.1 °C by direct current produced by a battery power source integrated into the device, to maintain the optimum performance of this portable device. The test strip is placed right below the glass, supported by an aluminium-supporting frame at the middle layer of the compartment, whereas the bottom layer of the compartment consists of a damp sponge, which sustains the humidity of the compartment. In addition, temperature and humidity sensors are installed in the internal part of the device, with a thermo-hygrometer placed at the exterior part to ensure the maintenance of temperature and RH over 30 min. Briefly, water is injected into the sponge to achieve the desired RH of the compartment at the desired temperature. Following the addition of sample, the testing compartment is closed for LFA. In line with the data produced by the temperature-humidity control chamber, this simple and portable device allows sensitive target detection under optimum environmental conditions.

3.5 Conclusion

In short, with the simple temperature-humidity control device, It was proven that temperatures of 25-30 °C, with a humidity > 40% give an optimum signal for amplicon detection in LFA. This compact, portable and cost-effective temperature-humidity control model, coupled with the test strip, offers rapid, specific and sensitive diagnosis

of infectious diseases in POC settings. It was expected that this study will raise concerns about the significance of the impact of environmental monitoring on biomolecule reactions in LFA, which could maximize the usage of paper-based material in biomedical areas. The outcome of this study could also lead to the development of a closed system, which provides an optimum temperature and RH for optimum LFA, coupled with an integrated paper-based sample-to-answer biosensor for sensitive target detection in the near future.

CHAPTER 4: AN INTEGRATED PAPER-BASED BIOSENSOR FOR EFFECTIVE DNA AMPLIFICATION AND LATERAL FLOW DETECTION AT THE POINT OF CARE

4.1 Introduction

NAT plays an essential role in many applications due to its relatively higher sensitivity and specificity than antigen or antibody detection (Akhtar et al., 2011; Katsanis & Katsanis, 2013; Krebs et al., 2014). However, the amount of target nucleic acid in a raw sample is usually too low to be directly detected, hence requiring an amplification process. Conventionally, nucleic acid amplification and detection (*e.g.,* PCR and electrophoresis) are separately performed, which are costly, labour-intensive, time-consuming and large equipment dependent, reducing their suitability for point-of-care (POC) applications (Martinez et al., 2010; Wang et al., 2012; Wang et al., 2010).

Nowadays, there exist a numbers of nucleic acid-based diagnostic equipment available in the market with the ability of performing isothermal amplification (e.g., LAMP and RPA)(Crannell et al., 2014; Francois et al., 2011) or/and amplicon detection. For instance, isothermal amplification with real time detection has been implemented in several systems such as SAMBA system by Diagnostics for the Real World (UK), Loopamp realtime turbidimeter (LA-200) by Eiken (Japan), Twista portable realtime florometer by TwistDX (UK) and bioluminescent assays in real-time (BART) instrument by Lumora (UK). Even though these instruments are simpler, more portable and enable more rapid detection as compared to that of conventional benchtop NAT equipment, most of them involve fluorescent detection, which requires implementation of UV light source, thus adding the entire cost. To this end, simpler colorimetric detection has been exemplified in the BeSt Cassette by BioHelix (USA) and XCP

nucleic acid detection device by Ustar Biotech (China). However, the amplification process requires an electric-heated thermostatic water bath or block heaters (Kaewphinit et al., 2013; Rigano et al., 2014), and is separately performed from detection, which entails multiple processing steps, hence restricting their use at the POC. Similar drawbacks have also been shown in several studies, which perform tube-based isothermal amplification, followed by colorimetric (Lau et al., 2015; Nie et al., 2014), fluorescent (Kao et al., 2005; Schilling et al., 2004) or chemiluminescent detection (Kumbhat et al., 2010a; Teles, 2011), either in real-time (Kao et al., 2005; Schilling et al., 2004) or endpoint detection (Conceicao et al., 2010; Lau et al., 2015; Nie et al., 2014; Teles, 2011). Therefore, the integration of both nucleic acid amplification and detection into a simpler and more cost-effective platform is in high demand, especially in resource-limited settings.

Paper has gained increasing interest as a promising platform for POCT due to its simplicity, cost-efficiency, biodegradability, and biocompatibility (Choi et al., 2015a; Hu et al., 2014). The porous structure of paper enables fluids to wick through via capillary action (Chen et al., 2015; Choi et al., 2015b), offering advantages such as sequential delivery of reagent (Fridley et al., 2012; Fu et al., 2010), sample mixing, and multiple-step processing (Lutz et al., 2011), which could potentially simplify the existing nucleic acid amplification technique. This emerging technique offers great potential to meet the Affordable, Sensitive, Specific, User-friendly, Rapid and Robust, Equipment-free, and Deliverable to end-users (ASSURED) criteria outlined by the World Health Organization (WHO) (Wu et al., 2005). In recent years, many studies have demonstrated LFA for amplicon detection due to its simple colorimetric readout, but a complex benchtop nucleic acid amplification process is still required prior to the detection, leading to an increased overall assay cost and time (Choi, 2015; Kaewphinit

et al., 2013; Rigano et al., 2014; Rigano et al., 2010). To address these limitations, paper-based isothermal amplification techniques have been introduced. Recent studies have demonstrated the use of paper as a platform for RPA (De Paula & Fonseca, 2004) and HDA (Linnes et al., 2014), followed by LFA for the detection of HIV and Chlamydia trachomatis, respectively. However, the paper-based amplification and LFA were still separately performed, which entails multiple processing steps, hence increasing the risk of reagent loss and even cross-contaminations. To date, a great challenge remains in integrating paper-based amplification platform into simple colorimetric LFA, which could tremendously simplify the operation steps. The challenge would be the requirement for on-chip fluidic control from nucleic acid amplification zone to lateral flow strip, with optimum temperature required for each step in a robust and portable manner. Developing an integrated LFA without relying on a large equipment (*e.g.,* thermal cycler, electric heater, incubator or water bath) for amplification, and an extra UV source for assay readout is of great importance for onsite NAT. However, in fact, no study has attempted to combine paper-based nucleic acid amplification and detection in an integrated lateral flow strip. In addition, a handheld battery-powered heater to be used for nucleic acid amplification is imperative to be coupled with the integrated LFA, which, however, has not yet been introduced for use in resource-poor endemic areas. Therefore, there is a strong demand to develop a new colorimetric integrated LFA that can achieve on-site naked-eye detection.

In this study, considering the simplicity of the biosensor in conjunction with the high efficiency of nucleic acid amplification, an integrated paper-based biosensor incorporating paper-based LAMP and LFA was developed. LAMP, a well-known novel nucleic acid amplification technique with high sensitivity and specificity under isothermal conditions is performed to produce a large number of amplicons, followed

by signal detection by LFA and quantification using a smartphone. The paper-based LAMP and lateral flow strip were initially separated by hydrophobic PVC layers, creating the "valves" to control the fluid flow from amplification zone to the test strip. The integrated paper-based biosensor was coupled with a handheld battery-powered heating device to enable target detection in remote settings without the need for an external electrical power supply. Recently, as dengue infections have become a serious healthcare concern worldwide, including underdeveloped and developing countries, there is an urgent need to develop simple, rapid and robust diagnostic tools for dengue detection in resource-poor settings. Therefore, dengue viral DNA was used as a model analyte in this study. The sensitivity of integrated paper-based amplification-to-detection biosensor was compared with the unintegrated platform (paper-based LAMP, followed by LFA). The performance of the integrated paper-based platform was evaluated by comparing it with the conventional tube-based platform. The biosensor permits the potential use of other isothermal amplification techniques, through adjusting the temperature. A simple paper-based sample preparation technique could be integrated into this integrated paper-based LAMP-LFA platform to create a fully integrated paper-based sample-to-answer biosensor, which is feasible for detection of a variety of target analytes in POC settings in the near future.

4.2 Materials and methods

4.2.1 Fabrication of an integrated paper-based LAMP-LFA biosensor

An integrated paper-based LAMP-LFA biosensor was specially developed for cost-effective nucleic acid amplification and lateral flow detection at the POC **(Fig. 4.1)**. The two-layer integrated biosensor was fabricated through the combination of the lateral flow strip (first layer) and the LAMP strip (second layer) with the fabrication process depicted in **Fig. 4.2**. The lateral flow strip was fabricated using the methods as

described in section 3.2.2. Briefly, the LAMP strip is composed of a piece of glass fiber pad (1 cm × 0.25 cm) protected by an adhesive tape and an adhesive PVC backing pad. The protective films at two ends of the backing pad were first removed to expose the adhesive surface. The glass fiber pad was then mounted onto one end of the backing pad, to create a glass fiber pad-backing pad LAMP strip, while another end of the backing pad was attached to the lateral flow layer. A piece of 3.5 cm × 2 cm disposable adhesive tape was folded in half, creating a small pocket that acts as a reaction chamber, into which the glass fiber pad of the LAMP strip is inserted. Both LAMP strip and lateral flow strip were combined together to create an integrated LAMP-LFA biosensor. The entire fabrication process required less than 1 min.

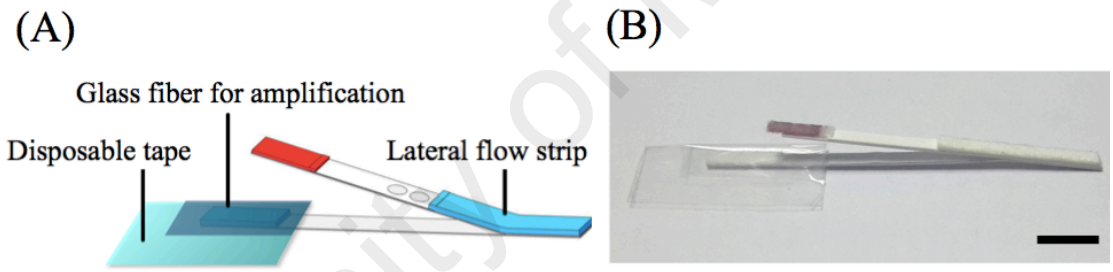

Figure 4.1: An integrated paper-based LAMP-LFA biosensor. (A) The schematic of integrated biosensor and (B) its image (Scale bar, 1 cm).

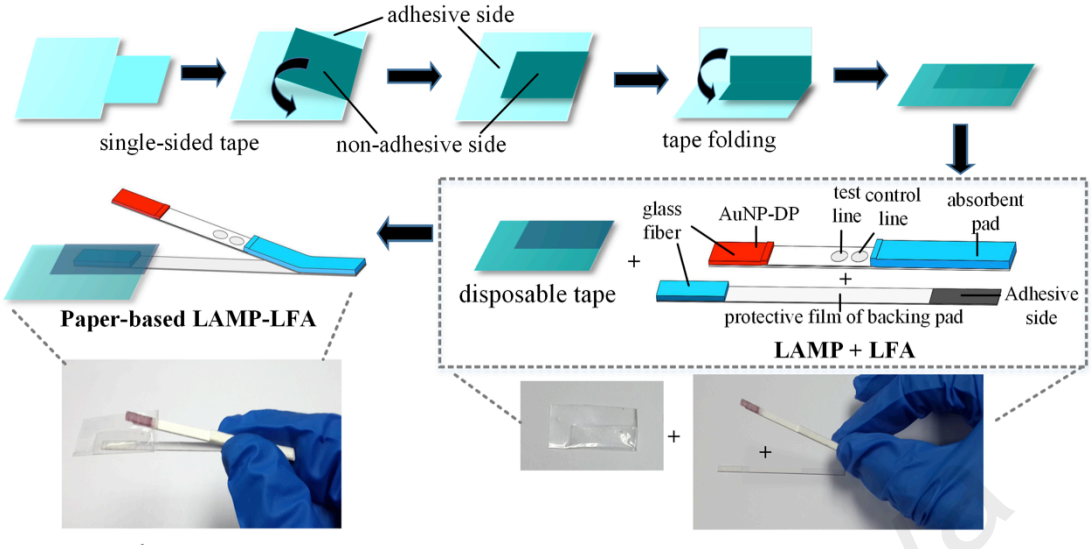

Figure 4.2: Fabrication of paper-based LAMP-LFA biosensor. The paper-based LAMP-LFA biosensor was fabricated by combining both lateral flow layer and LAMP layer. An adhesive tape was used to create a small pocket that acts as a LAMP reaction chamber.

4.2.2 LAMP optimization for the integrated paper-based LAMP-LFA biosensor

In NAT, detection of RNA viruses (*e.g.,* Dengue viruses) normally involves the process of RNA extraction, reverse-transcription and amplification and finally target DNA detection (Dauner et al., 2015; Teoh et al., 2015). In this study, synthetic Dengue viral DNAs were used as model analytes for proof-of-principle investigation of the potential of the prototype integrated LFA to perform both isothermal amplification and detection using the handheld battery-powered heating device. The oligonucleotide primers used in this study was DEN-1 Western Pacific (U88535) serotype specific primers which was synthesized based on the sequences reported in the literature (Umut, 2013) with specially designed control and detector probes (**Table 4.1**). Briefly, the conserved regions were identified using DNASIS software (Hitachi, Japan) and all the primers were designed using primer design software (Net Laboratory, Japan).

Table 4.1: DNA sequences used in this study

Name	Sequence (5'-3')
DENV detector probe	5'-tagaggttagaggaga-$(CH_2)_6$-SH-3'
DENV control probe	5'-tctcctctaacctcta/Biotin-3'
DENV F3	5'-gaggctgcaaaccatggaa-3'
DENV B3	5'-cagcaggatctctggtctct-3'
DENV FIP	5'-Biotin/gctgcgttgtgtcttgggaggttttctgtacgcatggggtagc-3'
DENV BIP	5'-cccaacaccaggggaagctgtttttttgttgttgtgcggggg-3'
DENV FLP	5'-ctcctctaaccactagtc-3'
DENV BLP	5'-accctggtggtaagga-3'
DENV target DNA for LAMP	5'-gaggctgcaaaccatggaagctgtacgcatggggtagcagactagtggttaga ggagacccctcccaagacacaacgcagcagcggggcccaacaccaggggaag ctgtaccctggtggtaaggactagaggttagaggagacccccccgcacaacaacaa acagcatattgacgctgggagagaccagagatcctgctg-3'

LAMP was performed in a total of 25 µL reaction mixture using a Loopamp DNA amplification kit (Eiken Chemical Co., Ltd., Japan) containing reaction mix (consisting of 40 mM Tris-HCl, 20 mM KCl, 16 mM MgSO4, 20 mM (NH4)2SO4, 0.2 % Tween 20, 1.6 M Betaine, 2.8 mM each of dNTPs), Bst DNA, 40 pmol each of primers FIP and BIP, 5 pmol each of outer primers F3 and B3, 20 pmol each of loop primers F (FLP) and B (FBP) and the specific amounts of target DNA (**Table 4.2**). In order to investigate the effectiveness of paper-based LAMP over a range of temperature, LAMP was performed in an unintegrated paper (glass fiber pad) being placed in the tube at a range of temperature (58, 60, 63, 65, and 68 °C) for 1 hr using a thermal cycler (Veriti, Applied Biosystem, Foster City, USA) and the data were compared with the control group (tube-based LAMP). With the optimum 63 °C, a serial concentration of DNA template (3×10^{10}, 3×10^{8}, 3×10^{6}, 3×10^{4} and 3×10^{2} copies) were tested at a range of incubation times (15, 30, 45, 60 and 90 min).

Table 4.2: Components of LAMP used per reaction

Component	Volume (µL)
Target DNA	Up to 10.2
2 × Reaction Mix	12.5
Primer: FIP	0.4 (40 pmol)
BIP	0.4 (40 pmol)
FLP	0.2 (20 pmol)
BLP	0.2 (20 pmol)
F3	0.05 (5 pmol)
B3	0.05 (5 pmol)
Bst DNA Polymerase	1
Distilled water (DW)	Top up to a final reaction volume of 25
Total	**25**

4.2.3 Endpoint target detection

Following the LAMP, the amplicon was collected through the centrifugation of the tube containing the glass fiber pad. The amplicon was then detected by gel electophoresis with 3 µL of the LAMP products being subjected to 1.5% agarose gel electrophoresis. Fluorescent staining was also performed with SYBR green I stain (Invitrogen, USA). The products were detected visually by a colour change from original orange to yellowish-green following the addition of 2 µL 1000-fold diluted SYBR Green I dye to the tube to obtain the final concentration of about 1×. The concentration of amplicon was further confirmed by measuring the absorbance value at 260 nm (OD 260) with the nanodrop ND-2000 (Thermo Scientific). As for the LFA, a denaturation step was required prior to the LFA by heating the amplicon in the tube at 95 °C with the optimum denaturation period of 0.5 min using a water bath. LFA was then performed using the 96 well plate with the addition of 50 µL SSC buffer. The images of all test strips were then captured and analyzed using a smartphone.

4.2.4 Nucleic acid amplification and detection using the integrated biosensor with the aid of a handheld battery-powered heating device

The integrated paper-based LAMP-LFA biosensor consists of a glass fiber pad for LAMP, a glass fiber pad for LFA, a nitrocellulose membrane, an absorbent pad and two PVC backing pads. A handheld battery-powered device was specially designed (Jingie, China) for performing nucleic acid amplification and detection in an integrated paper-based LAMP-LFA biosensor (**Fig. 4.3**). The entire process is briefly discussed in the discussion section. The battery-powered heating device is summarized in **Table 4.3**. Briefly, the glass fiber pads for LAMP and LFA were initially disconnected. The handheld device was pre-setted with the temperature of 63 °C for amplification and 95 °C for amplicon denaturation. The mixture of sample and LAMP reagents was first pipetted onto the glass fiber pad for LAMP protected by a disposable tape, followed by the amplification process at 63 °C at a range of incubation time (15, 30, 45, 60 and 90 min) in the closed heating compartment of the device. The entire process is briefly discussed in the discussion section.

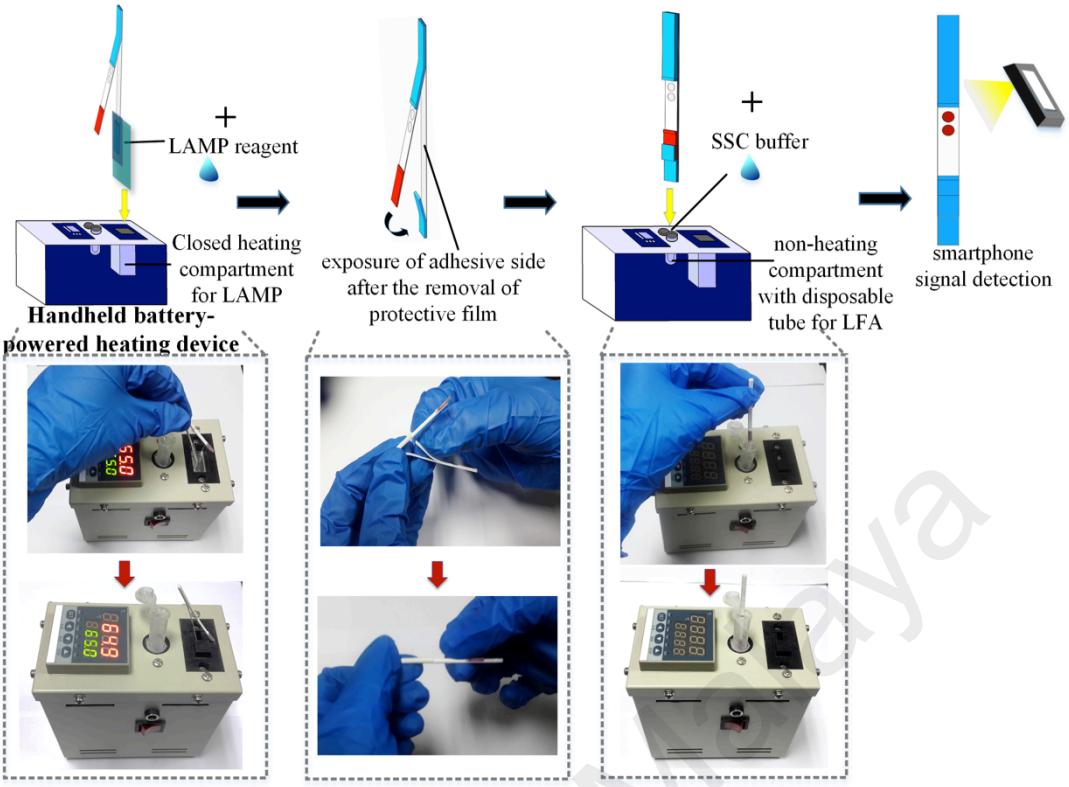

Figure 4.3: Paper-based amplification and detection using the integrated biosensor. A handheld battery-powered heating device was used for paper-based amplification and detection of nucleic acid, coupled with smartphone signal detection in resource-poor POC settings.

Table 4.3: Specifications of the handheld battery-powered heating device

Specifications	
Size of the device (L ×W ×H)	7 cm ×12 cm ×11 cm
Weight of the device	500 g
Temperature range	RT +5 - 100 °C
Temperature accuracy	±0.1 °C
Power supply	220V ± 10% 50 Hz
Maximum voltage	50 W
Material of heating compartment	aluminum alloy
Material of non-heating compartment	polyformaldehyde
Battery life-span	10 hr

Following the 95 °C denaturation step for an optimum 0.5 min (30 sec), both glass fiber pads were then connected through the removal of the protective film of the PVC backing pad. The integrated biosensor was moved into the non-heating compartment comprised of a disposable microcentrifuge tube to perform LFA following the addition of 50 μL SSC buffer into the tube. To determine the detection limit of the assay, a sensitivity assay was performed with a serial dilution of amplicon (3×10^{10}, 3×10^{8}, 3×10^{6}, 3×10^{4}, 3×10^{3} and 3×10^{2} copies) using the integrated paper-based biosensor. The data was compared with that using the tube-based LAMP, followed by LFA. The colour intensities of test zones were observed and their optical densities were determined.

4.2.5 Statistical analysis

Statistical analysis was performed using One-Way ANOVA with Tukey post-hoc test to compare the data among different groups. Data were expressed as mean ± standard error of the mean of three independent experiments (n=3). $p<0.05$ was reported as statistically significant.

4.3 Results

4.3.1 Integration of paper-based amplification into LFA to create an integrated paper-based LAMP-LFA biosensor

An integrated paper-based LAMP-LFA biosensor was developed for cost-effective nucleic acid amplification and lateral flow detection at the POC. The two-layer integrated biosensor was fabricated through the combination of the lateral flow strip (first layer) and the LAMP strip (second layer). A handheld battery-powered device was used for performing nucleic acid amplification and detection in an integrated paper-based LAMP-LFA biosensor. To investigate the potential risk of sample evaporation in the integrated biosensor, the mass of the biosensor was recorded before and after heating at 63 °C. By using a tape as a protector, the absence of sample evaporation was observed, as indicated by no significance difference in the mass of the biosensor before and after the amplification **(Fig 4.4)**.

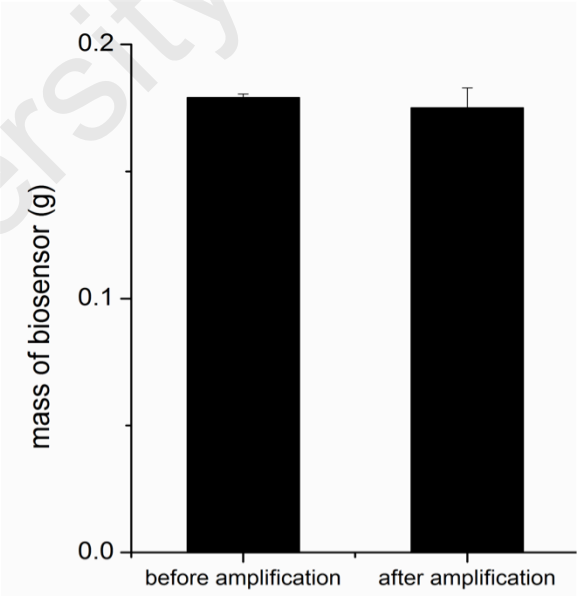

Figure 4.4: Evaluation of the risk of sample evaporation. There was no significant difference between the mass of biosensor before and after LAMP at 63 °C, indicating no risk of sample evaporation.

4.3.2 LAMP optimization

To optimize the LAMP reaction temperature, using Dengue DNA as a target analyte, the amplification process was performed at a range of temperature (58, 60, 63, 65 and 68 °C) for 60 min, followed by 95 °C denaturation for 5 min in conventional tube-based and paper-based platform, a glass fiber pad using the handheld heating device. Similar to the tube-based LAMP, the optimum temperature for paper-based LAMP was 63 °C, as indicated by more clearly visible bands shown in electrophoresis, a denser yellowish-green colour produced in SYBR Green I staining and a higher absorbance value obtained at 260 nm (OD 260) (**Fig. 4.5**).

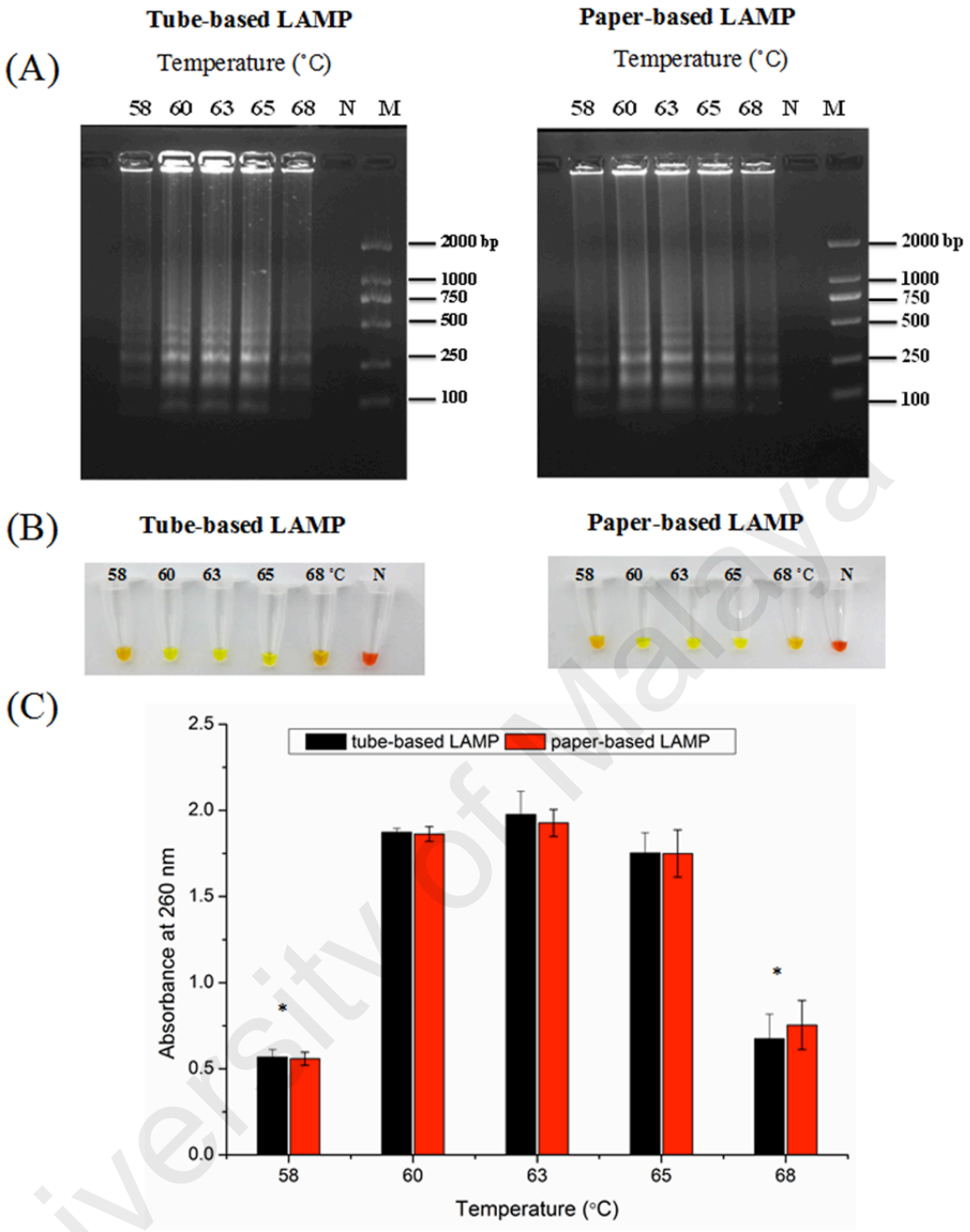

Figure 4.5: Optimization of LAMP temperature. The temperature of 63 °C, as the middle point, was the optimum LAMP temperature based on the visible bands in electrophoresis for both tube-based and paper-based platform (A), the comparable positive result shown (yellowish-green) after SYBR Green I staining (B) and absorbance value at 260 nm (* p<0.05) (C) (N = negative control, M= 100 – 2000 bp marker).

To evaluate the optimum denaturation time for optimum target amplification and detection, LAMP was performed in the tube at the optimum 63 °C, followed by denaturation at 95 °C for 0, 0.25, 0.5, 1, 3 and 5 min and LFA. The data showed that 0.5 min was the optimum denaturation period as it produced a significantly higher OD of test zone as compared to 0.25 min and showed no significant difference from 1 - 5 min of denaturation (**Fig. 4.6**).

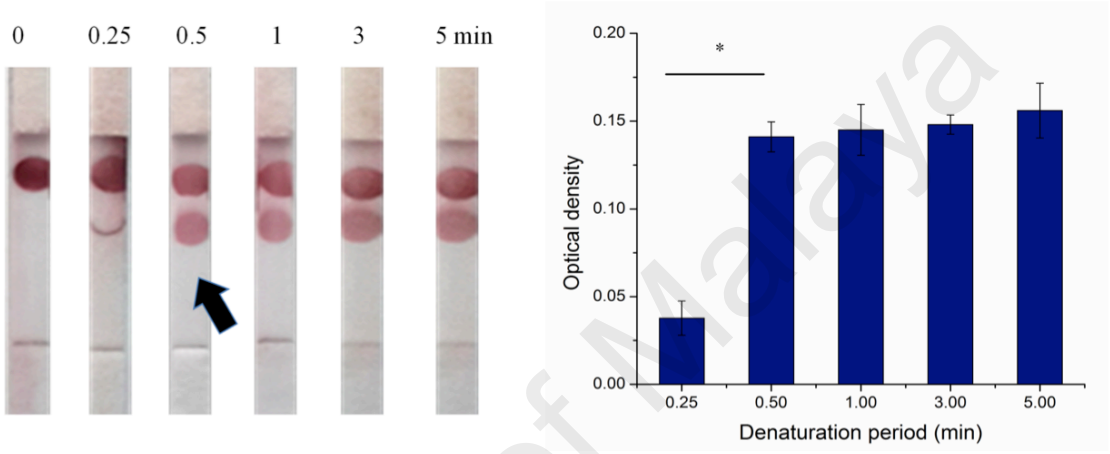

Figure 4.6: Optimization of denaturation period. Denaturation time of 0.5 min was selected as it produced a significantly higher optical density (OD) of test zone as compared to 0.25 min (*p<0.05).

To demonstrate the ability of paper-based platform to effectively support the amplification, at the optimum temperature of 63 °C and denaturation period of 0.5 min, LAMP incubation time was optimized. LAMP was performed in the glass fiber pad (*i.e.,* "unintegrated" paper-based LAMP) with a serial concentration of DNA template (3×10^{10}, 3×10^{8}, 3×10^{6}, 3×10^{4}, 3×10^{3} and 3×10^{2} copies) over a range of incubation time (15, 30, 45, 60 and 90 min) using the handheld heating device. The result of agarose gel electrophoresis shows that the longer the incubation time, the higher the amount of amplicons produced. The brightness of the bands appears to be proportional to the amount of DNA template used, as indicated by the detection limit of as low as 3×10^{6} copies achieved at the incubation time of at least 60 min. This data was further supported by SYBR Green I staining (**Fig. 4.7**).

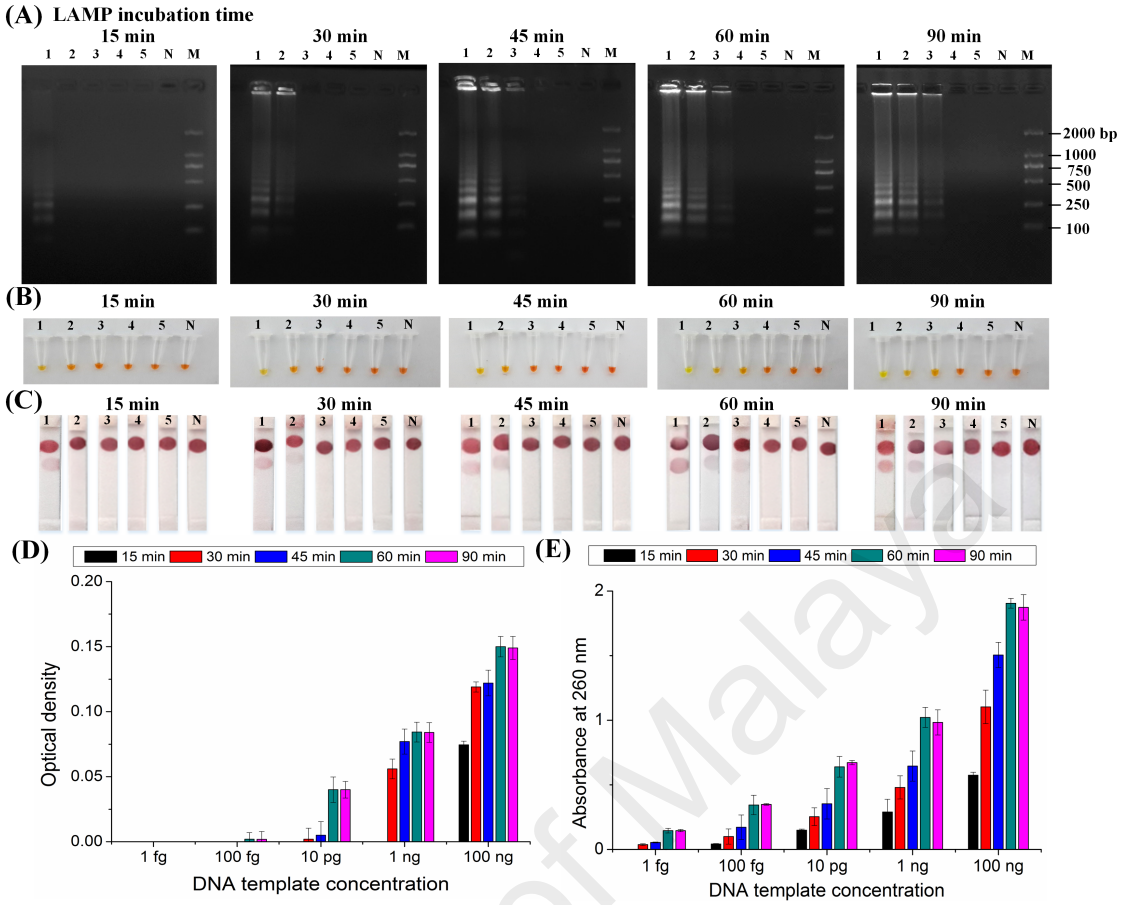

Figure 4.7: Unintegrated Paper-based LAMP and LFA. With the optimum LAMP temperature (63 °C), LAMP performed with a serial concentration of DNA template in the paper-based platform at different incubation time. The data of gel electrophoresis showed a directly proportional relationship between the brightness of the bands and the concentration of DNA template for LAMP (A). The positive result was further supported by the yellowish-green colour solution observed after the SYBR Green I staining (B), LFA (C & D) and absorbance value at 260 nm (E) (1= 3×10^{10} copies, 2= 3×10^{8} copies, 3= 3×10^{6} copies, 4= 3×10^{4} copies, 5= 3×10^{2} copies, N = negative control, M= 100 – 2000 bp marker).

In line with the results of electrophoresis and fluorescent staining, LFA showed a significantly higher optical density in the sample with a higher quantity of DNA template and a longer incubation time. A detection limit in LFA could be achieved of as low as 3×10^{6} copies at the optimum incubation time of 60 min. The amplification efficiency was further confirmed by the measurement of absorbance value (OD260) of amplicon. Collectively, 60 min was indicated as the optimum incubation time to achieve the lowest detection limit of the assay (**Fig. 4.7**).

4.3.3 Target DNA detection using the integrated LAMP-LFA biosensor

To investigate the potential of this simple and portable testing device to facilitate the integrated paper-based LAMP-LFA biosensor in remote settings, integrated test assays were performed using the handheld device. Interestingly, the optimum amplification period of 60 min was found to be capable of successfully achieving a detection limit of as low as 3×10^3 copies for dengue viral DNA (**Fig. 4.8**), which was more sensitive than that of unintegrated paper-based LAMP and LFA (3×10^6 copies). There was no significant difference between the detection limit of tube-based LAMP-LFA and integrated paper-based LAMP-LFA (**Fig. 4.8**).

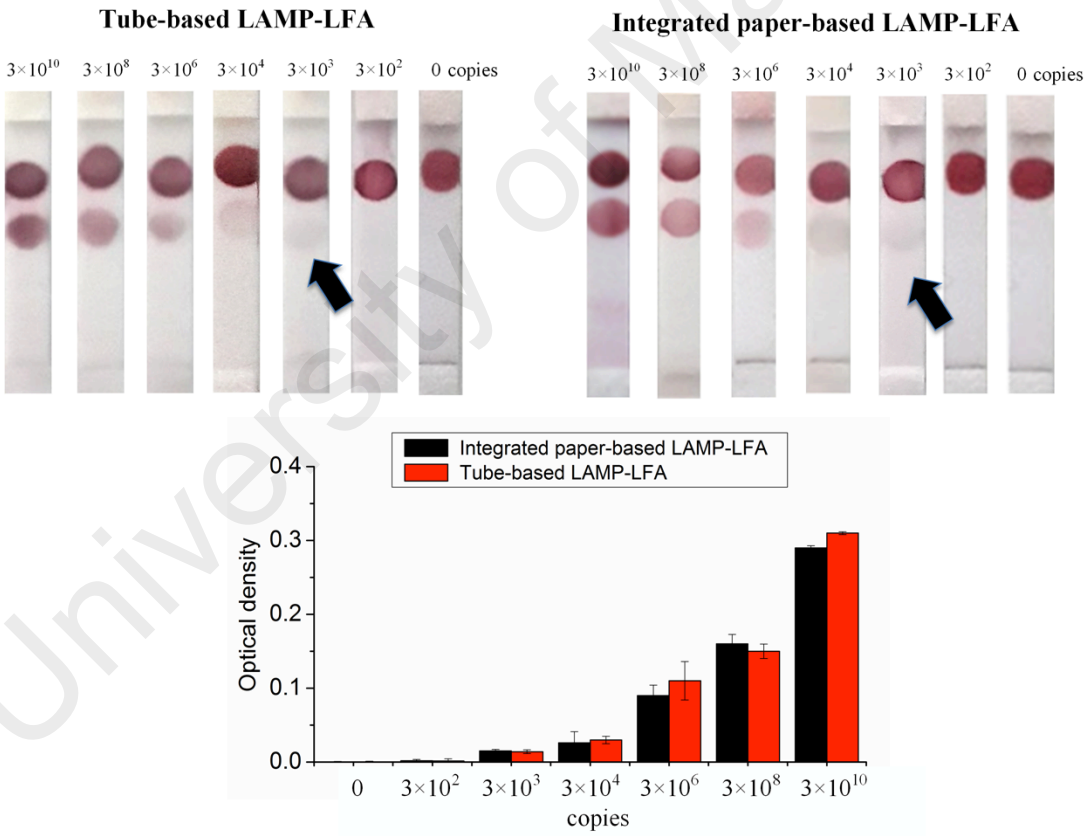

Figure 4.8: An integrated paper-based LAMP-LFA biosensor coupled with a handheld battery-powered heating device for target detection. The integrated paper-based biosensor could achieve the detection limit of as low as 3×10^3 copies at the optimum 60 min incubation time, which was comparable with that of tube-based LAMP-LFA in an unintegrated format.

4.4 Discussion

With the optimum reagent concentration and environmental factors obtained from the previous study (Choi, 2015), the functionality of the assay was improved by integrating paper-based nucleic acid amplification into LFA. In fact, in NAT, RNA viruses such as Dengue Virus (Vickers, 2001), Human Immunodeficiency Virus (HIV) (Ellis, 2004; Moher et al., 2001; Vickers et al., 2004) and Hepatitis C Virus (HCV) (Cribbie & Jamieson, 2000; Vickers et al., 2004) normally require reverse transcription and amplification prior to target detection. However, DNAs have been commonly used for evaluation of the performance of prototypes for various medical diagnostics (De Paula & Fonseca, 2004; Razali & Wah, 2011; Vickers, 2005). In this study, the proof-of-principle investigation of the potential of the prototype integrated LFA was conducted with both amplification and detection using the handheld battery-powered heating device. Synthetic Dengue viral DNAs were used as model analyte and it was suggested that this technique can be broadly applied to other target DNA/RNA.

Briefly, following the amplification process, a denaturation step is required to separate the double-stranded DNAs into single stranded DNA at denaturation temperature of 95 °C at an optimum period of 0.5 min **(Fig. 4.9)**. The single-stranded target would then bind to the single-stranded DP coupled with AuNP (AuNP-DP). After diffusing across the nitrocellulose membrane, the biotinylated amplicons would be captured by the streptavidin at the test zone to produce a red signal, with an optimum streptavidin concentration of 2 mg/mL. The remaining AuNP-DP would then hybridize with the control probe to form a red signal. In line with the results of electrophoresis and fluorescent staining, LFA showed a significantly higher optical density in the sample with a higher quantity of DNA template and a longer incubation time. A detection limit in LFA could be achieved of as low as 3×10^6 copies at the optimum

incubation time of 60 min. The amplification efficiency was further confirmed by the measurement of absorbance value (OD260) of amplicon. Collectively, 60 min was indicated as the optimum incubation time to achieve the lowest detection limit of the assay.

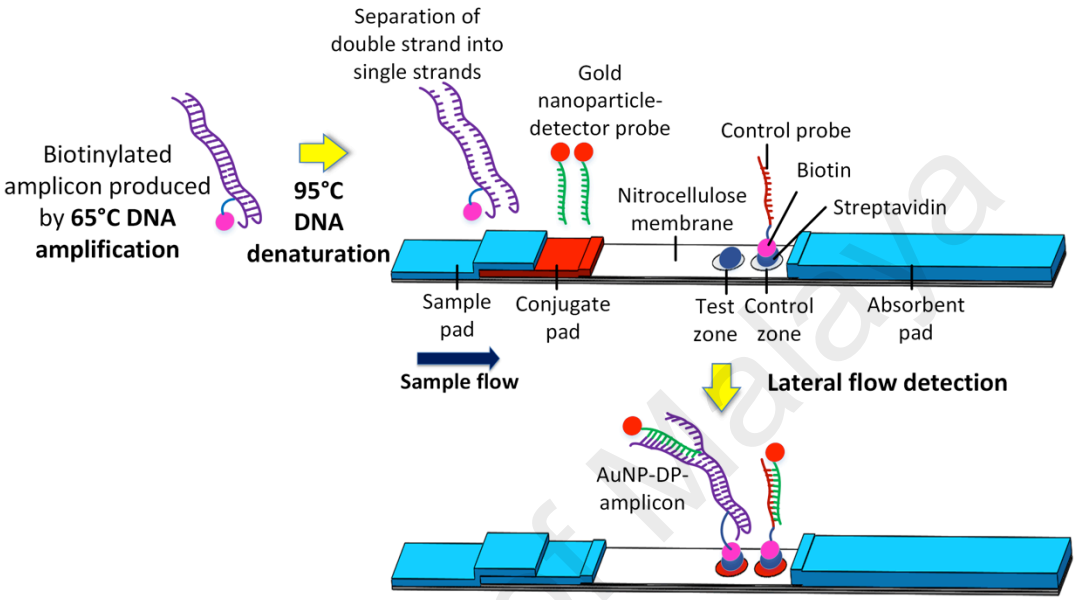

Figure 4.9: A schematic of lateral flow-based endpoint detection. Following the amplification process, 95 °C DNA denaturation is performed to separate the double-stranded DNAs into single strands. The single-stranded DNA would then bind to the single-stranded gold-nanoparticle-detector probe. After diffusing across the nitrocellulose membrane, the biotinylated amplicon is captured by the streptavidin at the test zone, and the remaining AuNP-DP is hybridized with the control probe to produce a red signal.

To simplify the processing step and achieve maximum sensitivity of the assay, integrating paper-based LAMP into LFA is proposed, in order to create an integrated paper-based LAMP-to-LFA biosensor for optimum amplicon detection. In fact, using unintegrated paper-based LAMP and LFA initially, it was found that there was a loss of more than half amount of solution from the original volume of 25 µL, with the average solution volume of 9.67 ± 0.33 µL left in the tube throughout the process. This might be due to the need for an additional step of centrifugation for amplicon collection between the process of paper-based LAMP and LFA, which could be successfully solved using the integrated biosensor. The challenge of combining paper-based LAMP and LFA

would be the requirement for on-chip fluidic control from LAMP zone and lateral flow strip with different temperature and time required for each zone. The challenge was addressed by creating the "valves" made by hydrophobic polyvinyl chloride (PVC) to control the fluid flow from one zone to another through connecting the PVC layers. The top PVC layer supports the lateral flow strip, which consists of a glass fiber pad, a nitrocellulose membrane and an absorbent pad. The bottom layer comprised of glass fiber pad, which acts as a platform for LAMP. A piece of disposable adhesive tape was folded into half, creating a small pocket to cover the amplification zone (glass fiber pad) to prevent from sample evaporation and contamination. There was also no risk of contamination throughout the process, as evidenced by the negative result shown by all the negative controls.

As high temperature is normally required for nucleic acid amplification, utilizing a handheld battery-powered heating device is essential to be coupled with the integrated paper-based biosensor for target detection in resource-limited settings where electricity may not be available (LaBarre et al., 2011). Therefore, a handheld battery-powered heating device was used for nucleic acid amplification and detection in an integrated paper-based biosensor. This handheld heating device consists of a closed heating compartment for amplification, a non-heating testing compartment for target analyte detection, an integrated battery, an integrated temperature controller and a charger. The heating compartment is made internally of aluminium alloy with external insulation wall, whereas the testing compartment is made of chemical-resistant polyformaldehyde, which could fit well with various sizes of disposable microcentrifuge tube for target analyte detection. A battery is integrated into the heating device with a programmable temperature controller for temperature control with a range of room temperature +5 °C to 100 °C, with the resolution of ±0.1 °C. The temperature sensor is installed in the internal part of the device, with the temperature displayed at the exterior part to ensure

the maintenance of the optimum temperature for the process. The heating process is required only for amplification, therefore the device could be turned off for LFA for power saving. Both nucleic acid amplification and detection could also be simultaneously performed with this handheld heating device.

To investigate the potential of this simple and portable testing device to facilitate the integrated paper-based amplification-to-detection biosensor in remote settings, test assays were performed using this device. Following the amplification at 63 °C and denaturation at 95 °C in the closed heating compartment, both amplification zone and lateral flow strip were then connected. LFA was then performed in the non-heating compartment, followed by signal detection by a smartphone. Interestingly, the optimum amplification period of 60 min was found to be capable of successfully achieving a detection limit of as low as 3×10^3 copies for dengue viral DNA, which was more sensitive than that of unintegrated paper-based LAMP and LFA (3×10^6 copies) due to the ability to retain the optimum amount of amplicons for detection in the integrated biosensor. There was no significant difference between the detection limit of tube-based LAMP-LFA and integrated paper-based LAMP-LFA, highlighting its potential use for sensitive target detection in the near future. The sensitivity of the integrated biosensor was comparable or even higher than that of the existing studies (Khunthong et al., 2013; Song et al., 2014). Even though some studies have reported more sensitive target detection (~100 copies) (Lourens et al., 2014; Umut, 2013), the amplification and detection were separately performed. Besides that, different targets and probes may yield different detection sensitivity. Therefore, it was successfully shown that the simple and cost-effective integrated paper-based biosensor offers a great potential to substitute the conventional tube-based assay for POC use.

4.5 Conclusion

In short, an integrated paper-based biosensor was developed to perform both nucleic acid amplification and detection with the aid of a handheld battery-powered heating device, which promises sensitive and specific target detection. The capabilities of producing colorimetric signal detectable by the naked eyes, eliminating the requirement for UV source for assay readout. The utilization of a handheld heating device eradicates the need for high-end equipment commonly used for amplification such as thermal cycler, electrical heater or water bath, suggesting its potential use in POC settings. Given that this handheld device is regulated by a programmable temperature controller with the temperature ranging from 25 to 100 °C, it is suggested that other amplification techniques could also be applied. The technique described here could also be used to detect a variety of target nucleic acid. It was suggested that in the future, the integration of a simple paper-based extraction method into this biosensor could facilitate sample-in-answer-out NAT in remote settings.

CHAPTER 5: A FULLY INTEGRATED PAPER-BASED SAMPLE-TO-ANSWER BIOSENSOR FOR NUCLEIC ACID EXTRACTION, AMPLIFICATION AND LATERAL FLOW DETECTION AT THE POINT OF CARE

5.1 Introduction

NAT, a molecular diagnostic technique that involves nucleic acid extraction, amplification and detection, conventionally relies on well-established laboratories, high-end instrumentation and highly trained operators, limiting its use in resource-poor settings (Martinez et al., 2010; Wang et al., 2012; Wang et al., 2010). With increasing incidence of infectious diseases and food and water contamination, particularly in developing and underdeveloped countries with poor infrastructure (Feasey et al., 2012; Oberholster et al., 2012), there is an urgent need to develop simple, inexpensive, portable and rapid molecular diagnostic tools, which can be readily implemented in remote settings (Choi et al., 2015a). Recent advances in POCT, especially LFAs, make it possible to achieve simple and cost-effective NAT at the POC (Choi, 2015; Tamama et al., 2011; Yoshida et al., 2009). LFAs are able to produce results in a simple way (visible colour formation) in less than 30 min. However, as biological samples (*e.g.*, blood, urine, saliva) are generally complex and contain low amounts of target nucleic acids, a substantial off-chip extraction and amplification process (*e.g.*, tube-based extraction and PCR) is normally required prior to lateral flow detection (Kaewphinit et al., 2013; Rigano et al., 2014; Rigano et al., 2010). Recently, paper-based extraction and amplification has been introduced for detection of various diseases (*e.g.*, HIV (De Paula & Fonseca, 2004), *Chlamydia trachomatis* (Linnes et al., 2014) and Influenza A (Rodriguez et al., 2015)). However, these essential steps have been separately performed from LFAs, which entail multiple processing steps, hence increasing the risk

of reagent loss and cross-contamination. Therefore, it is of great importance to integrate nucleic acid extraction, amplification and lateral flow detection in an integrated paper-based biosensor for use in remote settings.

Although there has been a growing interest in developing low-cost integrated sample-to-answer biosensors for POC applications (Choi et al., 2015b), there are only a few studies which report on this. For instance, Whitesides' group has developed an integrated "paper machine" by incorporating sample preparation, nucleic acid amplification and signal detection (Nguyen et al., 2012). However, an electrically-powered heater and an external UV source were used for amplification and fluorescence signal detection, respectively. To date, a great challenge remains in integrating LFA into one single biosensor, which could tremendously simplify the final read out. The challenge would be the requirement for on-chip fluidic control from nucleic acid extraction zone to amplification zone and lateral flow strip, with optimum temperature required for each NAT step in a robust and portable manner. In fact, even though the integration of DNA extraction and amplification into a paper-based biosensor has been reported, a combination of LFA with the aforementioned steps for simple colorimetric readout has not yet been demonstrated. In addition, a handheld battery-powered heater to be used for nucleic acid amplification is imperative to be coupled with the integrated biosensor, which, however, has not yet been introduced for use in low-resource endemic areas. Therefore, there is a strong demand for a new colorimetric integrated paper-based molecular biosensor that can achieve rapid on-site naked-eye detection.

In the present study, a prototype paper-based biosensor was developed, where FTA card and glass fiber were integrated into a lateral flow strip for nucleic acid extraction and amplification, followed by naked eye detection and quantification using a

smartphone. All paper matrices were initially separated by hydrophobic PVC layers, creating the "valves" to control the fluid flow from nucleic acid extraction zone to amplification zone and lateral flow strip. The integrated biosensor was coupled with a handheld battery-powered heating device to support highly sensitive and specific LAMP, eliminating the need for an electrically-powered heater or thermal cycler. The *Escherichia coli (E. coli)* as target analyte, was spiked into the drinking water, milk, blood, and spinach to demonstrate its ability in medical diagnostics, environmental monitoring and food safety. The biosensor permits the potential use of other amplification techniques (*e.g.*, SDA or RPA) in remote settings, through adjusting the temperature of the handheld device. This integrated biosensor could be broadly applied to other target analytes at the POC, holding great potential for a wide range of applications.

5.2 Materials and methods

5.2.1 Bacteria culture

E. coli ATCC 25922 was used as a model organism in this study. Initially, the bacteria was streaked onto Luria-Bertani (LB) agar containing 100 mg/mL of ampicillin and incubated at 37 °C for 16 hours to allow bacteria growth. An isolated *E. coli* colony was picked and cultured in 10 mL of LB medium at 37 °C for 16 hr with agitation at 150 rpm. The *E. coli* culture was used as a standard stock for all experiments. The turbidity of bacteria suspension was measured at a wavelength of 600 nm (OD 600). The bacteria stock was then diluted from 1- to 10-fold in phosphate buffered saline (PBS) and spread on LB-ampicillin plates (**Fig 5.1)**. The single colonies were then counted after overnight incubation at 37 °C. Bacteria concentrations were determined by plate colony counting. The concentration that produces 30-300 colonies was determined which was then used

to calculate colony forming units per mL (CFU/mL), and confirmed with OD 600 (Liu et al., 2014).

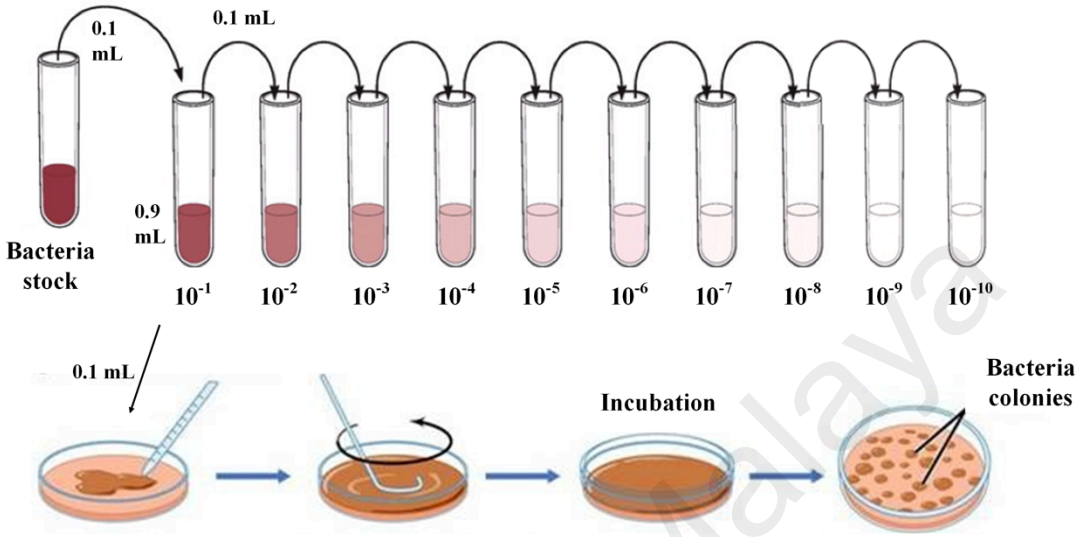

Figure 5.1: Bacteria culturing for bacteria concentration determination. The bacteria stock was diluted from 1- to 10-fold in PBS. Each concentration of bacteria was then spread on the LB-ampicillin plates for bacteria culturing.

5.2.2 Fabrication of a fully integrated paper-based sample-to-answer biosensor

The integrated paper-based biosensor consists of 4 layers (**Fig 5.2)**. The top PVC layer is the lateral flow layer supported by a PVC backing pad (6 cm × 0.25 cm) (J-B6, Jiening, China), which consists of a glass fiber (1 cm × 0.25 cm) (Pall 8964, Saint Germain-en-Laye, France), nitrocellulose membrane (1.9 cm × 0.25 cm) (HFB 18002, Millipore, USA), and an absorbent pad (2.5 × 0.25 cm) (H-1, Jiening, China). The second layer is comprised of glass fiber for highly specific and sensitive nucleic acid amplification technique (*i.e.*, LAMP). The third layer consists of a FTA card (Whatman, UK), with a diameter of 0.25 cm, for sample addition and nucleic acid extraction. The bottom layer is comprised of an absorbent pad. The waste produced from the washing step was absorbed by the absorbent pad, which was then being removed. The fabrication

process was similar to that of integrated paper-based LAMP-LFA biosensor previously described in **Fig 4.3** with the addition of two layers (*i.e.,* the third and the bottom layer).

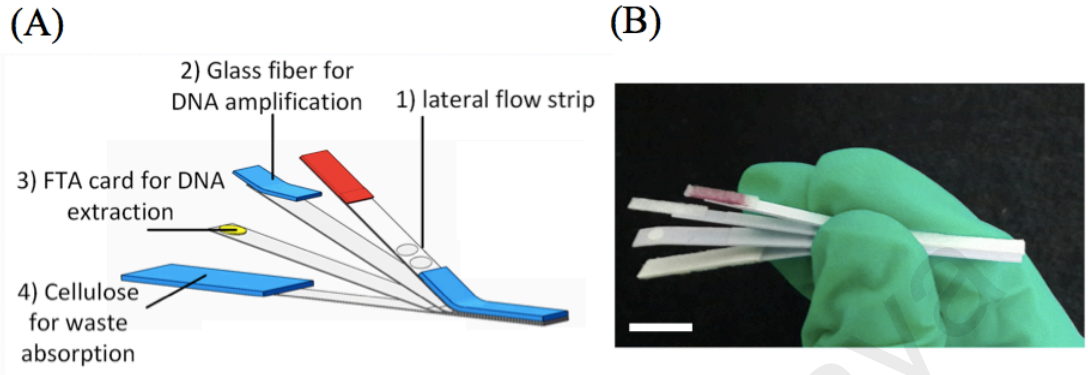

Figure 5.2: Development of a fully integrated paper-based sample-to-answer biosensor. (A) The biosensor consists of four PVC layers. The first layer is a lateral flow layer for LFA, the second layer consists of glass fiber for DNA amplification, the third layer consists of a FTA card for DNA extraction, whereas the bottom layer consists of cellulose for waste absorption after the process of sample purification and washing. (B) The image of biosensor (Scale bar, 1 cm).

By using Matrix ^{TM} 2360 Programmable Shear (Kinematic Automation Inc., CA, USA), the assembled pads were cut into small strips with 2.5 mm width. All materials were assembled to create an integrated paper-based sample-to-answer biosensor. A piece of 3.5 cm × 2 cm adhesive tape was folded in half, creating a small pocket to cover the amplification zone (glass fiber and FTA card) to avoid evaporation. About 0.5 µL of 2 mg/mL streptavidin (Promega, USA) and 0.5 µL of 100 µM control probe were dispensed onto the nitrocellulose membrane to create test zone and control zone, respectively on the lateral flow strip.

5.2.3 Optimization of FTA card paper-based extraction for the fully integrated biosensor

The whole operation process is shown in **Fig 5.3**, which will be discussed in details in the discussion **Section 5.4**.

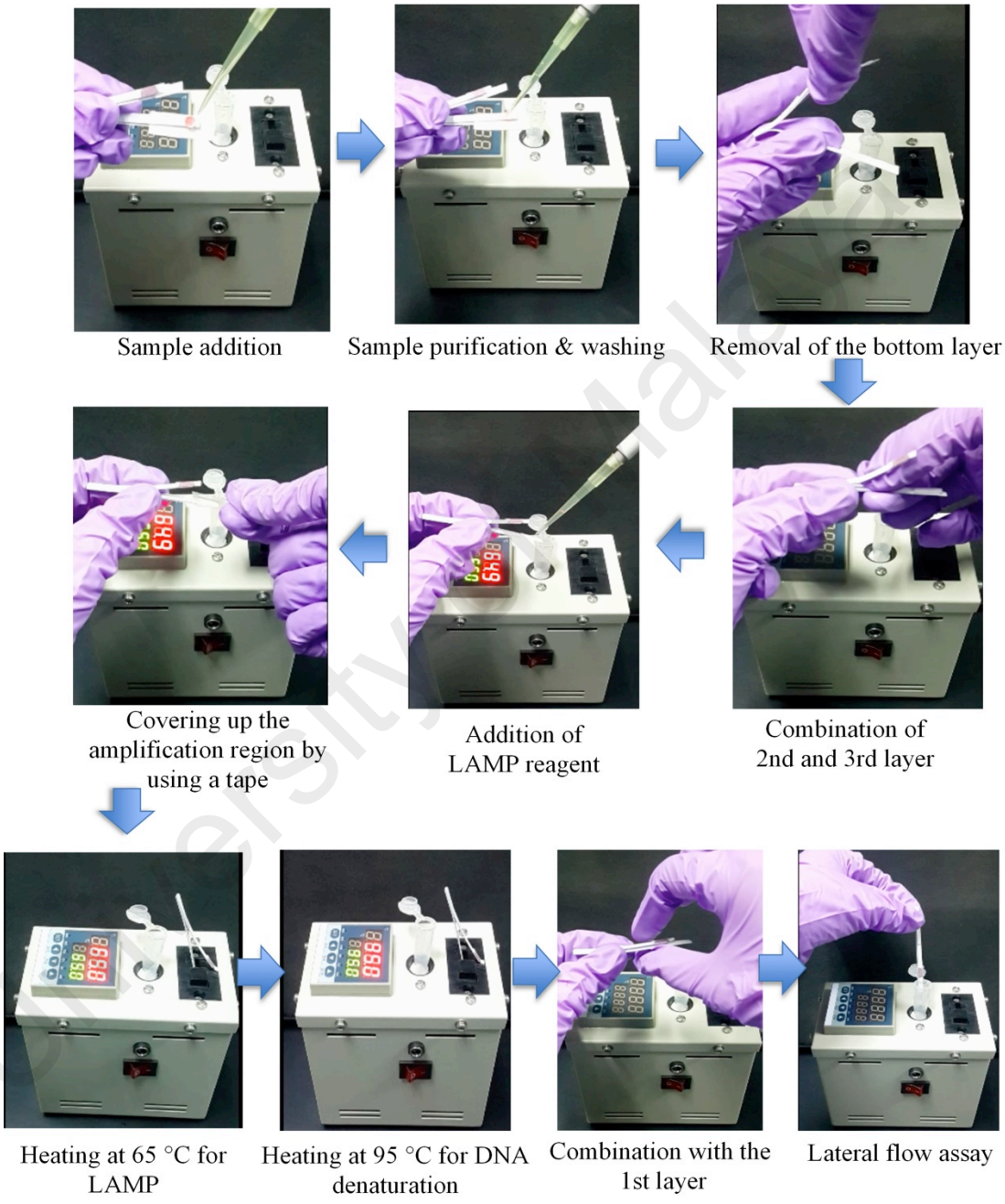

Figure 5.3: Paper-based sample-to-answer process. Following the sample addition, purification and washing were performed. The bottom layer was then removed, followed by the combination of the second and third layer. LAMP reagent was added, and the process of amplification and denaturation were performed. The first layer was then combined with the second and third layer for LFA.

In optimization of the extraction process, the biological sample was first pipetted onto the FTA card and kept at room temperature for nucleic acid extraction. To achieve rapid nucleic acid extraction for POCT, a range of drying period (*i.e.*, the cell lysis period) for FTA card were tested, *e.g.*, 5, 10, 15, 30, 45 and 60 min. qPCR **(Table 5.1 & Table 5.2)** was performed, followed by LFA to determine the extraction efficiency. The sequence used in qPCR will be stated in **Section 5.2.4**.

Table 5.1: Components of qPCR used per reaction

Component	**Volume (µL)**
DNA template	Up to 1
Forward primer (*E. coli* B3)	1 (0.2 µM)
Reverse primer (*E. coli* F3)	1 (0.2 µM)
2 × Reaction Mix	10
Nuclease-free water	Top up to a final reaction volume of 20
Total	**20**

Table 5.2: Thermal cycling profile for qPCR

Process	**Cycle**	**Temperature and duration per cycle**
Pre-denaturation	1	95 ^{o}C for 10 min
Denaturation	40	95 ^{o}C for 10 sec
Annealing	40	55 ^{o}C for 20 sec
Extension	40	72 ^{o}C for 15 sec

Following drying of the FTA card, a FTA purification reagent (Whatman, UK) and Tris-EDTA (TE) buffer (Sigma-Aldrich) were used to fully wash away the polymerase inhibitors prior to amplification. To determine the volume of FTA purification reagent and TE buffer used and number of washes required, both factors were optimized. Following the optimum 15 min of drying for FTA card, the biosensor was tested with various volumes of FTA purification reagent and TE buffer (*e.g.*, 20 µL and 40 µL, 40 µL and 80 µL, and 80 µL and 160 µL respectively). The necessity of one, two or three washes was tested to fully remove the polymerase inhibitors.

5.2.4 Optimization of paper-based LAMP temperature and incubation time for the fully integrated biosensor

The sequences used were obtained from Sangon Biotechnology Co., Ltd. (Shanghai, China) (**Table 5.3**). Briefly, following nucleic acid extraction, the second and third layers of PVC were combined, followed by the addition of amplification reagents onto the tape-covered glass fiber for amplification. The biosensor was then moved into the covered heating compartment of the handheld heating device for amplification process. To investigate the paper-based LAMP temperature, the amplification was performed with a range of temperatures (58, 60, 63, 65 and 68 °C) for 60 min, followed by detection by electrophoresis and SYBR Green I staining. The LAMP products were observed under visible light and UV light.

Table 5.3: DNA sequences used in the study

Name	**Sequence (5'-3')**
E.coli detector probe	5'-caaagggagaagggcatgg -$(CH_2)_6$-SH-3'
E.coli control probe	5'-ccatgcccttctccctttg/Biotin-3'
E.coli F3	5'-gccatctcctgatgacgc -3'
E.coli B3	5'-atttaccgcagccagacg -3'
E.coli FIP	5'-Biotin/cattttgcagctgtacgctcgcagcccatcatgaatgttgct -3'
E.coli BIP	5'-ctggggcgaggtcgtggtattccgacaaacaccacgaatt -3'
E.coli FLP	5'-taacaacctgtcatcgac -3'
E.coli BLP	5'-atcaatctcgatatccatgaaggtg -3'

5.2.5 LFA in the fully integrated biosensor

Following the amplification, DNA denaturation was performed at 95 °C for 30 s, followed by LFA based on the method as described in **Section 4.2.4**.

5.2.6 Various biological sample testing

The bacteria were first diluted in PBS for optimization of paper-based extraction and LAMP. To further show the potential of the biosensor to be applied in medical diagnostic, environmental monitoring and food safety, the bacteria was spiked into drinking water, milk, blood, and spinach samples with the final concentrations ranging from 1 to 10^5 CFU/mL. Discarded whole blood was used in this study. Bottled water, milk (containing 3% energy, 5% protein, 6% fat, 2% carbohydrate, 3% sodium and 13% calcium) and spinach samples were obtained from a local grocery store. Spinach leaves were washed and then spiked with *E. coli* before mixing with 100 mL of ultrapure water in a blender. The mixture was then filtered using a 70 μM-cell strainer to remove the residues of the leaves before testing. The mixture of each biological sample and *E. coli* were vortexed for 30 sec prior to NAT. All the samples were then tested using the integrated biosensor. A schematic of whole process is shown in **Fig. 5.4**.

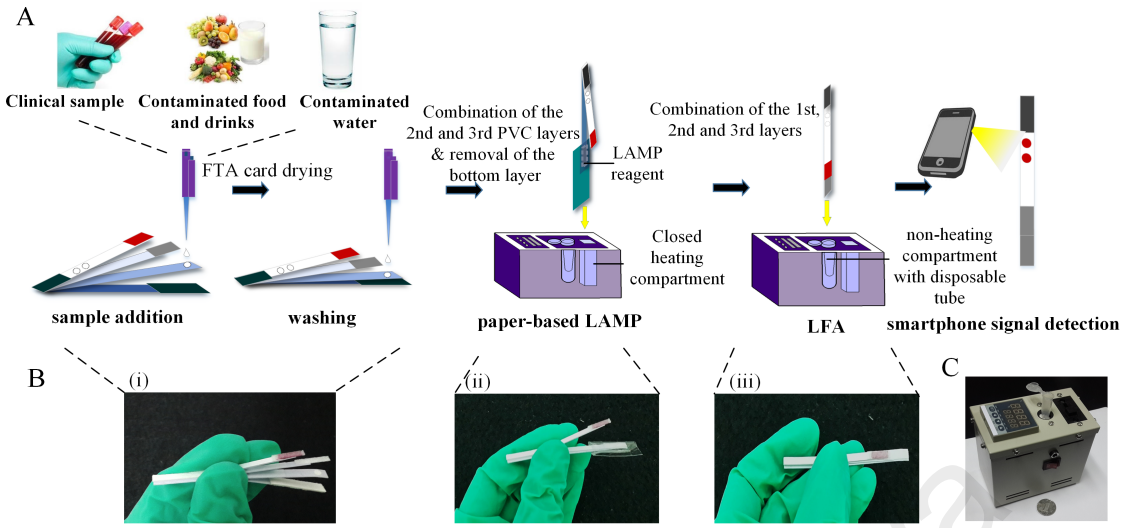

Figure 5.4: A schematic of biological sample testing using a fully integrated paper-based sample-to-answer biosensor coupled with a heating device. (A) A schematic of the experimental procedure. (B) Images of the biosensor during the steps of (i) extraction, (ii) amplification and (iii) lateral flow detection. (C) An image of a handheld battery-powered heating device.

5.2.7 Statistical analysis

Statistical analysis was performed using One-Way ANOVA with Tukey post-hoc test to compare the data among different groups. Data were expressed as mean ± standard error of the mean of three independent experiments (n=3). $p<0.05$ was reported as statistically significant.

5.3 Results

5.3.1 Determination of bacteria concentration

To determine the bacteria concentration for paper-based NAT, the bacteria stock was then diluted from 1- to 10-fold in PBS and spread on LB-ampicillin plates, followed by plate colony counting after incubation. It was found that 10-fold bacteria dilution produced an average of 178 ± 11.27 colonies (1.8 x 10^{13} CFU/mL) from the readings of bacteria culturing (n=3), with the average absorbance value of ~1.27 ± 0.017 at 600 nm (OD 600) (**Fig. 5.5)**. This concentration was selected as a reference as it falls within the range of 30-300 colonies (Liu et al., 2014).

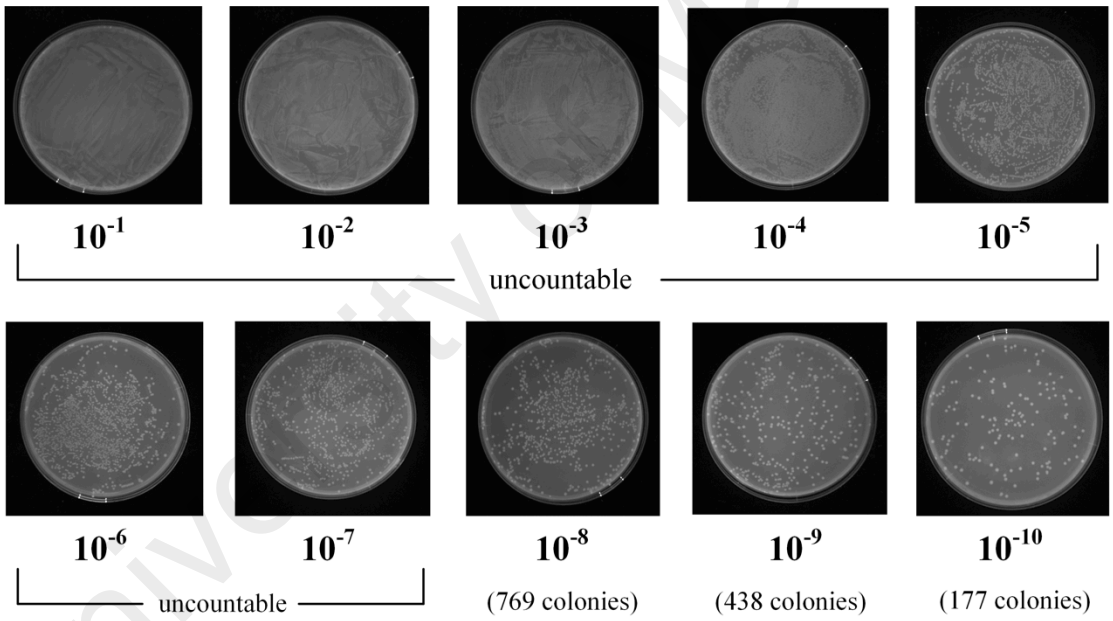

Figure 5.5: Determination of bacteria concentration. From 1- to 10-fold bacteria dilution, it was found that the concentration of 10-fold dilution produced an average of 178 ± 11.27 colonies (1.8 x 10^{13} CFU/mL) from the colony counting (n=3).

5.3.2 Optimization of FTA card paper-based extraction

To achieve rapid nucleic acid extraction for POCT, the effect of FTA card drying period (5, 10, 15, 30, 45 and 60 min) was tested, *i.e.*, the cell lysis period, on the biosensor. The extraction efficiency was determined by qPCR and LFAs. The data from PCR showed that a minimum of 15 min was able to achieve a lower cycle threshold (CT) values, which indicates a lower number of cycles required for the fluorescent signal to reach the threshold level **(Fig. 5.5)**. To further confirm the result, LFAs were performed. Likewise, it was found that 15 min FTA card drying produced a significantly (p<0.05) higher optical density of the test zone as compared to that of 5 and 10 min **(Fig. 5.6)**.

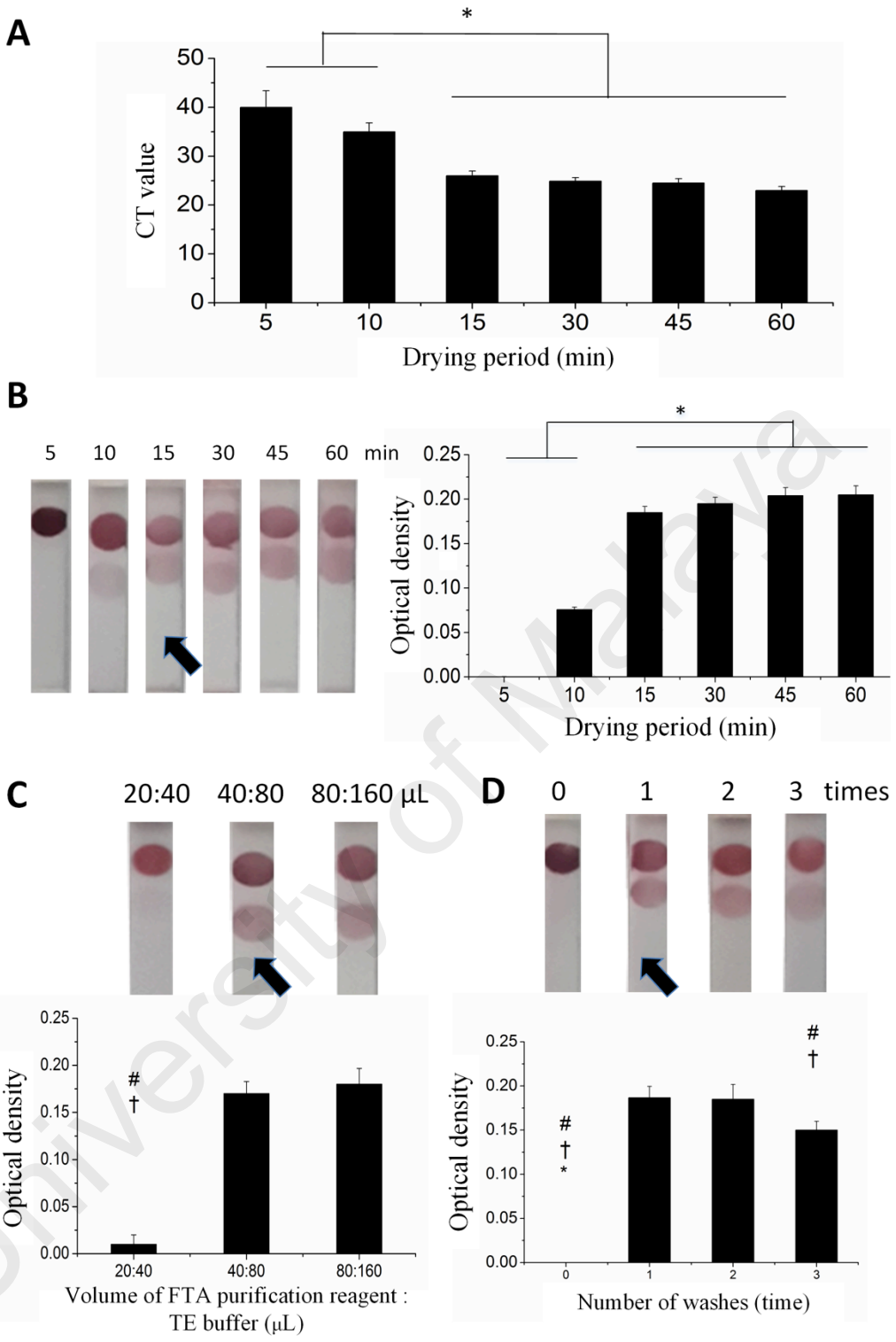

Figure 5.6: Optimization of paper-based DNA extraction. A duration of 15 min was selected as the optimum FTA card drying period based on the lower CT value in qPCR (* p<0.05) (A) and higher optical density in LFA (* p<0.05) (B) as compared to the shorter drying period. (C) A volume of 40 µL of FTA purification reagent and 80 µL of TE buffer was selected as optimum wash volume due to the significant higher optical density of test zone as compared to that of lower volume († p<0.05 relative to 40:80, # p<0.05 relative to 80:100). (D) One wash was able to provide significant higher optical density than that of without wash (* p<0.05 relative to 1 wash, † p<0.05 relative to 2 washes, # p<0.05 relative to 3 washes).

To make the integrated biosensor simpler and easier to use, a low volume of buffer with a reduced number of washes is essential. Therefore, both factors were optimized in the extraction process **(Fig. 5.6)**. In reagent volume optimization, a larger volume of TE buffer was used to wash away the excess FTA purification reagent that might affect the amplification (Connelly et al., 2015). The FTA purification reagent and TE buffer volumes tested were 20 µL and 40 µL, 40 µL and 80 µL, and 80 µL and 160 µL respectively for a total of two washes, where the volumes were about 10 times lower than that stated in the conventional protocol. It was found that 40 µL of FTA purification reagent and 80 µL of TE buffer produced a significantly (p<0.05) higher optical density of test zone as compared to that of 20 µL purification reagent and 40 µL buffer.

With the optimum volume of 40 µL of FTA purification reagent and 80 µL of TE buffer, the number of washes required to completely wash away the polymerase inhibitors from the FTA cards were investigated. It was found that there was no significant difference (p>0.05) in optical density of the test zones between one and two washes. However, three washes significantly (p<0.05) reduced the signal of the assay **(Fig. 5.6)**.

5.3.3 Optimization of paper-based amplification

To optimize the LAMP incubation time in the present study, LAMP was performed in the integrated biosensor at an optimum temperature of 65 °C and a range of incubation times (15, 30, 45 and 60 min) with a serial concentration of *E. coli* (1, 10, 10^2, 10^3, 10^4 and 10^5 CFU/mL), **Figure 5.7**. It was found that the longer the incubation time, the lower the detection limit of the assay. The detection limit of 45 min and 60 min incubation time (10 CFU/mL) were lower than that with 15 and 30 min (10^4 CFU/mL

and 10^2 CFU/mL, respectively) of amplification. Similar result was obtained through the observable red signal in the test zone (**Fig. 5.7**) and optical density from grey scale analysis of the test zone (**Fig. 5.7**).

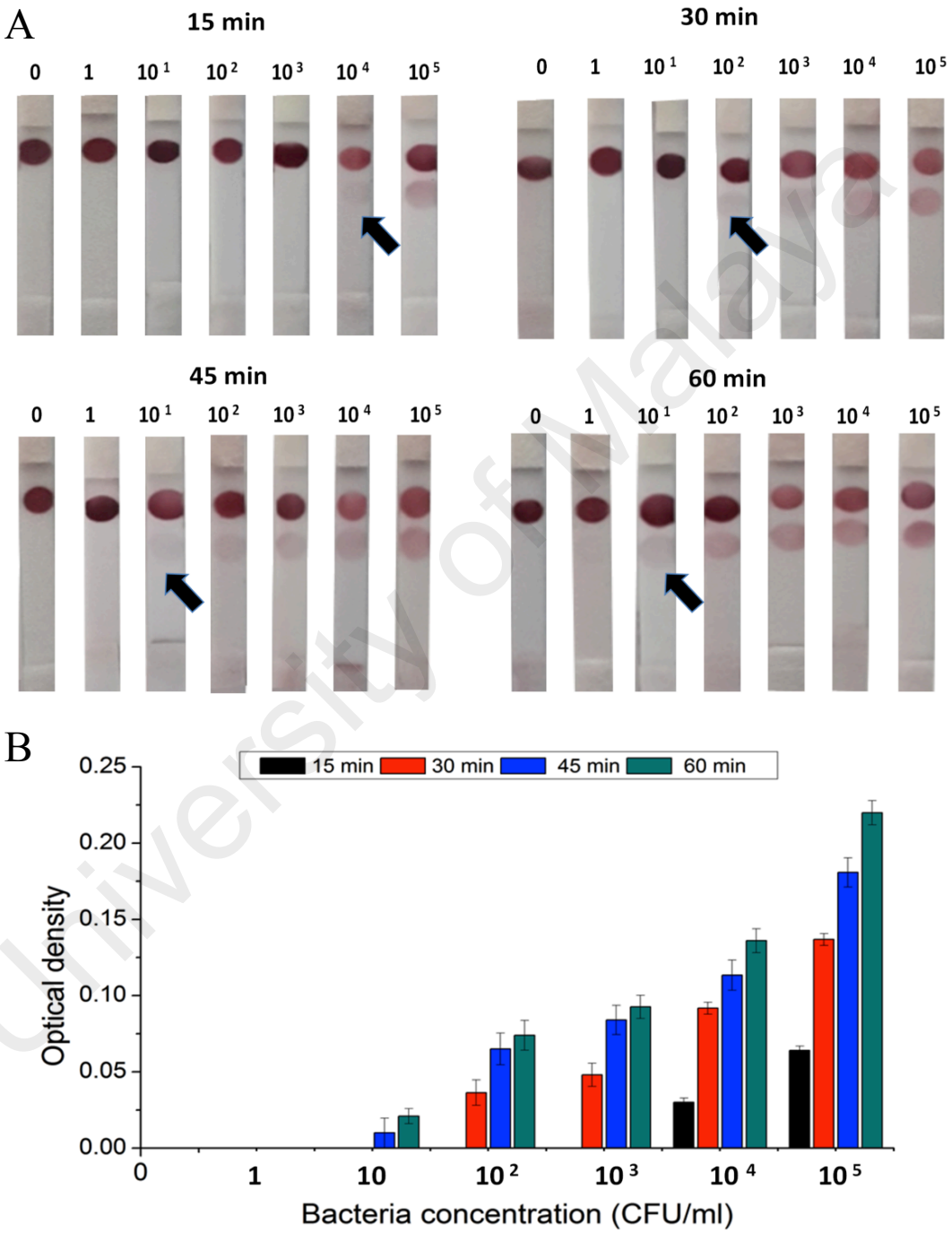

Figure 5.7: Optimization of paper-based LAMP. The detection limit of 45 and 60 min incubation time were lower as compared to 15 and 30 min of amplification. A minimum of 45 min incubation time was able to achieve a detection limit of as low as 10 CFU /mL of bacteria as indicated by the red signal shown at the test zone (A) and optical density obtained through gray scale analysis of the test zone (B).

5.3.4 *E. coli* spiked sample testing

To demonstrate the potential use of the biosensor for various applications, the biosensor was tested with *E. coli*-spiked whole blood samples, drinking water, milk and spinach with a range of bacteria concentrations (1, 10, 10^2, 10^3, 10^4 and 10^5 CFU /mL). It was successfully proven that the integrated biosensor could effectively detect real sample from drinking water, milk, blood, and spinach in a simple manner, with the detection limit of 10, 10, 100, 1000 CFU/mL, respectively, demonstrating its ability in medical diagnostics, environmental monitoring and food safety analyses (**Fig. 5.8)**.

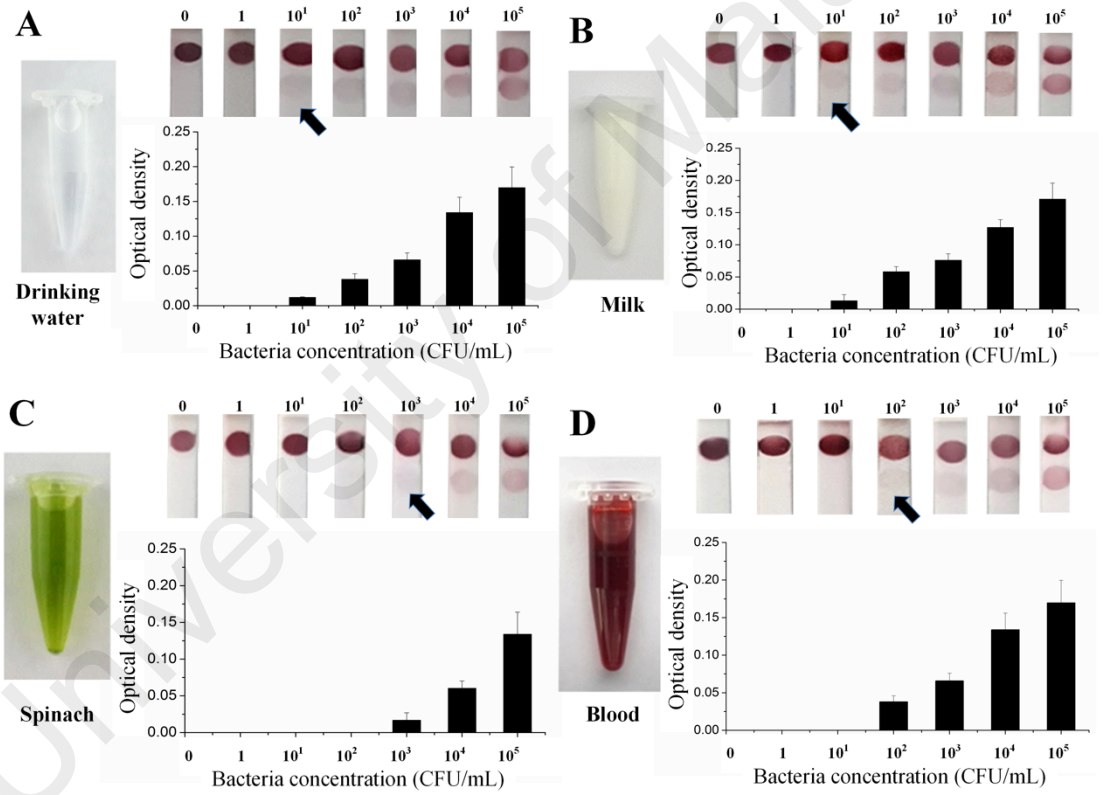

Figure 5.8: Biological sample testing. The integrated *E.coli* biosensor could effectively detect real sample from drinking water (A), milk (B), spinach (C) and whole blood (D) with the detection limit of 10, 10, 1000, 100 CFU/mL, respectively, showing its great potential for future food and water safety analyses and medical diagnostics.

5.4 Discussion

To achieve complete NAT in POC settings, a prototype fully integrated paper-based biosensor was further developed, where FTA card and glass fiber were integrated into a lateral flow strip for nucleic acid extraction and amplification, followed by naked eye detection and quantification using a smartphone. All paper matrices were initially separated by hydrophobic PVC layers, creating the "valves" to control the fluid flow from nucleic acid extraction zone to amplification zone and lateral flow strip. The fully integrated biosensor was also coupled with a handheld battery-powered heating device to support highly sensitive and specific LAMP.

FTA cards are impregnated with a patented chemical formulation for DNA storage, lysis and extraction. As they have been extensively used for DNA collection and storage, it was suggested that besides enabling immediate sample processing, the biosensor also allows sample storage in remote settings prior to analysis, which are greatly useful when further laboratory tests are required to confirm the diagnosis, especially for diagnosis of chronic diseases (*e.g.,* cancer). As compared to other available paper-based biosensors (Linnes et al., 2014; Rodriguez et al., 2015), which do not allow sample storage, the prototype allows sample storage at ambient temperature by protecting DNA from degradation for downstream analysis (Beckett et al., 2008), making them a very attractive tool for both onsite sample collection and storage (Lange et al., 2014; Liang et al., 2014), and immediate analysis.

Following the addition of the sample onto the FTA card, the card was allowed to dry and the impregnated chemicals lysed cells at room temperature. As these chemicals may interfere with the downstream analysis, washing steps are required for chemical removal. The bottom layer responsible for waste absorption was removed, and the

second and third PVC layers were combined, followed by the addition of amplification reagents onto the tape-covered glass fiber for amplification. The tape-covered zone was then moved into the covered heating compartment of the handheld device for amplification. Following the amplification, denaturation was performed to separate the double-stranded DNAs into single strands to be hybridized with AuNP-DP. The second and third layers were then combined with the top lateral flow layer, and were moved into the non-heating compartment containing the disposable microcentrifuge tube for LFA. At the end of each assay, the result could be detected by the naked eye or/and quantified by using a smartphone. The simple integrated paper-based biosensor coupled with this handheld device enables a rapid and accurate detection of targets at the POC.

To demonstrate the potential use of the biosensor for applications such as medical diagnostics, environmental monitoring and food safety analysis, the biosensor was tested with *E. coli*-spiked whole blood samples, drinking water, milk and spinach with a range of bacteria concentrations (1, 10, 10^2, 10^3, 10^4 and 10^5 CFU /mL) at the optimum temperature (65 °C) and incubation time (45 min). In detection of *E. coli* in drinking water, the biosensor achieved a detection limit of as low as 10 CFU/mL, which is similar to that in PBS solution. The data prove that the biosensor can sensitively detect target analytes in contaminated water, which is comparable to the existing paper-based assays (10-10^2 CFU/mL) (Hu et al., 2013; Morales-Narváez et al., 2015; Røsland et al., 2009; Wu et al., 2015), offering great potential in applications of environmental and water safety analyses.

To evaluate the potential use of the biosensor in food safety analysis, it was tested with *E. coli*-spiked milk and spinach sample. Similar to the data of PBS and drinking water, the assay achieved the detection limit of 10 CFU /mL of bacteria in a

milk sample. Even though milk components (*e.g.,* Ca^{2+}) have been reported to inhibit the amplification process by reducing the exposure of DNA to the polymerase (Durel et al., 2015), the result did not show such a negative impact, which further proved the successful removal of the amplification-inhibitory components through the purification and washing process. In detection of *E. coli*-spiked spinach sample, it was found that the detection limit was 10^3 CFU/mL, which was higher as compared to other samples. This might be due to the requirement for pre-processing steps (*e.g.,* filtration) to remove the residue of spinach leaves prior to the detection, resulting in the loss of bacteria. The ability to detect 10 and 10^3 CFU/mL of *E.coli* in milk and spinach samples respectively was comparable or even more sensitive than the other existing paper-based assays (~10^3-10^6 CFU/mL) (Hossain et al., 2012; Song et al., 2016), Considering the simplicity and accuracy of the assay, the all-in-one prototype offers great potential for food and water safety analyses.

On the other hand, sepsis is known as the current leading cause of death (Laakso & Mäki, 2013). The blood culture method represents the gold standard for determination of sepsis, which is however time-consuming (2-5 days) and highly dependent on skilled operators, thus less suitable for POC applications. Rapid molecular diagnosis is critical for early patient management to reduce the risk of disease transmission. To investigate the potential use of the integrated biosensor in medical diagnosis (especially in sepsis diagnosis), it was tested with *E. coli*-spiked human whole blood sample. It was found that the detection limit was 100 CFU/mL, which was higher as compared to PBS, drinking water and milk sample. This might be due to the presence of a significant amount of white blood cells, which would also be lysed by the FTA card, hence reducing the space available for binding and lysing of bacterial cells. However, with the ability of sensitively detecting *E. coli* in whole blood with comparable or even

lower detection limit than conventional assays (10-500 CFU/mL) (Laakso & Mäki, 2013), the biosensor holds great potential to complement conventional culture-based techniques to achieve rapid, sensitive and specific clinical diagnosis.

Unlike the previously reported equipment-dependent paper-based assays (Connelly et al., 2015; De Paula & Fonseca, 2004; Linnes et al., 2014; Rodriguez et al., 2015), the proposed fully integrated biosensor does not rely on large equipment (*e.g.,* thermal cycler, electric heater, incubator or water bath) for the amplification process, which demonstrates its potential use in remote settings. Most importantly, by using the prototype, the colorimetric signal can be easily detected by the naked eye without the need for an extra device (*e.g.*, UV lamp), which is deliverable to the end-users, highlighting its advantages over the existing fluorescent detection paper-based biosensors (Connelly et al., 2015; Dos Santos et al., 2010; Song et al., 2013a).

In addition, by performing the LAMP, the prototype permits highly sensitive and specific target detection as compared to other amplification techniques (Fernández-Soto et al., 2014; Minnucci et al., 2012). The high sensitivity of the proposed biosensor is demonstrated by its ability to achieve the detection limit of as low as 10 CFU/mL in *E. coli* detection, which is comparable or even more sensitive than the recently reported nucleic acid-based LFAs (~10^2-10^4 CFU/mL) (Pöhlmann et al., 2014; Terao et al., 2015). Even though a few studies have reported the ability of ultrasensitive detection of *E. coli* in LFAs (~5-10 CFU/mL), sophisticated off-chip extraction and amplification is required prior to lateral flow detection, hence restricting their use for POC testing (Wu et al., 2015). The current prototype could be used to detect various target nucleic acids, holding great potential for various POC applications in the near future.

5.5 Conclusion

In short, an integrated paper-based biosensor was proposed, which could perform simple nucleic acid extraction, amplification and detection in about 1 hr. The proposed prototype produces a simple colorimetric signal detectable by the naked eyes, eradicating the need for an extra UV source for assay readout. A handheld heating device is coupled with this biosensor, which eliminates the requirement for large heating systems (*e.g.,* thermal cycler, electric heater, incubator or water bath), making it more suitable for use in remote settings. Even though the integrated biosensor has ability to detect spiked *E.coli*, evaluation of its ability to detect clinical blood sample is essential for future clinical assessment. Furthermore, the concentration of target analyte in clinical blood sample is normally low, necessitating the sensitivity enhancement of LFA. Therefore, further test should include incorporating simple sensitivity enhancement method into LFA for highly sensitive clinical sample testing.

CHAPTER 6: POLYDIMETHYLSILOXANE-PAPER HYBRID LATERAL FLOW ASSAY FOR HIGHLY SENSITIVE SAMPLE-TO-ANSWER NUCLEIC ACID TESTING

6.1 Introduction

In recent studies, AuNP-based LFAs have been demonstrated as a potential diagnostic tool for NAT with simple visual detection, which offers great capability of rapid diagnosis at the POC (Yoshida et al., 2009). However, the poor sensitivity of AuNP-based LFAs limits its widespread application (Choi et al., 2016a). To this end, significant efforts have been made to improve their sensitivity using various approaches such as enzyme-based signal enhancement (He et al., 2011), probe-based signal enhancement (Hu et al., 2013), sample concentration (Chiu et al., 2014; Moghadam et al., 2015) and thermal contrast (Qin et al., 2012). However, these techniques require either special design of DNA sequences (Hu et al., 2013), external electrical power sources (Moghadam et al., 2015; Qin et al., 2012), or multiple operation steps (Chiu et al., 2014; Houseley & Tollervey, 2009), limiting their use for POC testing. In contrast, fluidic control in LFA could significantly improve the sensitivity of the assay with simple strip fabrication and operation steps, which have currently attracted significant research interest (Parolo et al., 2013; Rivas et al., 2014).

Several studies have reported various methods of controlling fluid flow and reagent transport in LFA by creating wax barriers (Rivas et al., 2014; Tai et al., 2005) or alteration of the geometry of the paper network (Parolo et al., 2013). Despite their potential of improving the analytical sensitivity of an assay through fluidic delays, most of these methods are less suitable to be integrated into LFAs with sample-in-answer-out capabilities (*i.e.,* integrated extraction, amplification and colorimetric detection) due to

several reasons. Importantly, to develop a miniaturized sample-to-answer lateral flow strip for rapid NAT which involves the aforementioned three main steps, a heat-dependent amplification process is normally required prior to detection. In this context, a wax barrier on the strip may melt during the heating process (Xu et al., 2014), hence affecting the fluidic control strategy. On the other hand, increasing the fluidic path length or width or sample pad modification as suggested by the existing study (Parolo et al., 2013) makes the total size of the strip larger, and consumes a higher volume of reagent and sample, which undermines the unique advantages of POC use. In addition, the irregular size of such a biosensor makes the manufacturing process more complicated. Therefore, to meet the increasing need for portable, rapid, robust, inexpensive, easily performable and importantly, highly sensitive NAT for POC testing, integrating a simple fluidic control strategy into a sample-to-answer biosensor without involving incompatible chemical is highly desirable.

In the present study, a novel strategy of incorporating a paper-based shunt and a PDMS barrier into the strip was demonstrated. PDMS was selected, because it is inexpensive, inert, non-toxic and (unlike wax suggested by the existing studies (Rivas et al., 2014; Tai et al., 2005)) heat-resistant (Choi et al., 2012), complementing the heating process normally required for sample-to-answer NAT. The shunt or PDMS barrier alone were integrated into the lateral flow strip for signal enhancement. Since creating a PDMS barrier alone would not sufficiently enhance the signal and implementing a larger shunt alone would be sample-consuming, both an optimum size of shunt and an optimum amount of PDMS droplets were further combined with LFA to achieve an optimum fluidic delay for analytical sensitivity enhancement without consuming a large volume of sample. The phenomena of fluidic delays were further evaluated by mathematical simulation. The developed LFA would offer great promise to sensitively

detect various targets for a wide range of applications including biomedical diagnosis, food safety control and environmental monitoring.

6.2 Materials and methods

6.2.1 Preparation of lateral flow strip implemented with shunt, PDMS droplets and the combination of both

All DNA sequences used in the study were obtained from the Sangon Biotechnology Co., Ltd. (Shanghai, China) (**Table 6.1**). To demonstrate the potential of implementing a shunt into LFA for fluidic delay to enhance the assay sensitivity, test strips with different lengths of shunt (0.5, 0.75, 1, 1.25 and 1.5cm) were prepared (**Fig. 6.1A**). The width of shunt was maintained the same as that of the test strip to keep the fabrication process simple. The shunt was placed between the conjugate pad (glass fiber) and the nitrocellulose membrane, with a 0.5 cm × 0.25 cm overlapping region between the two conjugate pads, and also between the conjugate pad and the shunt. The surface area of the overlapping region between the conjugate pad and the nitrocellulose membrane was 0.1 cm × 0.25 cm in unmodified lateral flow strip, which was similar to that between the nitrocellulose membrane and the absorbent pad of all test strips.

Table 6.1: DNA sequences used in the study

Name	Sequence (5'-3')
HBV detector probe	5'- atgaatctggccacctgggt -$(CH_2)_6$-SH-3'
HBV control probe	5'- acccaggtggccagattcat/Biotin-3'
HBV F3	5'- cttctgtggagttactctctt-3'
HBV B3	5'- gctgactactaattccctgg-3'
HBV FIP	5'-Biotin/ctcccgatacagagcagaggtttgccttctgacttctttcc-3'
HBV BIP	5'- ttgttcacctcaccatacagcatgggtcttccaaattacttcc-3'
HBV FLP	5'- ggtgtcgaggagatctcgaata-3'
HBV BLP	5'- attctgtgttggggtgagtt-3'
HBV target DNA	5'- acccaggtggccagattcat -3'

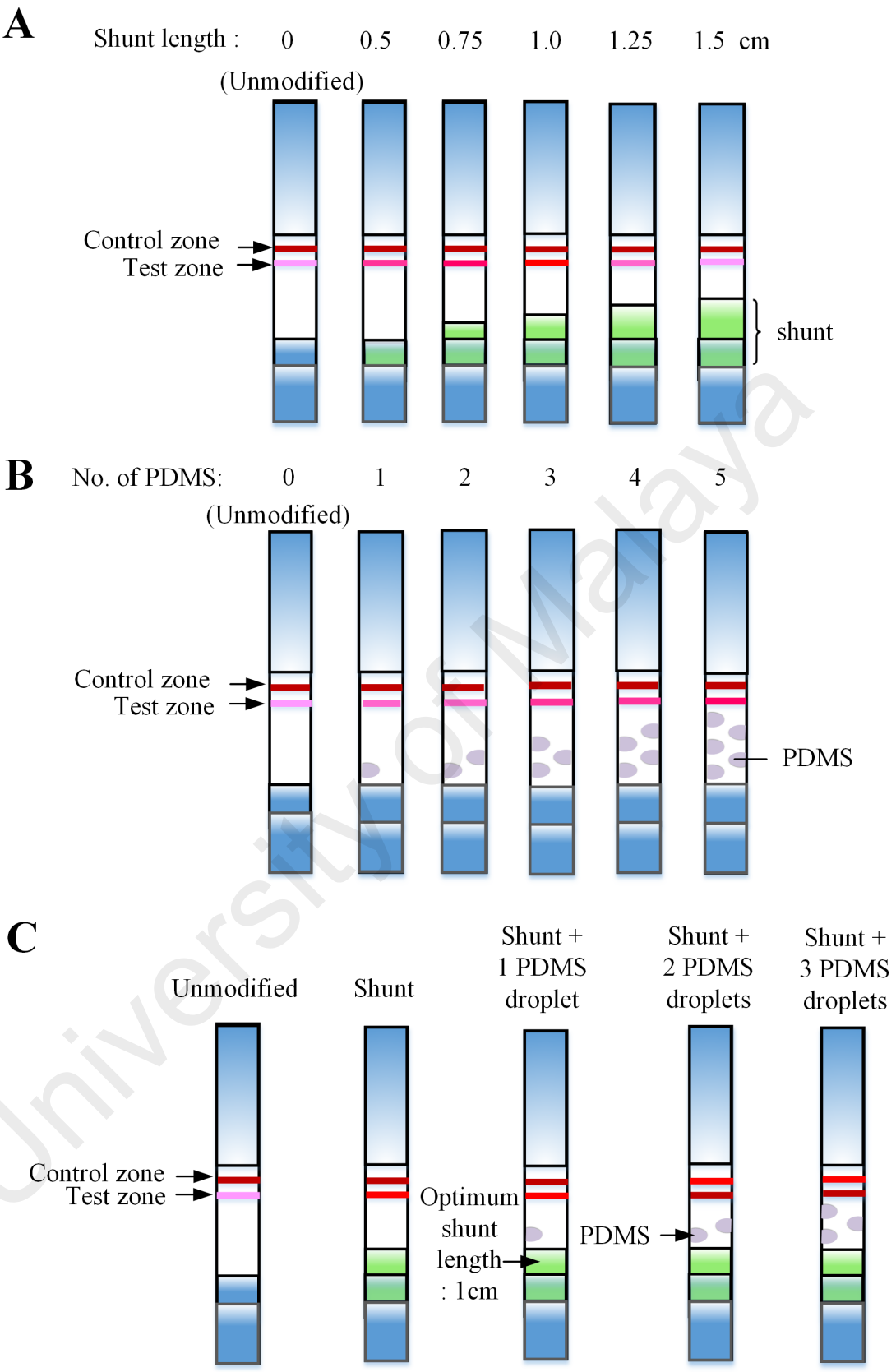

Figure 6.1: A schematic of modified lateral flow strip. Lateral flow strip with (A) a glass fiber shunt, (B) a PDMS barrier or (C) combination of both for detection sensitivity enhancement.

To evaluate the possibility of incorporating PDMS droplets into LFA for sensitivity improvement, different number of PDMS droplets (one, two, three, four and five droplets) was added onto the nitrocellulose membrane (**Fig. 6.1B**). The volume of each PDMS droplet was 0.1 μL and the distance between each droplet was maintained at 2 mm. Following the dispension of the droplets onto the nitrocellulose membrane, the test strips were dried in an oven at 37 °C for about 1 hour. Thereafter, to further improve the sensitivity of LFA with optimum fluidic control, both shunt and PDMS droplets were incorporated into the lateral flow strip (**Fig. 6.1C**). The optimum length of shunt was combined with 1, 2 or a maximum of 3 droplets of PDMS to achieve optimum sensitivity of the assay. LFA was performed based on the method described in **Section 3.2.4**.

6.2.2 Mathematical simulation

To mathematically simulate the phenomena of liquid flow in LFA, a 3D physical model for a steady-state flow in a fluid-saturated strip (as heterogeneous porous medium) was presented in this study. The flow can be described by the Brinkman equation for the porous regions, in which the viscosity effect is taken into consideration:

$$\nabla p = -\frac{\mu}{K}\vec{V} + \mu_e \nabla^2 \vec{V} \qquad (6.1)$$

where $\vec{V}$, p, μ, μ_e and K are fluid velocity, pressure, fluid viscosity, effective viscosity for Brinkman term and permeability of porous medium, respectively. The fluid viscosity (μ) is approximate to that of the water at 20 °C. The effective viscosity (μ_e) is assumed to correspond to the fluid viscosity (μ) in thin porous layers (Liu et al., 2007). The permeability K for different type of porous materials was evaluated by the selected empirical equations. For random overlapping fiber porous materials, such as

the glass fiber and the absorbent pad in LFA, the empirical equation of the permeability K is given as follows (Liu et al., 2015):

$$K=r^2\frac{\pi\varepsilon\left(1-\sqrt{1-\varepsilon}\right)^2}{24\left(1-\varepsilon\right)^{1.5}} \qquad (6.2)$$

where ε is material porosity and r is average fiber radius in fiber porous material. As for the granular porous material, in this case, nitrocellulose membrane, permeability K was obtained through Kozeny-Carman equation (Brooks & Purcell, 1952):

$$K=\frac{d^2\varepsilon^3}{180\left(1-\varepsilon\right)^2} \qquad (6.3)$$

where d is average pore diameter. The porosity ε was obtained by empirical method through measuring the volume of liquid absorbed by the materials (Zaytseva et al., 2004). Both the average fiber radius r and average pore diameter d were obtained from the scanning electron microscopy (SEM) figures of the material.

The boundary conditions are summarized as follows: The inlet velocity of LFA was calculated with the known sample volume (100 μL), the inlet cross-section and the period required for fluid absorption. The pressure at the outlet is equal to the atmospheric pressure. All other bounding walls are under non-slip conditions. The mathematical simulation was done using the Brinkman equation module of Comsol Multiphysics 5.0 software.

6.2.3 Clinical sample testing

To prove the potential of integrating the optimum fluidic control strategy into the prototype fully integrated paper-based sample-to-answer biosensor previously describe in **Section 5.2.2** for sensitive sample-to-answer target detection, the prototype was tested with HBV blood clinical sample according to the published protocol (Zaytseva et al., 2005). The fabrication and operation processes were previously described in **Section**

5.2.2 and **Section 5.2.3**, respectively. With prior informed written consent, the human blood samples from 16 HBV patients were obtained from the First Affiliated Hospital of Xi'an Jiaotong University. The study was approved by the Institute Research Ethics Committee of The First Affiliated Hospital. The positive blood samples were confirmed by conventional DNA analysis, involving tube-based extraction using Purelink Genomic DNA Mini Kits (Invitrogen), followed by quantitative-real time PCR (qPCR) (**Table 6.2**). Tube-based LAMP and electrophoresis were also performed according to the manufacturer's instruction. To further confirm the specificity of the assay using the prototype, two clinically confirmed HCV-positive samples, two Cytomegalovirus-positive samples and three blood samples from healthy donors were also tested with the modified sample-to-answer biosensor.

Table 6.2: HBV-positive clinical samples confirmed by qPCR

Sample	Concentration (IU/mL)
a	3.18×10^5
b	7.33×10^6
c	1.96×10^5
d	1.34×10^2
e	3.07×10^3
f	1.56×10^2
g	2.72×10^4
h	1.92×10^7
i	2.92×10^4
j	5.35×10^8
k	3.42×10^8
l	2.04×10^2
m	2.64×10^3
n	7.07×10^6
o	2.72×10^4
p	1.59×10^2

6.2.4 Statistical analysis

One-Way ANOVA with a Tukey post-hoc test was used to compare the data among different groups in all assays. Data were expressed as mean ± standard error of the mean of three independent experiments (n=3). $p<0.05$ was reported as statistically significant.

6.3 Results

6.3.1 Sensitivity enhancement by incorporating a glass fiber shunt

In fact, the flow rate in paper is significantly dependent on the physical characteristics of paper (*e.g.,* pore size). Therefore, selection of an appropriate material for shunt is essential for effective fluidic control. For this, different type of pads including cellulose (GF-08), glass fiber Fusion 5 (Whatman, Inc., Florham Park, NJ) and borosilicate glass fiber (Pall 8964) were compared in terms of the final analytical sensitivity. It was found that Fusion 5 with an average pore size of 10 μm showed a significantly lower analytical sensitivity with a higher sample wicking rate, as indicated by 6.5 ± 0.18 min required to reach the test zone as compared to that of cellulose (10.5 ± 0.2 min) and glass fiber Pall 8964 (8.4 ± 0.1 min), resulting in a shorter interaction time between the target and AuNP-DP and hence lowering the assay sensitivity **(Fig. 6.2)**.

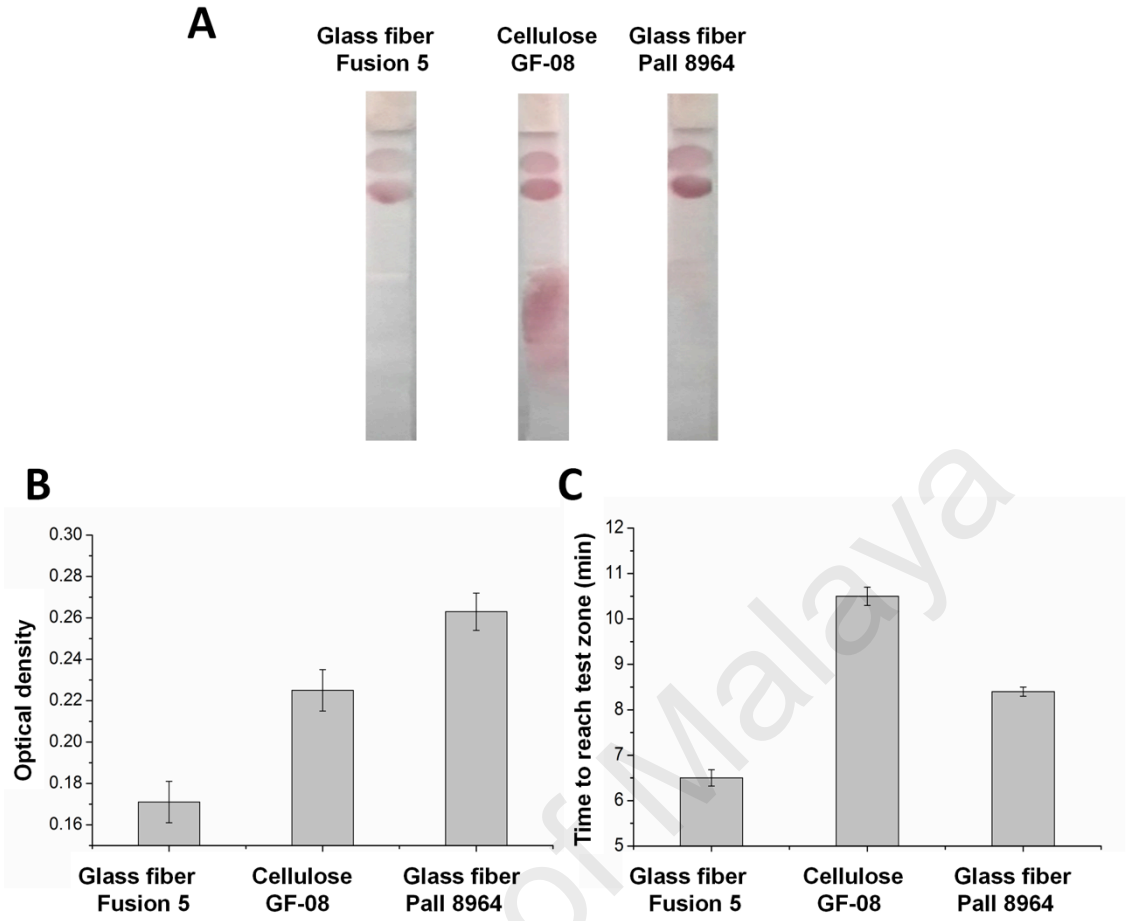

Figure 6.2: Selection of an appropriate shunt material. (A-B) Glass fiber Pall 8964 showed a significant higher optical density of the test zone (0.225 ± 0.01) with (C) desirable sample wicking duration required to reach the test zone as compared to that of Fusion 5 and Cellulose.

Cellulose with a smaller pore size (0.5 μm) showed a significant fluidic delay as compared to fusion 5 and glass fiber Pall 8964. This significant fluidic delay might cause a failure of the considerable amount of AuNP-DP-target to completely wick through the nitrocellulose membrane, resulting in the presence of the residual AuNP-DP or AuNP-DP-target (in red) on the glass fiber. The low amount of AuNP-DP captured by the streptavidin at the test zone results in a significantly lower signal produced in LFA. Unlike cellulose, the glass fiber Pall 8964 with confined pore size (~ 8 μm) enables all fluid to wick through the shunt and nitrocellulose membrane for target capturing. By reducing the fluid wicking rate, the glass fiber Pall 8964 allows the AuNP-DP and target to have sufficient reaction time before being captured by the

streptavidin, hence resulting in a significantly higher (p<0.05) optical density of the test zone (0.263 ± 0.009) as compared to that of fusion 5 (0.171 ± 0.01) and cellulose (0.225 ± 0.01). Therefore, glass fiber Pall 8964 was selected as a material of choice for shunt.

To induce a desirable time delay, which is the duration required for the fluid front to reach the test zone as compared to the unmodified LFA and enhance the sensitivity of LFA, different lengths of shunts (0.5, 0.75, 1, 1.25, 1.5 cm) with the same width to that of lateral flow strip (0.25 cm) were compared. The surface area of overlapping region between the sample pad and conjugate pad, and that between the conjugate pad and the shunt were remained the same (0.5 cm × 0.25 cm). The width of shunt was maintained the same as that of the strip to keep the fabrication process simple.

It was found that the sensitivity of the assay increased with increasing length of shunt as indicated by a more clearly visible test zone, a higher optical density of test zone and a significantly lower (p<0.05) detection limit of LFA. For instance, the detection limit for 1 cm-length shunt was 10 pM target DNA, which represents about 5-fold signal enhancement over unmodified LFA (50 pM) **(Fig. 6.3)**.

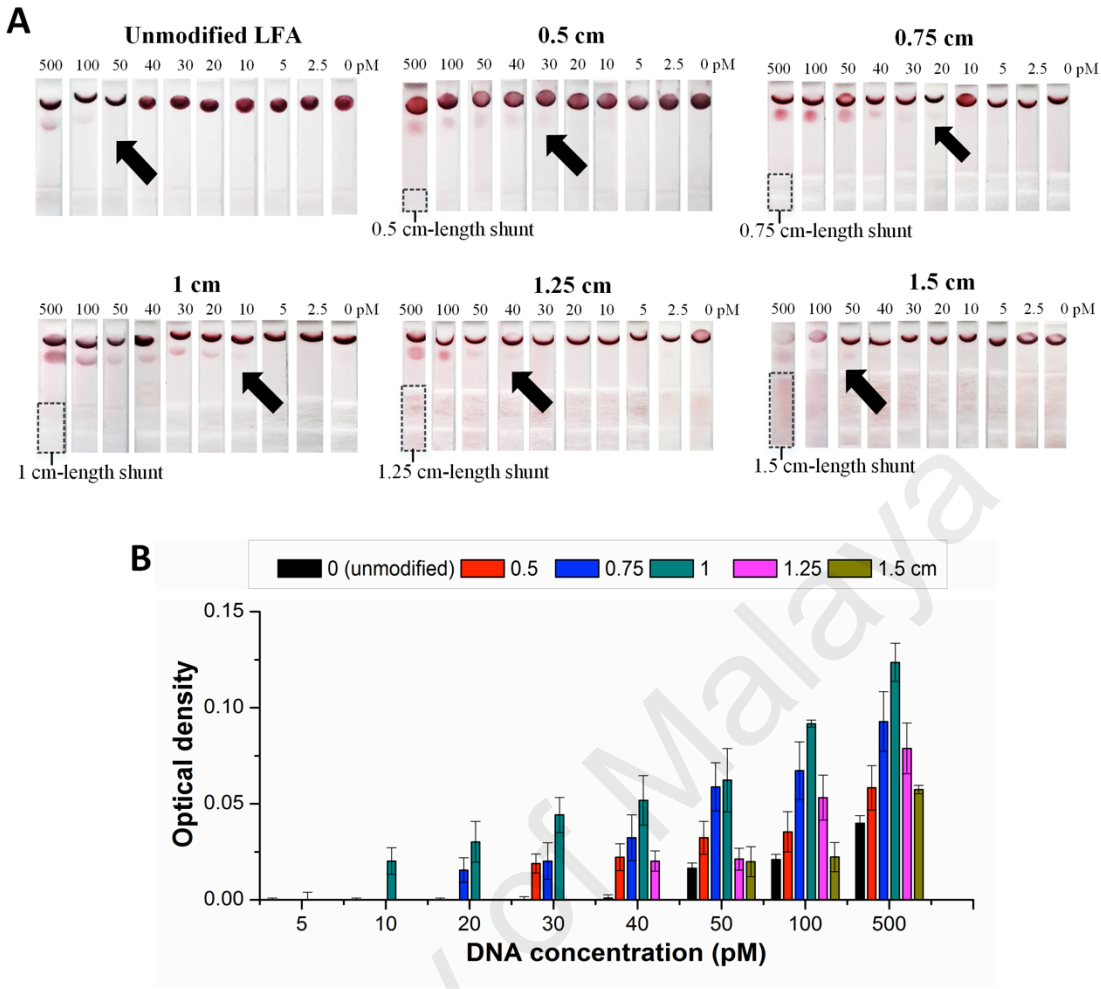

Figure 6.3: Sensitivity enhancement of LFA by implementation of glass fiber shunt. The shunt with the length of 1 cm achieved the highest sensitivity with a detection limit of as low as 10 pM, representing 5-fold signal enhancement over unmodified LFA as indicated by the observable colour intensity of the test zone (A) and optical density of the test zone after analysis (B).

This is basically due to a more desirable time delay produced by the shunts with 1 cm length, as evidenced by 156 ± 3.36 sec fluidic delays produced from the shunt region to the test zone as compared to that of the unmodified strip, resulting in an increased interaction rate between the AuNP-DP and target DNA **(Fig. 6.4)**.

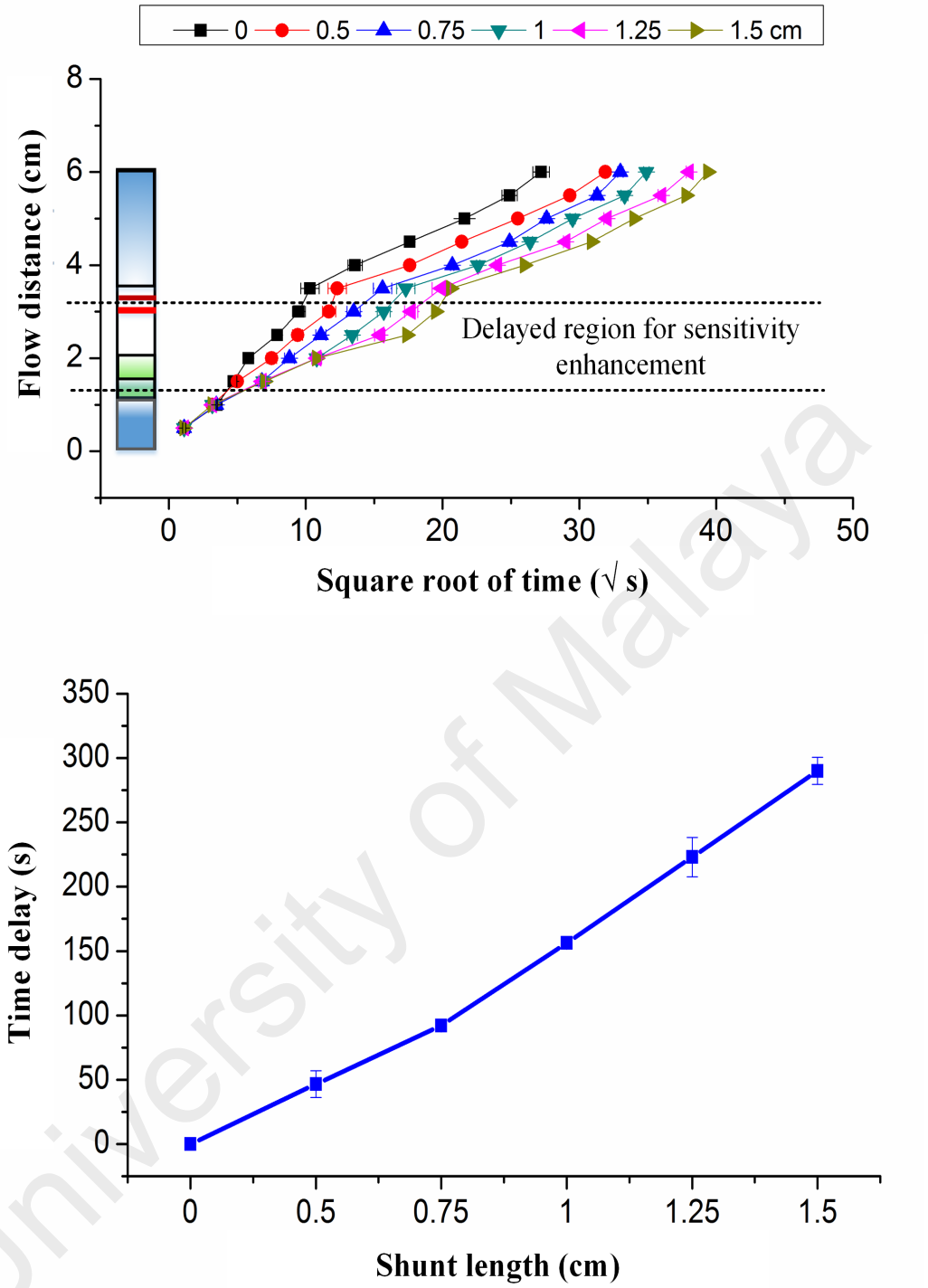

Figure 6.4: Fluidic delay in LFA with different length of shunt. The desirable fluidic delay (156.3 ± 3.36 sec) achieved by using 1 cm-length shunt allows optimum interaction of biomolecules, which leads to a significant enhancement in sensitivity of LFA.

Theoretically, in the presence of shunt, a significant amount of the fluid from the nitrocellulose membrane is diverted into the shunt, resulting in a reduced flow rate in the nitrocellulose membrane. In the absence of the shunt, the distance moved by the fluid front (*L*) is described by Washburn's equation (Toley et al., 2013), where *L* is directly proportional to the square root of time ($t^{½}$). It was noted that after reaching the shunt, the absorption of fluid by the shunt reduces the fluid front in the nitrocellulose membrane, as indicated by an increased $t^{½}$ **(Fig. 6.4)**.

However, as previously mentioned, shunts with a length longer than 1 cm (1.25 cm and 1.5 cm) showed a lower optical density of test zone, and a lower analytical sensitivity (40 and 50 pM, respectively) **(Fig. 6.3)**. This might be due to the higher water absorption capacity (54 μL/cm^2), which results in a failure of the fluid to completely wick through the strip. As a result, a significant amount of AuNP-DP and AuNP-DP-target remain along the glass fiber and nitrocellulose membrane, leading to a significant background signal as compared to the unmodified LFA and shorter-shunt LFA (< 1 cm shunt length).

The phenomena of a shunt-induced reduction of fluid velocity were also evaluated using mathematical simulations. For each group, the average velocity at the test zone was calculated. The velocities were calculated to be 0.354, 0.289, 0.272, 0.247, 0.218 and 0.208 mm/s for unmodified, the shunt with a length of 0.5, 0.75, 1.0, 1.25 and 1.5 cm, respectively (**Fig. 6.5)**.

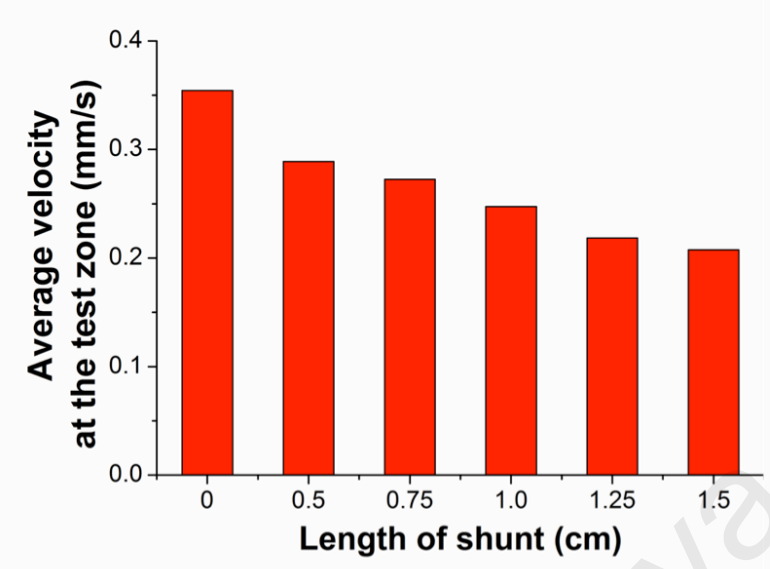

Figure 6.5: The average velocity at the test zone with different length of shunt. The longer the length of the shunt, the lower the average velocity at the test zone.

As shown in **Fig. 6.6A,** the red lines in the shunt indicate the movement of fluid throughout the shunt. This further supports the experimental data, which reveals that the longer the shunt, the larger the space for biomolecule reaction. Additionally, the longer shunt promotes the flow resistance, which results in the reduction of fluid velocity **(Fig. 6.6B**) and thus affects the detection sensitivity.

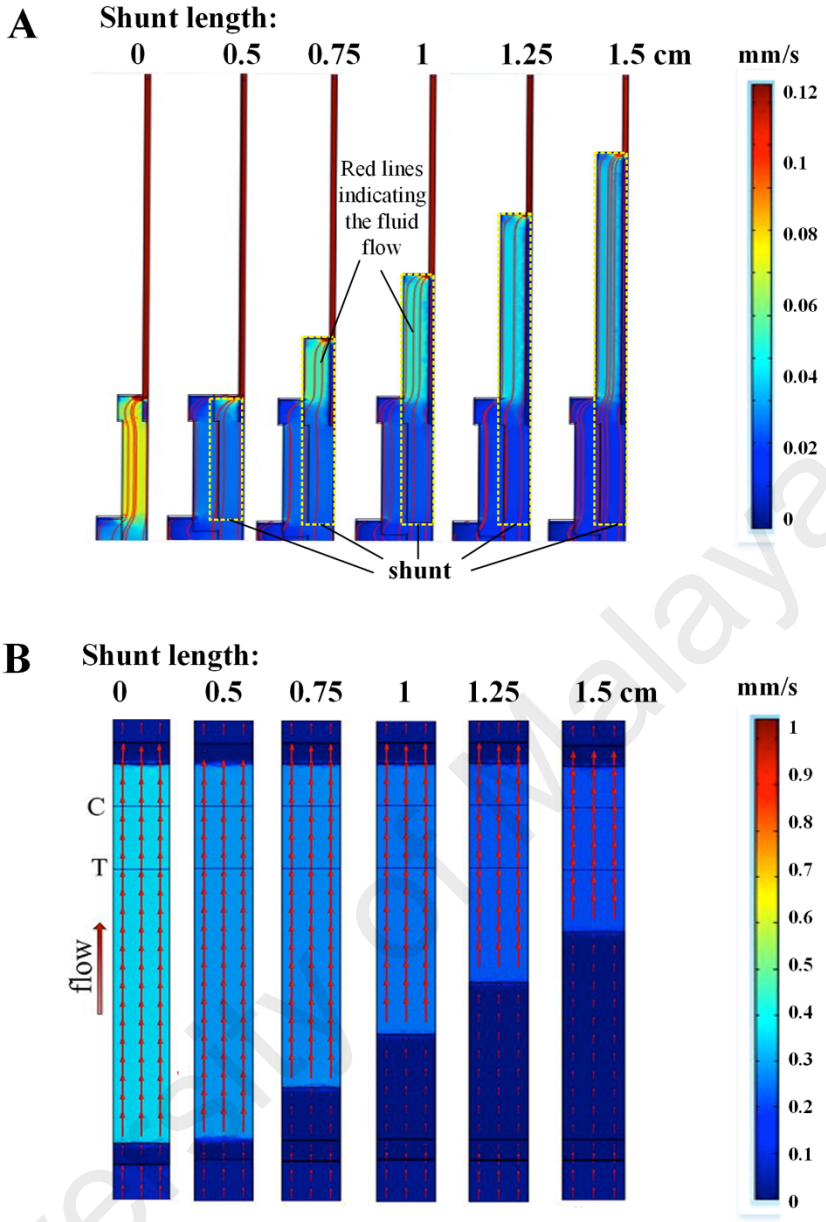

Figure 6.6: Flow velocity simulation of the test strip with a shunt. The flow velocity was mathematically simulated, indicating that the longer the shunt, the slower the wicking rate of fluid (A-B).

6.3.2 Sensitivity enhancement by creating PDMS barrier

As 5-fold signal enhancement induced by the glass-fiber shunt might not be sufficient for most medical diagnostic, it was suggested that adding a hydrophobic barrier (*i.e.,* PDMS barrier) for further sensitivity enhancement. To prove the potential of the PDMS barrier to control the fluid flow in LFA, the LFA was performed by creating a different number of PDMS droplets on the strip without implementing the shunt.

In fact, applying the PDMS onto the nitrocellulose membrane allows the penetration of PDMS into the membrane and creates the hydrophobic zone. To confirm if the PDMS truly acts as a barrier across the nitrocellulose membrane, characterization was performed. SEM reveals the penetration of PDMS droplets into the nitrocellulose membrane, which creates a barrier to obstruct the fluid flow **(Fig. 6.7)**.

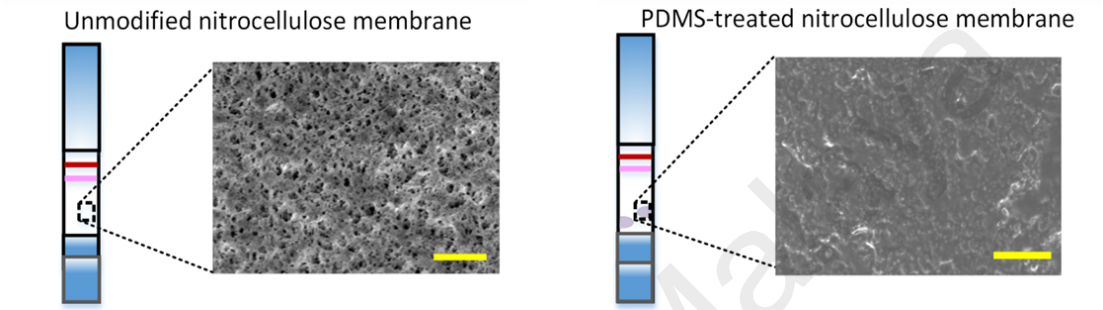

Figure 6.7: Characterization of PDMS-paper hybrid LFA using SEM. The SEM images of unmodified nitrocellulose membrane and PDMS treated nitrocellulose membrane (Scale bars, 50 μm), where the modified showed the penetration of PDMS into the nitrocellulose membrane, creating a barrier in lateral flow strip.

To determine the effect of the number of PDMS droplets on the sensitivity of LFA, one, two, three, four or five drops of PDMS with the volume of 0.1 μL respectively were dropped onto the nitrocellulose membrane of different group. Five drops of PDMS is maximal due to the limited space available on the nitrocellulose membrane. It was found that increasing PDMS droplets slightly increases the sensitivity of LFA, as indicated by the detection limit of as low as 40, 40, 30, 30 and 20 pM target achieved by one, two, three, four and five PDMS droplets, respectively **(Fig. 6.8)**. About 2.5-fold signal enhancement was observed in the strip with 5 PDMS droplets over unmodified LFA.

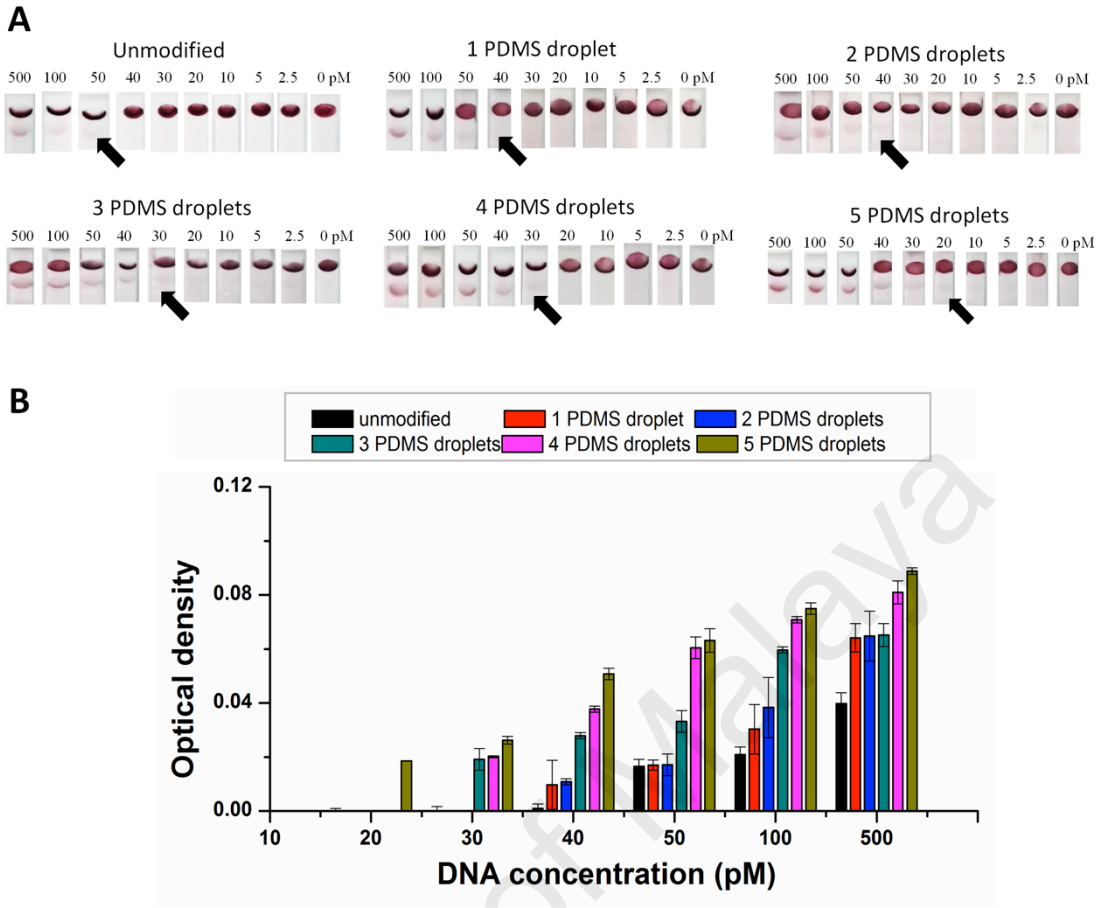

Figure 6.8: Sensitivity enhancement of LFA by creating PDMS barrier. The higher the number of PDMS droplets, the lower the detection limit achieved as indicated by the detection limit of as low as 20 pM achieved with 5 PDMS droplets, through the observation of colour intensity of the test zone (A) and optical density of the test zone after analysis (B).

It was suggested that the sensitivity enhancement might also be associated with the increased biomolecule interaction rate as induced by the fluidic delays, as indicated by the more significant time delay produced by a higher number of PDMS droplets. The time delays were determined by the duration of fluid flow from the region of the first PDMS droplet (from the bottom of the strip) to the test zone, showing 97.2 ± 0.4 sec delay produced with 5 PDMS droplets over 6.84 ± 4.7 sec, 25.8 ± 3.8 sec, 43.8 ± 2.36 sec, 97.2 ± 8.58 sec produced with one, two, three and four droplets, respectively **(Fig. 6.9)**.

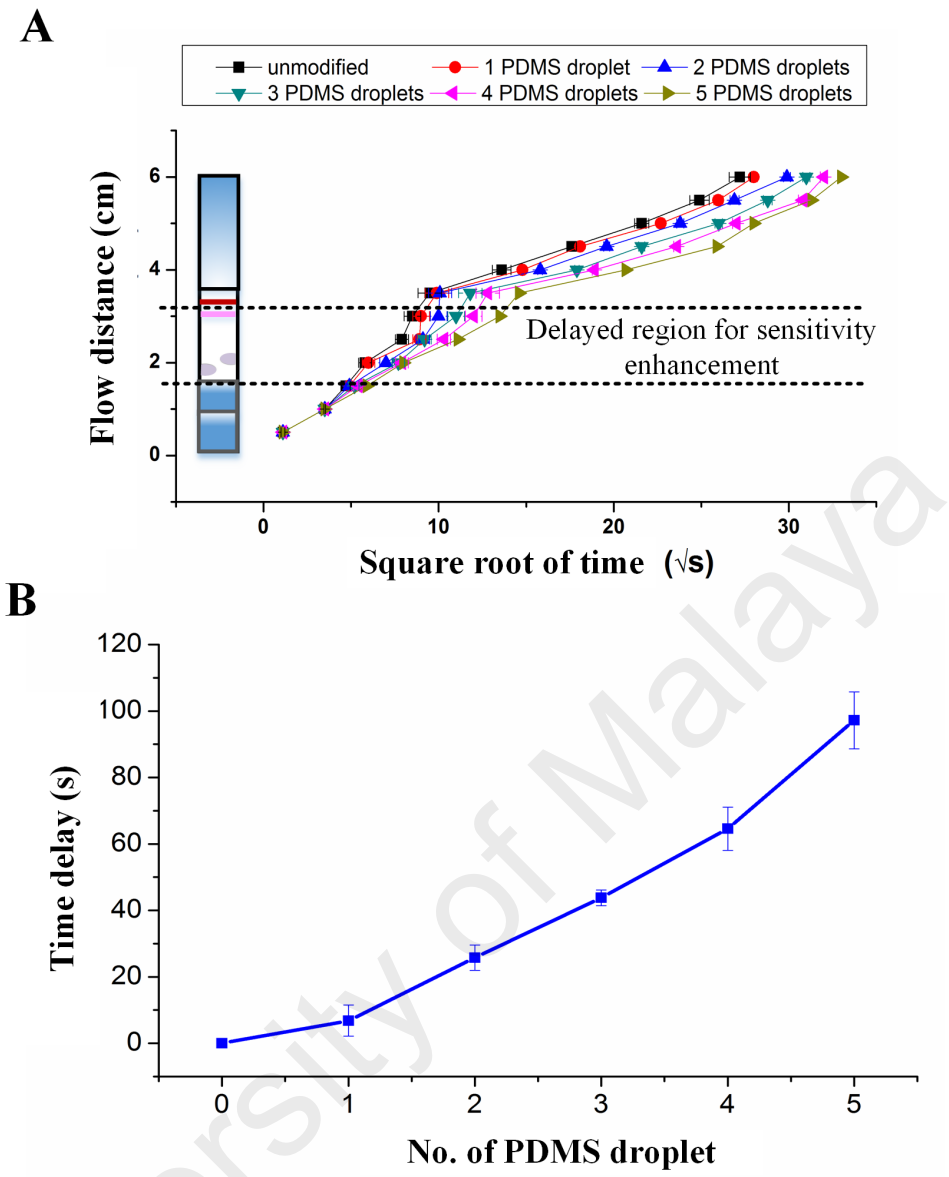

Figure 6.9: Fluidic delay in LFA with different number of PDMS droplets. The significant fluidic delay was shown with a higher number of PDMS droplets, resulting in a significant improvement in sensitivity of LFA.

The phenomena of PDMS-induced reduction of fluid velocity were also evaluated using mathematical simulations **(Fig. 6.10)**.

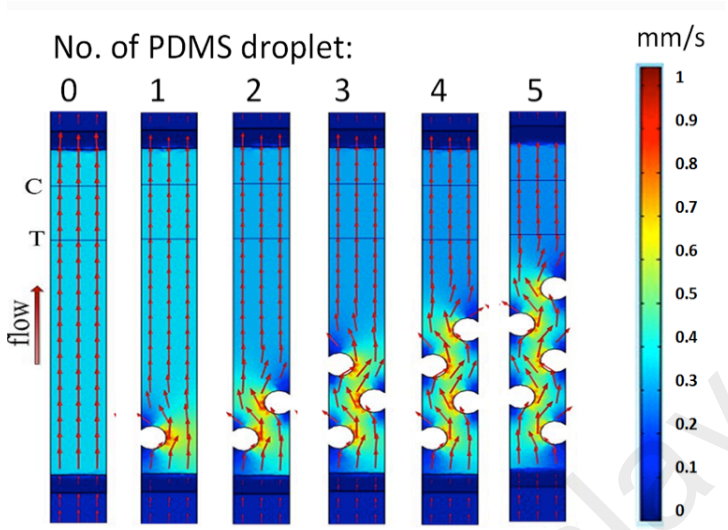

Figure 6.10: Flow velocity simulation of the test strip with PDMS barrier. The flow velocity was mathematically simulated, indicating that the higher the number of PDMS droplets, the lower the wicking rate of fluid.

The velocities at the test zone were calculated to be 0.354, 0.352, 0.325, 0.296, 0.289 and 0.279 mm/s for unmodified, 1 PDMS droplet, 2 PDMS droplets, 3 PDMS droplets, 4 PDMS droplets and 5 PDMS droplets, respectively **(Fig 6.11)**, indicating that the higher the number of PDMS droplet, the lower the flow velocity, which is in accordance with the experimental data.

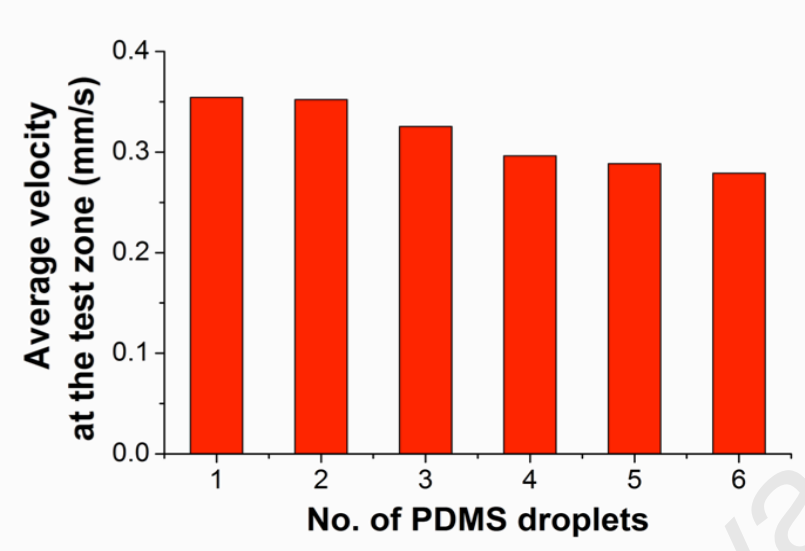

Figure 6.11: The average velocity at the test zone with different number of PDMS droplets. The higher the number of PDMS droplets, the lower the average velocity at the test zone.

It was observed that the PDMS barrier obstructs the fluid flow leading to the different flow magnitude and direction, as indicated by the red arrows shown in **Figure 6.10**. The present results suggest that the higher the number of PDMS droplets, the longer the nitrocellulose membrane involved in tortuosity. This effect promotes fluid mixing, which could enhance the biomolecule interaction and hence improve the sensitivity of LFA.

6.3.3 Sensitivity enhancement by a combination of glass fiber shunt and PDMS barrier

To demonstrate the potential of combining both shunt and PDMS barrier in LFA for enhancing sensitivity with optimum fluidic control, the number of PDMS droplets required to be combined with the optimum 1cm-length of shunt that would not significantly consuming large volume of reagent or sample was determined**.** One, two or a maximum of three PDMS droplets (due to the limited space available to create PDMS barrier in the presence of shunt) were dropped onto the lateral flow strip. It was found

that the detection limits of LFAs were 10 pM, 5 pM and 5 pM target with one, two and three PDMS droplets, respectively **(Fig. 6.12)**.

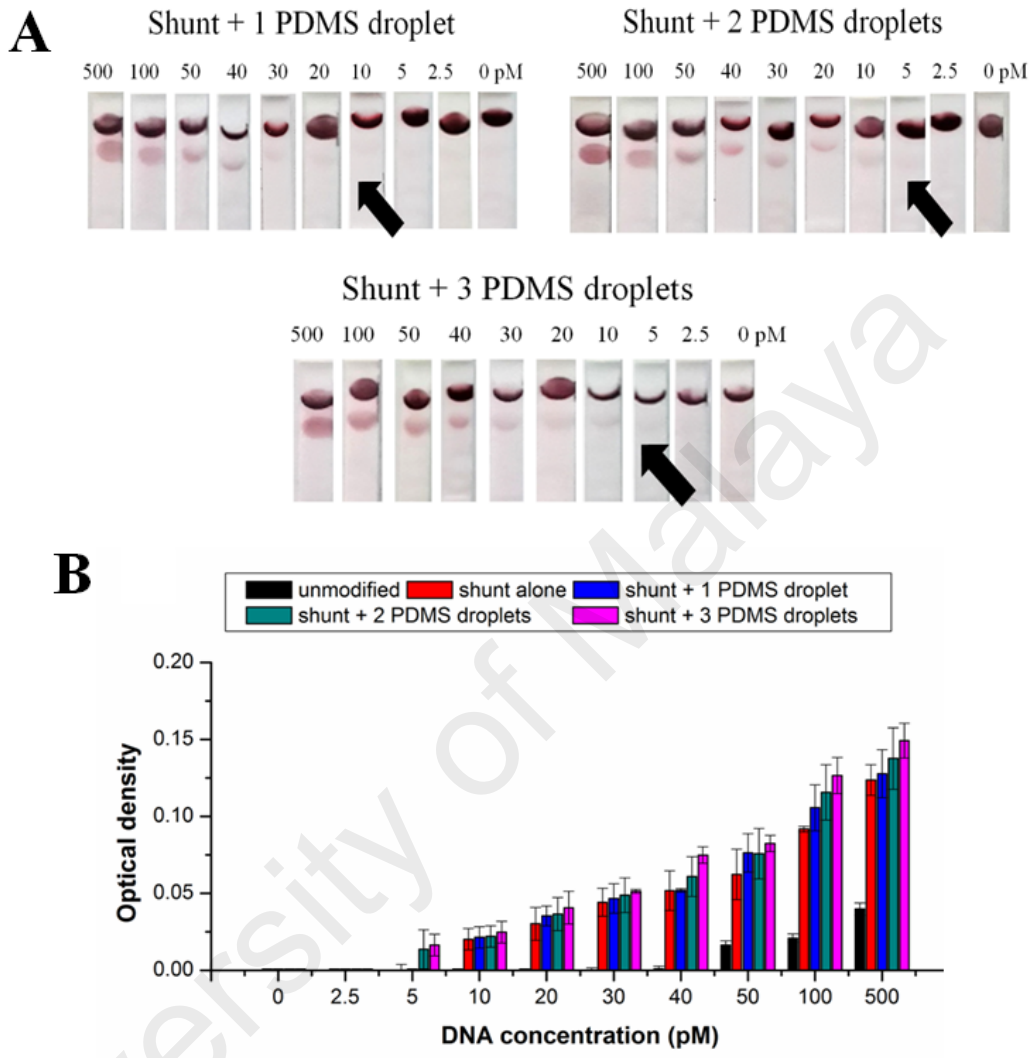

Figure 6.12: Sensitivity enhancement of LFA by incorporating both shunt and PDMS barrier. The optimum of two PDMS droplets in combination with a piece of 1cm × 2.5 cm shunt achieved a higher sensitivity as indicated by the detection limit as low as 5 pM, representing 10-fold signal enhancement over unmodified LFA, as indicated by the observable colour intensity of the test zone (A) and optical density of the test zone after analysis (B).

A shunt and two PDMS droplets could achieve a 10-fold signal enhancement over unmodified LFA, which is again associated with the optimum biomolecule interactions as previously discussed. In contrast, three drops of PDMS creates fluidic delays of 255.8 ± 6.5 sec **(Fig. 6.13)**, where there is no significant difference from two drops of PDMS in terms of time delay, thus producing the same detection limit of 5 pM.

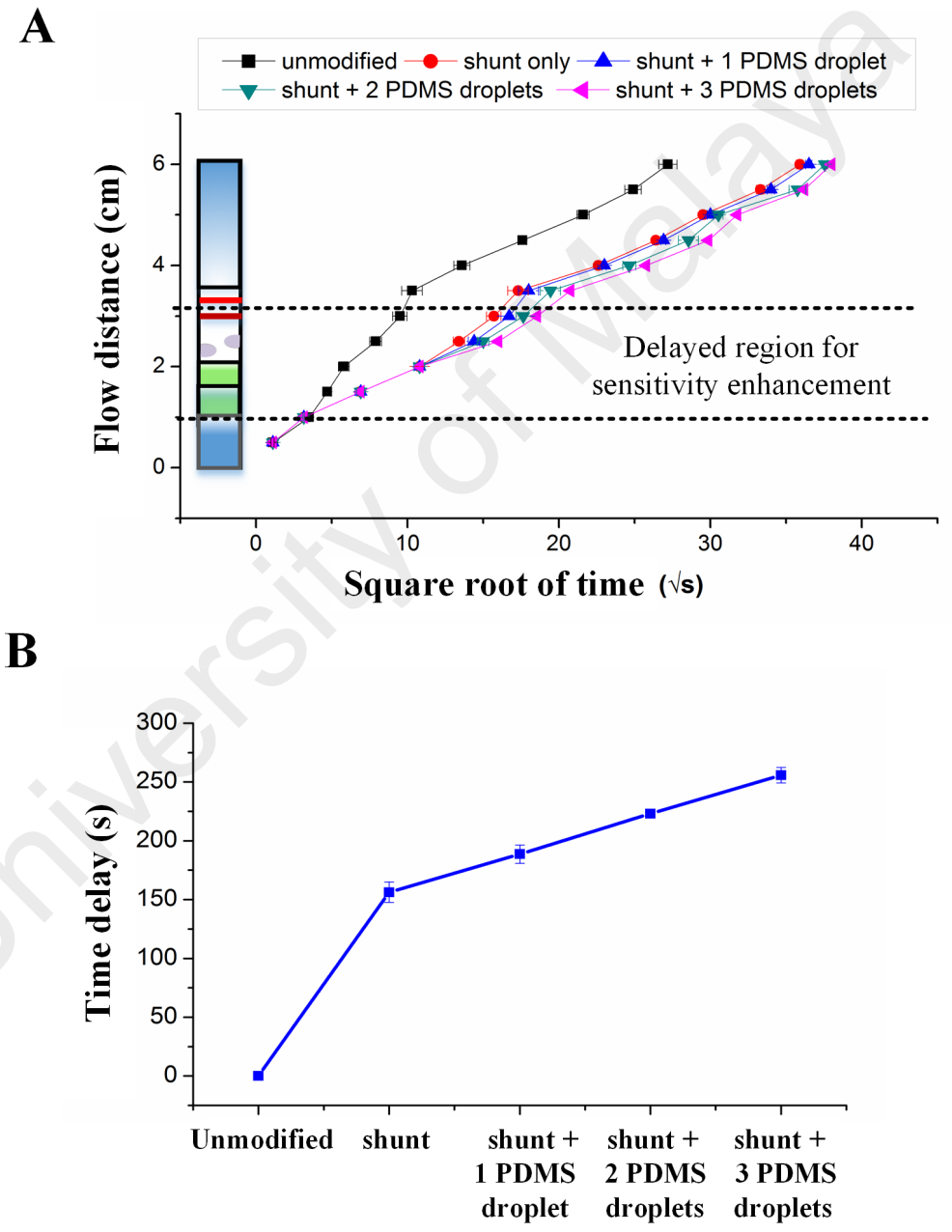

Figure 6.13: Fluidic delay in LFA coupled with a shunt and PDMS droplets. The optimum fluidic delay achieved by the combination of one shunt and two PDMS droplets.

The phenomena of fluid velocity control by these techniques were also further confirmed using mathematical simulations **(Fig. 6.14)**.

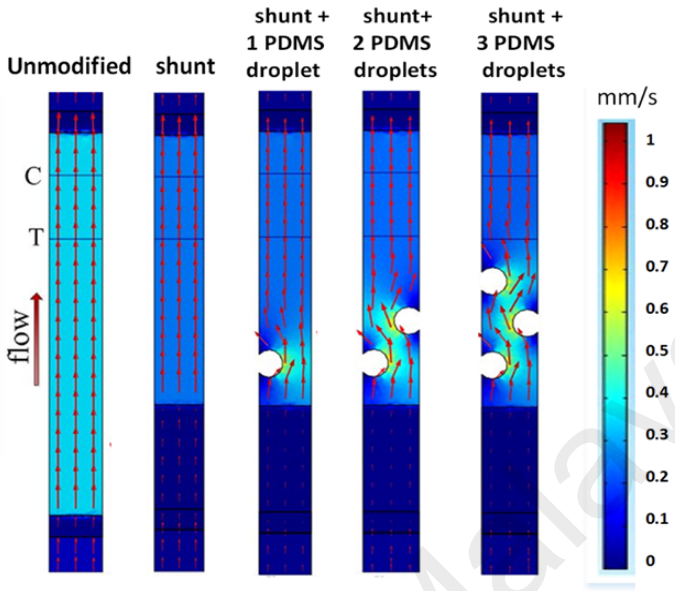

Figure 6.14: Flow velocity simulation of the test strip coupled with a shunt and PDMS barrier. The flow velocity was mathematically simulated, indicating that with a 1cm-length shunt, the higher the number of PDMS droplets, the lower the wicking rate of fluid.

The velocities at the test zone were 0.354, 0.242, 0.228 and 0.221 mm/s for unmodified, combination of shunt with 1 PDMS droplet, combination of shunt with 2 PDMS droplets and combination of shunt with 3 PDMS droplets, respectively **(Fig. 6.15)**.

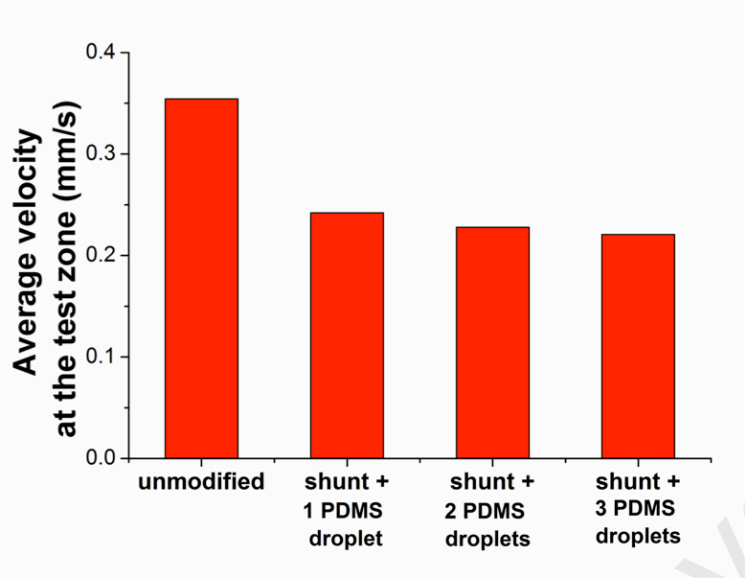

Figure 6.15: The average velocity at the test zone of lateral flow strip coupled with a shunt and PDMS droplets. The combination of both shunt and PDMS droplets decreases the average velocity at the test zone.

This indicates that with a fixed length of shunt (1 cm), the higher the number of PDMS droplets, the lower the fluid velocity, which supports the experimental data. In addition, consistent with the data in **Fig. 6.14**, a higher number of PDMS droplets leads to a longer nitrocellulose membrane involved in tortuosity, resulting in a higher biomolecule reaction rates and thus a higher signal intensity of the test zone.

6.3.4 Integration of sensitivity enhancement techniques into sample-to-answer biosensor with clinical sample testing

As there is an urgent need for the development of a sample-to-answer biosensor for sensitive medical diagnosis in resource-poor settings, the potential of integrating the optimum fluidic control strategy into the prototype fully integrated paper-based sample-to-answer biosensor was evaluated **(Fig. 6.16)**.

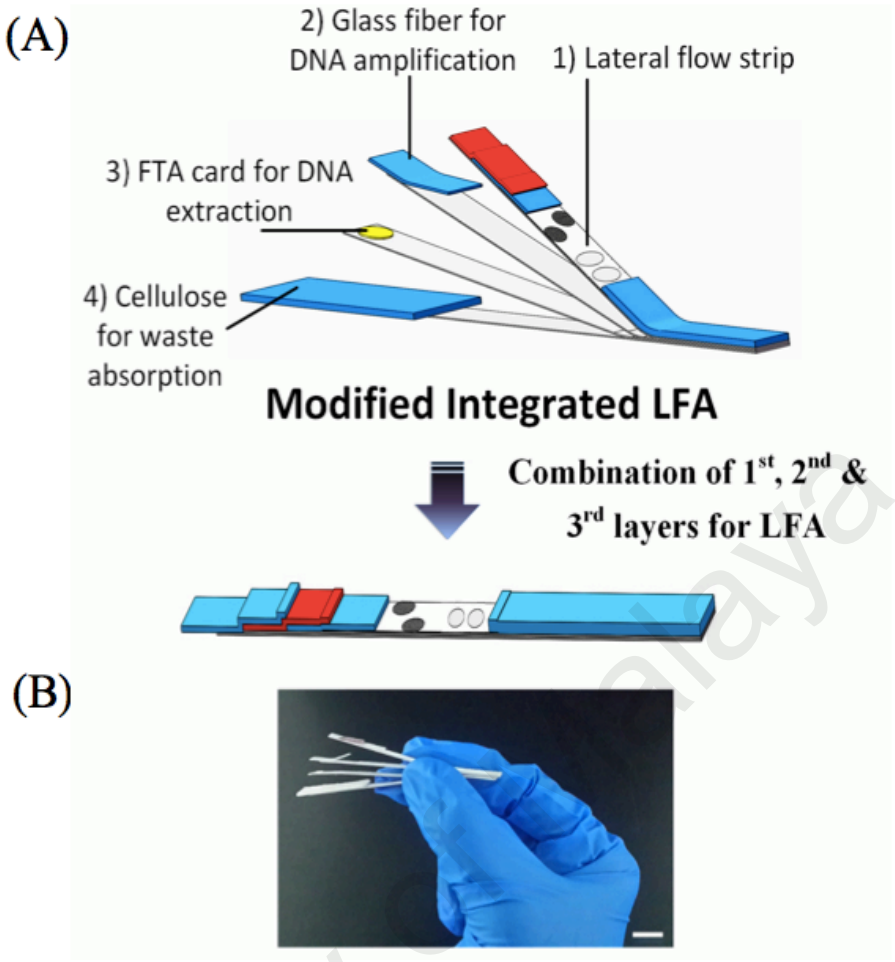

Figure 6.16: A schematic diagram of integrating both sensitivity enhancement techniques into an integrated paper-based biosensor for clinical sample testing. (A) Schematic of a modified paper-based sample-to-answer biosensor for DNA extraction, amplification and sensitive lateral flow detection and (B) its image (Scale bar, 1 cm).

To prove the potential use of this modified LFA for sensitive clinical diagnosis, Hepatitis B Virus was selected as model analyte in clinical assessment. About 16 HBV-positive clinical samples, which were confirmed by gold standard qPCR (**Table 6.2**), were initially tested with conventional benchtop DNA analysis, involving tube-based DNA extraction, tube-based LAMP and electrophoresis. In accordance with the result of gold standard qPCR, electrophoresis showed clearly visible band with high viral DNA concentration (10^7 to 10^8 IU/mL) and light colour of bands with low viral DNA concentration (10^2 to 10^4 IU/mL) **(Fig. 6.17A)**.

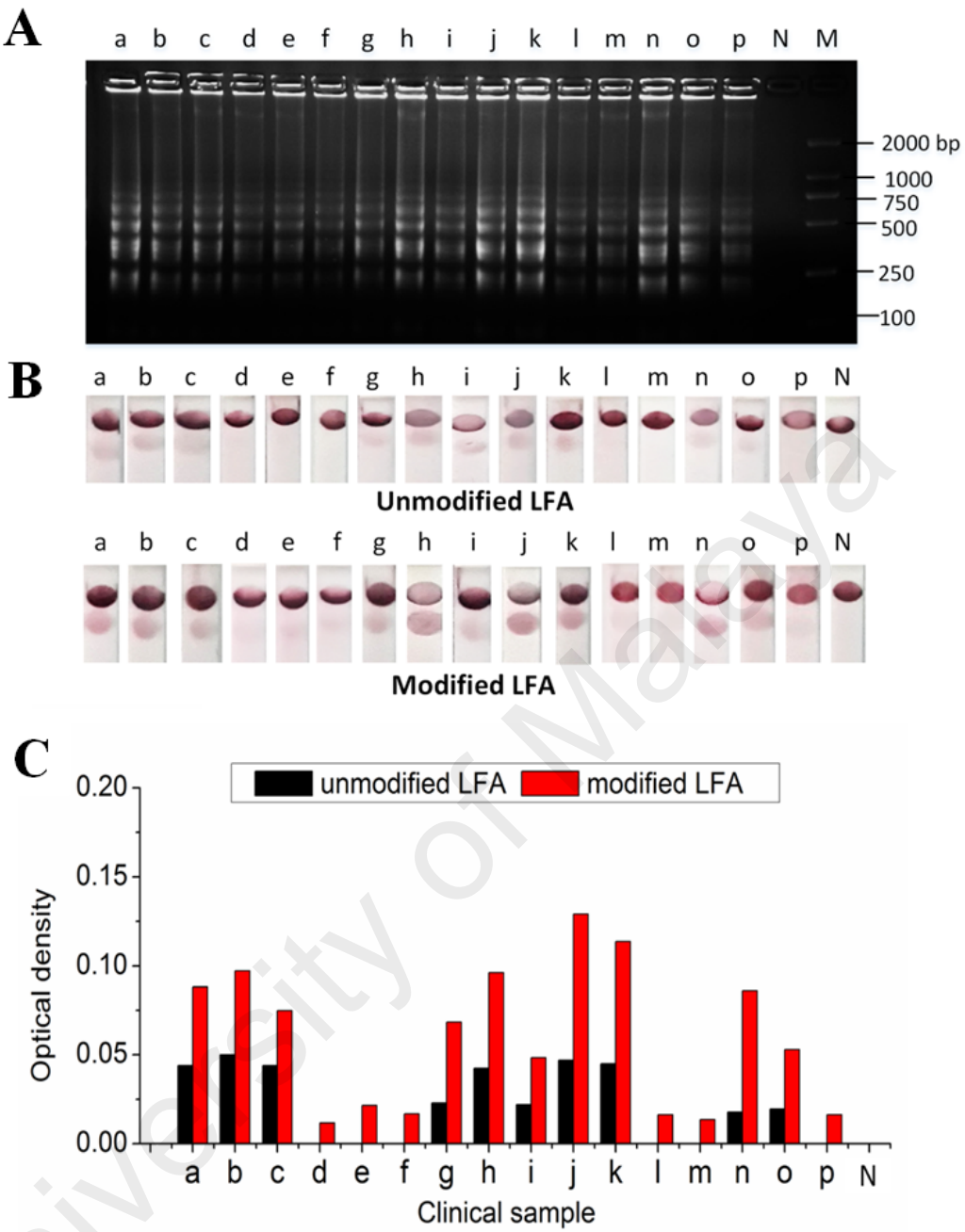

Figure 6.17: Integration of both sensitivity enhancement techniques into a paper-based sample-to-answer biosensor for clinical sample testing. In accordance with the result of gold standard qPCR, 16 HBV positive samples (Sample a-p) showed clearly visible bands in electrophoresis (A) (N = negative control, M= 100-2000 bp marker). By integrating the fluidic control techniques into the prototype paper-based sample-to-answer biosensor, it was found that at high target concentration, a higher intensity of red signal was observed at the test zone in modified LFA as compared to that of unmodified LFA, whereas at low target concentration, the red signal can still be observed in modified LFA but are absent in unmodified LFA (B), which are corresponding to the optical densities obtained through grey scale analysis (C).

To demonstrate the potential of the sample-to-answer biosensor to sensitively detect HBV, fluidic control techniques were incorporated into the prototype. Interestingly, it was found that testing with the patient blood with high concentration of HBV results in a higher optical density of test zone using the modified sample-to-answer biosensor whereas a lower intensity of test zone was observed in the unmodified sample-to-answer biosensor. On the other hand, in the presence of low HBV concentration in blood, modified sample-to-answer biosensor (with modified LFA) showed a lower intensity of test zone whereas unmodified LFA showed no signal at the test zone **(Fig. 6.17B-C)**.

Additionally, the good specificity of the modified sample-to-answer biosensor was also evidenced by the only positive result shown in HBV-positive clinical samples, whereas other samples such as Hepatitis C virus (HCV 1 & 2), cytomegalovirus (CMV 1 & 2) and samples from healthy donors (Healthy 1, 2 & 3) showed negative results **(Fig. 6.18)**.

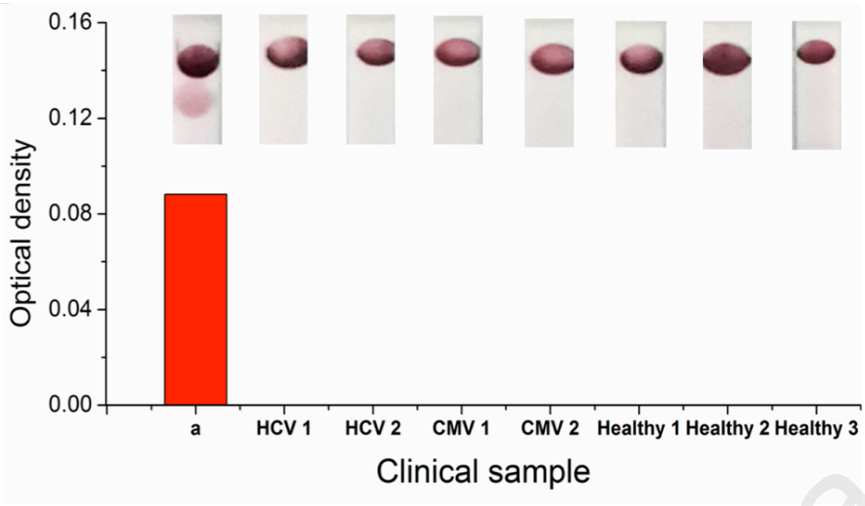

Figure 6.18: Specificity assay using the modified integrated paper-based sample-to-answer biosensor. Good specificity was demonstrated by the only positive result shown in HBV sample (Sample a) whereas the two HCV samples (HCV 1 and 2), two cytomegalovirus sample (CMV 1 and 2) and three blood samples from healthy donors (Healthy 1, 2 and 3) showed negative result.

6.4 Discussion

To date, the poor sensitivity of LFA has limited its widespread applications. Therefore, in this study, a novel strategy of integrating a simple fluidic control strategy into LFA was proposed, by delaying the fluid flow. Generally, there are two ways of reducing the reagent transport rate in LFA without modification of strip size. The first way is incorporating an additional porous medium (*e.g.*, cellulose) to absorb the fluid and thus reduce its flow rate in the paper (Toley et al., 2013), while the other way is creating hydrophobic barriers (*e.g.*, wax barrier) to obstruct the regular flow in the paper (Rivas et al., 2014). In LFAs, it was proposed that both ways enable analytical sensitivity enhancement by increasing the binding and reaction rates of biomolecules before being captured by the capturing molecules (in this case, streptavidin).

In fact, various kinds of nitrocellulose membranes with different lengths and capillary flow rates are available in the market, which may contribute to the assay

sensitivity. The nitrocellulose membrane used in this study (2.0 cm length with a flow rate of 180 sec/4 cm) is commonly used in research institutes and industries, which has been utilized in the previous studies (Bind et al., 2014; Choi, 2015; Choi et al., 2016b; Tang et al., 2016). In the present study, to evaluate the effect produced by the shunt and PDMS barrier, the nitrocellulose membrane with an even lower capillary flow rate was not used. The length of the membrane was not modified as increasing the length may cause more sample or reagent consumption, whereas reducing the length may result in poor sensitivity due to the lower biomolecule interaction rate and shorter time for the biomolecules to reach the test zone (Rivas et al., 2014).

In an effort towards miniaturization of the biosensor with a simple fabrication process, which is compatible with POC applications, the size of the conventional strip is maintained (~ 6 cm × 2.5 cm), including the size and shape of sample and conjugate pads. Additionally, the unmodified conjugate pad could fix the AuNP-DP deposition site, thus producing a consistent result. Therefore, a piece of shunt and PDMS barrier were added into LFA without modifying the shape and size of the pad. The number of shunt was not manipulated, to avoid the potential risk of creating gaps between the adjacent layers, which would inconsistently affect the fluid flow. Also, the shunt thickness was not modified, as the glass fiber used in the study is commercially available with limited choice of thickness.

As 5-fold signal enhancement induced by the glass-fiber shunt might not be sufficient for most medical diagnostic, it was suggested to further improve the analytical sensitivity by creating an additional hydrophobic barrier. As discussed earlier, increasing the length of shunt showed potential risk of sample loss due to the increased absorbent capacity of shunt, resulting in a low sensitivity of LFA. Therefore, it was

suggested that adding a hydrophobic barrier for further sensitivity enhancement would be a better choice, which acts as an obstacle to delay the sample flow without consuming a large volume of sample. To prove the potential of the PDMS barrier to control the fluid flow in LFA, the LFA was performed by creating a different number of PDMS droplets on the strip without implementing the shunt.

As our group currently focuses on developing handheld apparatus to facilitate both fabrication and operation of the biosensor in remote settings, PDMS dropping was performed, which could be potentially achieved by using a portable apparatus instead of microstructures patterning, which normally requires the bench-top equipment like high-end inkjet printers and electrically-powered heaters. In the present study, a handheld pipette is used to dispense the PDMS onto the nitrocellulose membrane, followed by drying using the prototype handheld battery-powered heating device. A portable PDMS printing device was currently developed to achieve accurate, precise and highly reproducible modified lateral flow strips. The entire fabrication and operation process is simple and rapid, which is readily performable in remote settings.

In short, the rate of the fluid flow through the lateral flow strip is altered by incorporation of the shunt and the PDMS barrier. In the presence of shunt with the optimum length of 1 cm, a significant amount of the sample from the nitrocellulose membrane is diverted into the shunt, causing a fluidic delay in the nitrocellulose membrane. The shunt acts as a reaction space for AuNP-DP and target DNA, hence increasing their interaction rate. The process results in more formation of AuNP-DP-target complexes, which eventually bind to the streptavidin at the test zone and produce a high intensity of test zone, thus enhancing the analytical sensitivity of the assay. In addition to the shunt, incorporating the optimum two droplets of PDMS induces the

tortuosity effects, which obstructs the fluid flow and leads to the different flow magnitude and direction. This effect promotes fluid mixing, which could enhance the AuNP-DP and target DNA interaction, thus further enhancing the sensitivity of LFA. The optimum fluidic delay (223.1 ± 2.36 sec) was achieved in the presence of paper-based shunt and two PDMS droplets, achieving optimum biomolecule interactions and hence enhancing the detection sensitivity. The fluidic control strategy allows highly sensitive target detection, achieving a 10-fold signal enhancement over conventional unmodified LFA.

As there is an urgent need to develop a highly sensitive sample-to-answer biosensor for medical diagnosis in resource-poor settings, the potential of integrating the optimum fluidic control strategy into the prototype sample-to-answer biosensor was evaluated, using Hepatitis B Virus (HBV) as a target analyte. Generally, in acute HBV infections, the concentration of HBV could be as low as 10^2 to 10^4 IU/mL (Nie et al., 2010; Rehermann & Nascimbeni, 2005). Using the modified sample-to-answer biosensor, the prototype was able to detect the clinical samples with HBV concentrations of as low as ~10^2 IU/mL, highlighting its potential application in rapid and early detection of HBV infection.

The proposed modified LFA offers several advantages over the existing fluidic control methods. Unlike the LFAs with implemented temperature-sensitive wax-barriers, incorporating heat-resistant PDMS barrier enables all types of temperature-dependent amplification in NAT. In contrast to the LFA with architecture modifications, the proposed LFA allows easier manufacturing process and reduces the volume of sample and reagent required. Collectively, the modified prototype enables low cost, portable and rapid sample in-to-answer out detection of target analyte with comparable

performance to the conventional laboratory-based DNA analysis. The current prototype could be broadly applied to other target analytes, offering great potential for a wide range of applications.

6.5 Conclusion

In this study, a novel strategy of integrating a simple fluidic control strategy into LFA was proposed. The strategy involves incorporating a piece of paper-based shunt and a polydimethylsiloxane (PDMS) barrier to the strip to achieve optimum fluidic delays for LFA signal enhancement. With an optimum size of shunt and number of PDMS droplets, the fluidic transport can be greatly controlled in LFA without consuming a large volume of sample. The phenomena of fluidic delay, which contributes to the sensitivity enhancement, were evaluated by the mathematical simulation, through which the fluid movement throughout the shunt and the tortuosity effects in the presence of PDMS were revealed. This fluidic control strategy allows highly sensitive medical diagnosis, resulting in 10-fold signal enhancement over conventional unmodified LFA. Additionally, integrating this strategy into the prototype sample-to-answer biosensor enables highly sensitive detection of HBV (~10^2 IU/mL), which is comparable to the conventional laboratory-based assays. The proposed modified sample-to-answer biosensor shows great promise to sensitively detect various target analytes for a broad range of applications in the near future.

Future work should focus on evaluation of different parameters of shunt, including the different shunt number (with different pattern of stacking) and shunt thickness (synthetic shunts with different thicknesses) to be compared with that of shunt length for LFA sensitivity improvement. Future work should also include the development of a portable PDMS printing device to achieve accurate, precise and

highly reproducible lateral flow strips, allowing rapid strip fabrication and sensitive target detection in remote settings.

CHAPTER 7: CONCLUSIONS AND FUTURE PERSPECTIVES

7.1 Conclusions

In the present study, a novel fully integrated paper-based biosensor incorporating nucleic acid extraction, amplification and lateral flow detection was demonstrated for the first time. Firstly, the concentration of reagent and environmental factors was optimized. It was found that the optimum reagent concentrations are 2 mg/ml, 3 nM and 4 × for streptavidin, AuNP-DP and SSC buffer, respectively. It was also successfully proven that temperatures of 25-30 °C and a relative humidity beyond 50% give an optimum signal for biotinylated DNA detection in LFA.

Subsequently, an integrated LAMP-LFA biosensor was developed with the aid of a handheld battery-powered heating device for effective amplification and detection of targets in resource-poor settings. With optimum reagent concentration and environmental factors, target DENV DNA amplification and detection were performed using an integrated paper-based platform, achieving a detection limit of as low as 3×10^3 copies, which is comparable to that of conventional tube-based LAMP-LFA in an unintegrated format.

Paper-based extraction was further integrated into the biosensor to create a four-layer fully integrated paper-based sample-to-answer biosensor, which produces a simple colorimetric signal detectable by the naked eyes, eradicating the need for an extra UV source for assay readout. The integrated biosensor is coupled with the handheld heating device, which eradicates the need for the high-end equipment commonly used for amplification such as a thermal cycler, an electrical heater or a water bath. The biosensor can successfully detect *E. coli* in spiked drinking water, milk, blood, and

spinach with a detection limit of as low as 10-1000 CFU/mL, and HBV in clinical blood samples with detection limit of ~10^4 IU/mL, highlighting its potential use in medical diagnostics, food safety analyses and environmental monitoring.

The sensitivity of the integrated biosensor was enhanced by incorporating a piece of paper-based shunt and a PDMS barrier to the lateral flow strip to achieve optimum fluidic delays for LFA signal enhancement, resulting in 10-fold signal enhancement over unmodified LFA. This strategy enables highly sensitive detection of HBV in clinical sample, achieving a detection limit of as low as ~10^2 IU/mL, which is comparable to the conventional laboratory-based assays. The phenomena of fluidic delay was also evaluated by mathematical simulation, through which the fluid movement throughout the shunt and the tortuosity effects in the presence of PDMS barrier were revealed, factors which significantly enhance the sensitivity of the assay. The proposed modified fully integrated biosensor shows great promise in the sensitive detection of various target analytes for a broad range of applications in the near future.

7.2 Future perspectives

A number of limitations should be addressed for potential real world applications. To eliminate the requirement for laboratory unit (*e.g.,* refrigerator) for reagent storage and multiple processing steps (*e.g.,* pipetting) which increases the risk of contamination, future work should include on-chip reagent storage (*e.g.,* hydrogel as a fluid reservoir (Niedl & Beta, 2015) or on-chip dry reagent storage (Shu et al., 2003)) for simple device operation. The capability for reagent storage allows the activation of the biosensor upon the addition of buffer, making the biosensor more user-friendly. In addition, the ability of the biosensor to store the reagent at room temperature circumvents the need for laboratory storage facilities.

Additionally, to address the tedious operation steps, incorporating paper-based valve technology into the paper-based biosensor (Gerbers et al., 2014) is also essential to enable automated sequential fluid delivery without intermittent technical disruptions. Besides that, a low cost and disposable chemical heater (Buser et al., 2016; Lillis et al., 2014) could be used for coupling with the biosensor to substitute the battery-powered heater to provide heat for specific isothermal amplifications of NAT in remote settings.

In addition, as multiplex detection represents another major demand for integrated paper-based assays, future work should also include developing an integrated biosensor with an ability to detect multiple targets simultaneously in a single assay, which would immensely improve its usability. To realize the quantitative analysis of LFAs, the utilization of a handheld solar-powered reader or a readily available smartphone-based reader is also important to allow accurate quantification of the assay, which is particularly useful in resource-limited settings (Song et al., 2012). The result can be analyzed by end-users for quick decision-making or transferred to an off-site laboratory to be analyzed by trained personnel.

To achieve contamination-free and sensitive fully integrated NAT, future work should focus on developing a portable closed system with precise control of optimum temperature and relative humidity, for the entire sample-in-answer-out process in POC settings, coupled with a smartphone for data analysis (Ge et al., 2013; Zaki & Shanbag, 2010). An automated system starting from nucleic acid extraction, and proceeding through amplification to result analysis with minimal intermittent technical disruptions, is of paramount importance for NAT in resource-poor settings, and meets the ASSURED criteria outlined by the WHO, that is, to be affordable, sensitive, specific, user-friendly, rapid and robust, equipment-free, and deliverable to end users for target

detection. In the future there will be more studies focusing on paper-based sample-to-answer biosensors dedicated to a wide range of applications.

REFERENCES

Akhtar, Asifa, Fuchs, Elaine, Mitchison, Tim, Shaw, Reuben J., St Johnston, Daniel, Strasser, Andreas, . . . Zerial, Marino. (2011). A decade of molecular cell biology: Achievements and challenges. *Nature Reviews: Molecular Cell Biology, 12*(10), 669-674.

Aye, Khin Saw, Matsuoka, Masanori, Kai, Masanori, Kyaw, Kyaw, Win, Aye Aye, Shwe, Mu Mu, . . . Htoon, Myo Thet. (2011). Fta card utility for pcr detection of mycobacterium leprae. *Japanese Journal of Infectious Diseases, 64*(3), 246-248.

Barry, John F, & DeMille, David. (2012). Low-temperature physics: A chilling effect for molecules. *Nature, 491*(7425), 539-540.

Beckett, Sara M, Laughton, Stephen J, Dalla Pozza, Luciano, McCowage, Geoffrey B, Marshall, Glenn, Cohn, Richard J, . . . Ashton, Lesley J. (2008). Buccal swabs and treated cards: Methodological considerations for molecular epidemiologic studies examining pediatric populations. *American Journal of Epidemiology, 167*(10), 1260-1267.

Bhatt, Samir, Gething, Peter W, Brady, Oliver J, Messina, Jane P, Farlow, Andrew W, Moyes, Catherine L, . . . Sankoh, Osman. (2013). The global distribution and burden of dengue. *Nature, 496*(7446), 504-507.

Bind, M. A., Zanobetti, A., Gasparrini, A., Peters, A., Coull, B., Baccarelli, A., . . . Schwartz, J. (2014). Effects of temperature and relative humidity on DNA methylation. *Epidemiology, 25*(4), 561-569. doi: 10.1097/ede.0000000000000120

Blacksell, S. D., Bell, D., Kelley, J., Mammen, M. P., Jr., Gibbons, R. V., Jarman, R. G., . . . Newton, P. N. (2007). Prospective study to determine accuracy of rapid serological assays for diagnosis of acute dengue virus infection in laos. *Clinical and Vaccine Immunology, 14*(11), 1458-1464. doi: 10.1128/cvi.00482-06

Blacksell, Stuart D, Jarman, Richard G, Bailey, Mark S, Tanganuchitcharnchai, Ampai, Jenjaroen, Kemajittra, Gibbons, Robert V, . . . Lalloo, David G. (2011). Evaluation of six commercial point-of-care tests for diagnosis of acute dengue infections: The need for combining ns1 antigen and igm/igg antibody detection to achieve acceptable levels of accuracy. *Clinical and Vaccine Immunology, 18*(12), 2095-2101.

Blažková, Martina, Koets, Marjo, Rauch, Pavel, & van Amerongen, Aart. (2009). Development of a nucleic acid lateral flow immunoassay for simultaneous detection of listeria spp. And listeria monocytogenes in food. *European Food Research and Technology, 229*(6), 867-874. doi: 10.1007/s00217-009-1115-z

Brooks, C. S., & Purcell, W. R. (1952). *Surface area measurements on sedimentary rocks*.

Buser, Joshua, Zhang, Xiaohong, Byrnes, Samantha, Ladd, Paula D, Heiniger, Erin K, Wheeler, Maxwell D, . . . Weigl, Bernhard H. (2016). A disposable chemical heater and dry enzyme preparation for lysis and extraction of DNA and rna from microorganisms. *Analytical Methods*.

Carrilho, Emanuel, Phillips, Scott T, Vella, Sarah J, Martinez, Andres W, & Whitesides, George M. (2009). Paper microzone plates. *Analytical Chemistry, 81*(15), 5990-5998.

Cate, David M, Adkins, Jaclyn A, Mettakoonpitak, Jaruwan, & Henry, Charles S. (2014). Recent developments in paper-based microfluidic devices. *Analytical Chemistry, 87*(1), 19-41.

Chen, Yi-Hsun, Kuo, Zong-Keng, & Cheng, Chao-Min. (2015). Paper–a potential platform in pharmaceutical development. *Trends in Biotechnology, 33*(1), 4-9.

Chien, L. J., Liao, T. L., Shu, P. Y., Huang, J. H., Gubler, D. J., & Chang, G. J. (2006). Development of real-time reverse transcriptase pcr assays to detect and serotype dengue viruses. *Journal of Clinical Microbiology, 44*(4), 1295-1304. doi: 10.1128/jcm.44.4.1295-1304.2006

Chiu, R. Y., Jue, E., Yip, A. T., Berg, A. R., Wang, S. J., Kivnick, A. R., . . . Kamei, D. T. (2014). Simultaneous concentration and detection of biomarkers on paper. *Lab Chip, 14*(16), 3021-3028. doi: 10.1039/c4lc00532e

Choi, Heungyeal, Im, Kyuhyun, & Chang, Taihyun. (2012). Fractionation of poly (dimethyl siloxane) by interaction chromatography. *Macromolecular Research, 20*(1), 101-105.

Choi, J. R., Hu, J., Feng, S., Wan Abas, W. A. B., Pingguan-Murphy, B., & Xu, F. . (2015a). Paper-based point-of-care testing for diagnosis of dengue infections. *Critical Reviews in Biotechnology*.

Choi, J.R., Hu, J., Feng, S., Wan Abas, W.A.B., Pingguan-Murphy, B. & Xu, F. . (2015). Sensitive biomolecule detection in lateral flow assay with a portable temperature-humidity control device. *Biosensors and Bioelectronics, 79*, 98-107. doi: 10.1016/j.bios.2015.12.005

Choi, Jane Ru, Hu, Jie, Feng, Shangsheng, Abas, Wan Abu Bakar Wan, Pingguan-Murphy, Belinda, & Xu, Feng. (2016a). Sensitive biomolecule detection in lateral flow assay with a portable temperature–humidity control device. *Biosensors and Bioelectronics, 79*, 98-107.

Choi, Jane Ru, Hu, Jie, Tang, Ruihua, Gong, Yan, Feng, Shangsheng, Ren, Hui, . . . Pingguan-Murphy, Belinda. (2016b). An integrated paper-based sample-to-answer biosensor for nucleic acid testing at the point of care. *Lab Chip*.

Choi, Jane Ru, Tang, Ruihua, Wang, ShuQi, Abas, Wan Abu Bakar Wan, Pingguan-Murphy, Belinda, & Xu, Feng. (2015b). Paper-based sample-to-answer molecular diagnostic platform for point-of-care diagnostics. *Biosensors and Bioelectronics, 74*, 427-439.

Christopher, Paul, Robinson, Nikki, & Shaw, MichaelK. (2005). Antibody-label conjugates in lateral-flow assays. In RaphaelC Wong & HarleyY Tse (Eds.), *Drugs of abuse* (pp. 87-98): Humana Press.

Chun, Ai Lin. (2014). Diagnostics: Better paper-based assays. *Nature Nanotechnology*.

Conceicao, T. M., Da Poian, A. T., & Sorgine, M. H. (2010). A real-time pcr procedure for detection of dengue virus serotypes 1, 2, and 3, and their quantitation in clinical and laboratory samples. *Journal of Virological Methods, 163*(1), 1-9. doi: 10.1016/j.jviromet.2009.10.001

Connelly, John T, Nugen, Sam R, Borejsza-Wysocki, Wlodek, Durst, Richard A, Montagna, Richard A, & Baeumner, Antje J. (2008). Human pathogenic cryptosporidium species bioanalytical detection method with single oocyst detection capability. *Anal Bioanal Chem, 391*(2), 487-495.

Connelly, John Thomas, Rolland, Jason P, & Whitesides, George M. (2015). A" paper machine" for molecular diagnostics. *Analytical Chemistry*.

Crannell, Zachary Austin, Castellanos-Gonzalez, Alejandro, Irani, Ayesha, Rohrman, Brittany, White, Arthur Clinton, & Richards-Kortum, Rebecca. (2014). Nucleic acid test to diagnose cryptosporidiosis: Lab assessment in animal and patient specimens. *Analytical chemistry, 86*(5), 2565-2571.

Craw, P., & Balachandran, W. (2012). Isothermal nucleic acid amplification technologies for point-of-care diagnostics: A critical review. *Lab Chip, 12*(14), 2469-2486. doi: 10.1039/c2lc40100b

Cribbie, RA, & Jamieson, J. (2000). Structural equation models and the regression bias for measuring correlates of change. *Educational and Psychological Measurement, 60*, 893 - 907.

Cuzzubbo, A. J., Endy, T. P., Nisalak, A., Kalayanarooj, S., Vaughn, D. W., Ogata, S. A., . . . Devine, P. L. (2001). Use of recombinant envelope proteins for serological diagnosis of dengue virus infection in an immunochromatographic assay. *Clinical and Diagnostic Laboratory Immunology, 8*(6), 1150-1155. doi: 10.1128/cdli.8.6.1150-1155.2001

Dauner, Allison L., Mitra, Indrani, Gilliland Jr, Theron, Seales, Sajeewane, Pal, Subhamoy, Yang, Shih-Chun, . . . Wu, Shuenn-Jue L. (2015). Development of a pan-serotype reverse transcription loop-mediated isothermal amplification assay for the detection of dengue virus. *Diagnostic Microbiology and Infectious Disease, 83*(1), 30-36. doi: http://dx.doi.org/10.1016/j.diagmicrobio.2015.05.004

De Paula, S. O., & Fonseca, B. A. (2004). Dengue: A review of the laboratory tests a clinician must know to achieve a correct diagnosis. *Brazilian Journal of Infectious Diseases, 8*(6), 390-398. doi: /S1413-86702004000600002

de Paz, Hector David, Brotons, Pedro, & Muñoz-Almagro, Carmen. (2014). Molecular isothermal techniques for combating infectious diseases: Towards low-cost point-of-care diagnostics. *Expert Rev Mol Diagn, 14*(7), 827-843.

De Roy, Karen, Marzorati, Massimo, Negroni, Andrea, Thas, Olivier, Balloi, Annalisa, Fava, Fabio, . . . Boon, Nico. (2013). Environmental conditions and community evenness determine the outcome of biological invasion. *Nat Commun, 4*, 1383.

de Vargas Wolfgramm, Eldamária, de Carvalho, Fernanda Magri, da Costa Aguiar, Vitor Rezende, Sartori, Mariana Penha De Nadai, Hirschfeld-Campolongo, Gabriela CR, Tsutsumida, Weslley M, & Louro, Iúri Drumond. (2009).

Simplified buccal DNA extraction with fta® elute cards. *Forensic science international: Genetics, 3*(2), 125-127.

de Vries, Jutte JC, Barbi, Maria, Binda, Sandro, & Claas, Eric CJ. (2012). Extraction of DNA from dried blood in the diagnosis of congenital cmv infection *Diagnosis of sexually transmitted diseases* (pp. 169-175): Springer.

Dineva, M. A., Candotti, D., Fletcher-Brown, F., Allain, J. P., & Lee, H. (2005). Simultaneous visual detection of multiple viral amplicons by dipstick assay. *Journal of Clinical Microbiology, 43*(8), 4015-4021. doi: 10.1128/jcm.43.8.4015-4021.2005

Dos Santos, Francisco, Andrade, Pedro Z, Boura, Joana S, Abecasis, Manuel M, Da Silva, Claudia Lobato, & Cabral, Joaquim. (2010). Ex vivo expansion of human mesenchymal stem cells: A more effective cell proliferation kinetics and metabolism under hypoxia. *Journal of Cellular Physiology, 223*(1), 27-35.

Dossi, Nicolò, Toniolo, Rosanna, Pizzariello, Andrea, Impellizzieri, Flavia, Piccin, Evandro, & Bontempelli, Gino. (2013). Pencil ‐ drawn paper supported electrodes as simple electrochemical detectors for paper ‐ based fluidic devices. *Electrophoresis, 34*(14), 2085-2091.

Dungchai, Wijitar, Chailapakul, Orawon, & Henry, Charles S. (2010). Use of multiple colorimetric indicators for paper-based microfluidic devices. *Analytica Chimica Acta, 674*(2), 227-233.

Durel, L, Benoit, F, Treilles, M, & Farre, M. (2015). Extraction of mastitis pathogen DNA from sample collecting cards: Practical consequences. *J Vet Sci Anim Husb, 3*(2), 202.

Eichmann, S. L., & Bevan, M. A. (2010). Direct measurements of protein-stabilized gold nanoparticle interactions. *Langmuir, 26*(18), 14409-14413. doi: 10.1021/la1027674

Ellis, MJ. (2004). Neoadjuvant endocrine therapy as a drug development strategy. *Clinical Cancer Research, 10*, 391S - 395S.

Fang, X., Tan, O. K., Tse, M. S., & Ooi, E. E. (2010). A label-free immunosensor for diagnosis of dengue infection with simple electrical measurements. *Biosensors and Bioelectronics, 25*(5), 1137-1142. doi: 10.1016/j.bios.2009.09.037

Fauci, Anthony S., & Morens, David M. (2012). The perpetual challenge of infectious diseases. *New England Journal of Medicine, 366*(5), 454-461. doi: doi:10.1056/NEJMra1108296

Feasey, Nicholas A, Dougan, Gordon, Kingsley, Robert A, Heyderman, Robert S, & Gordon, Melita A. (2012). Invasive non-typhoidal salmonella disease: An emerging and neglected tropical disease in africa. *The Lancet, 379*(9835), 2489-2499.

Feng, Shangsheng, Choi, Jane Ru, Lu, Tian Jian, & Xu, Feng. (2015). State-of-art advances in liquid penetration theory and flow control in paper for paper-based diagnosis. *Adv Porous Flow., 5*, 16-29.

Fernández-Soto, Pedro, Mvoulouga, Prosper Obolo, Akue, Jean Paul, Abán, Julio López, Santiago, Belén Vicente, Sánchez, Miguel Cordero, & Muro, Antonio. (2014). Development of a highly sensitive loop-mediated isothermal amplification (lamp) method for the detection of loa loa. *PloS One, 9*(4).

Francois, Patrice, Tangomo, Manuela, Hibbs, Jonathan, Bonetti, Eve‐Julie, Boehme, Catharina C, Notomi, Tsugunori, . . . Schrenzel, Jacques. (2011). Robustness of a loop‐mediated isothermal amplification reaction for diagnostic applications. *FEMS Immunology and Medical Microbiology, 62*(1), 41-48.

Fridley, Gina E, Le, Huy Q, Fu, Elain, & Yager, Paul. (2012). Controlled release of dry reagents in porous media for tunable temporal and spatial distribution upon rehydration. *Lab Chip, 12*(21), 4321-4327.

Fronczek, Christopher F., Park, Tu San, Harshman, Dustin K., Nicolini, Ariana M., & Yoon, Jeong-Yeol. (2014). Paper microfluidic extraction and direct smartphone-based identification of pathogenic nucleic acids from field and clinical samples. *RSC Advances, 4*(22), 11103-11110. doi: 10.1039/C3RA47688J

Fry, Scott R, Meyer, Michelle, Semple, Matthew G, Simmons, Cameron P, Sekaran, Shamala Devi, Huang, Johnny X, . . . Young, Paul R. (2011). The diagnostic sensitivity of dengue rapid test assays is significantly enhanced by using a combined antigen and antibody testing approach. *PLoS Neglected Tropical Diseases, 5*(6), e1199.

Fu, Elain, Lutz, Barry, Kauffman, Peter, & Yager, Paul. (2010). Controlled reagent transport in disposable 2d paper networks. *Lab Chip, 10*(7), 918-920.

Gan, Wupeng, Zhuang, Bin, Zhang, Pengfei, Han, Junping, Li, Cai-Xia, & Liu, Peng. (2014). A filter paper-based microdevice for low-cost, rapid, and automated DNA extraction and amplification from diverse sample types. *Lab Chip, 14*(19), 3719-3728.

Ge, Yiyue, Wu, Bin, Qi, Xian, Zhao, Kangchen, Guo, Xiling, Zhu, Yefei, . . . Wang, Hua. (2013). Rapid and sensitive detection of novel avian-origin influenza a (h7n9) virus by reverse transcription loop-mediated isothermal amplification combined with a lateral-flow device.

Gerbers, Roman, Foellscher, Wilke, Chen, Hong, Anagnostopoulos, Constantine, & Faghri, Mohammad. (2014). A new paper-based platform technology for point-of-care diagnostics. *Lab Chip, 14*(20), 4042-4049. doi: 10.1039/C4LC00786G

Giokas, Dimosthenis L, Tsogas, George Z, & Vlessidis, Athanasios G. (2014). Programming fluid transport in paper-based microfluidic devices using razor-crafted open channels. *Analytical Chemistry, 86*(13), 6202-6207.

Goldsborough, M.D., & Fox, D.K. (2006). Methods for the storage and synthesis of nucleic acids using a solid support: Google Patents.

Gomes, Bruna Carrer, Franco, Bernadette Dora Gombossy de Melo, & De Martinis, Elaine Cristina Pereira. (2013). Microbiological food safety issues in brazil: Bacterial pathogens. *Foodborne Pathogens and Disease, 10*(3), 197-205.

Guzman, M. G., Alvarez, M., Rodriguez-Roche, R., Bernardo, L., Montes, T., Vazquez, S., . . . Halstead, S. B. (2007). Neutralizing antibodies after infection with dengue 1 virus. *Emerging Infectious Diseases, 13*(2), 282-286. doi: 10.3201/eid1302.060539

Guzman, M. G., & Kouri, G. (2004). Dengue diagnosis, advances and challenges. *International Journal of Infectious Diseases, 8*(2), 69-80.

Han, Yu Long, Wang, Shuqi, Zhang, Xiaohui, Li, Yuhui, Huang, Guoyou, Qi, Hao, . . . Xu, Feng. (2014). Engineering physical microenvironment for stem cell based regenerative medicine. *Drug Discovery Today, 19*(6), 763-773. doi: http://dx.doi.org/10.1016/j.drudis.2014.01.015

Hawkins, Kenneth R., & Weigl, Bernhard H. (2010). *Microfluidic diagnostics for low-resource settings*.

He, Y., Zeng, K., Gurung, A. S., Baloda, M., Xu, H., Zhang, X., & Liu, G. (2010). Visual detection of single-nucleotide polymorphism with hairpin oligonucleotide-functionalized gold nanoparticles. *Analytical Chemistry, 82*(17), 7169-7177. doi: 10.1021/ac101275s

He, Yuqing, Zhang, Sanquan, Zhang, Xibao, Baloda, Meenu, Gurung, Anant S., Xu, Hui, . . . Liu, Guodong. (2011). Ultrasensitive nucleic acid biosensor based on enzyme–gold nanoparticle dual label and lateral flow strip biosensor. *Biosensors and Bioelectronics, 26*(5), 2018-2024. doi: http://dx.doi.org/10.1016/j.bios.2010.08.079

Hossain, SM Zakir, Ozimok, Cory, Sicard, Clémence, Aguirre, Sergio D, Ali, M Monsur, Li, Yingfu, & Brennan, John D. (2012). Multiplexed paper test strip for quantitative bacterial detection. *Analytical and bioanalytical chemistry, 403*(6), 1567-1576.

Houseley, J, & Tollervey, D. (2009). The many pathways of rna degradation. *Cell, 136*(4), 763 - 776.

Hu, Jie, Cui, Xingye, Gong, Yan, Xu, Xiayu, Gao, Bin, Wen, Ting, . . . Xu, Feng. (2016). Portable microfluidic and smartphone-based devices for monitoring of cardiovascular diseases at the point of care. *Biotechnol Adv*.

Hu, Jie, Wang, Lin, Li, Fei, Han, Yu Long, Lin, Min, Lu, Tian Jian, & Xu, Feng. (2013). Oligonucleotide-linked gold nanoparticle aggregates for enhanced sensitivity in lateral flow assays. *Lab Chip, 13*(22), 4352-4357.

Hu, Jie, Wang, ShuQi, Wang, Lin, Li, Fei, Pingguan-Murphy, Belinda, Lu, Tian Jian, & Xu, Feng. (2014). Advances in paper-based point-of-care diagnostics. *Biosensors and Bioelectronics, 54*(0), 585-597. doi: http://dx.doi.org/10.1016/j.bios.2013.10.075

Huang, Min Joon, Xie, Hui, Wan, Qiangqiang, Zhang, Li, Ning, Yong, & Zhang, Guo-Jun. (2013). Serotype-specific identification of dengue virus by silicon nanowire array biosensor. *Journal of nanoscience and nanotechnology, 13*(6), 3810-3817.

Hue, Kien Duong Thi, Tuan, Trung Vu, Thi, Hanh Tien Nguyen, Bich, Chau Tran Nguyen, Le Anh, Huy Huynh, Wills, Bridget A, & Simmons, Cameron P.

(2011). Validation of an internally controlled one-step real-time multiplex rt-pcr assay for the detection and quantitation of dengue virus rna in plasma. *Journal of Virological Methods, 177*(2), 168-173.

Hunsperger, E. A., Yoksan, S., Buchy, P., Nguyen, V. C., Sekaran, S. D., Enria, D. A., . . . Peeling, R. W. (2009). Evaluation of commercially available anti-dengue virus immunoglobulin m tests. *Emerging Infectious Diseases, 15*(3), 436-440. doi: 10.3201/eid1503.080923

Johnson, B. W., Russell, B. J., & Lanciotti, R. S. (2005). Serotype-specific detection of dengue viruses in a fourplex real-time reverse transcriptase pcr assay. *Journal of Clinical Microbiology, 43*(10), 4977-4983. doi: 10.1128/jcm.43.10.4977-4983.2005

Kaewphinit, Thongchai, Arunrut, Narong, Kiatpathomchai, Wansika, Santiwatanakul, Somchai, Jaratsing, Pornpun, & Chansiri, Kosum. (2013). Detection of mycobacterium tuberculosis by using loop-mediated isothermal amplification combined with a lateral flow dipstick in clinical samples. *BioMed research international, 2013*.

Kahn, Kalju, & Plaxco, Kevin W. (2010). Principles of biomolecular recognition *Recognition receptors in biosensors* (pp. 3-45): Springer.

Kao, C. L., King, C. C., Chao, D. Y., Wu, H. L., & Chang, G. J. (2005). Laboratory diagnosis of dengue virus infection: Current and future perspectives in clinical diagnosis and public health. *Journal of Microbiology, Immunology, and Infection. Wei Mian Yu Gan Ran Za Zhi, 38*(1), 5-16.

Katsanis, Sara Huston, & Katsanis, Nicholas. (2013). Molecular genetic testing and the future of clinical genomics. *Nat Rev Genet, 14*(6), 415-426. doi: 10.1038/nrg3493

Kersting, S., Rausch, V., Bier, F. F., & von Nickisch-Rosenegk, M. (2014). Rapid detection of plasmodium falciparum with isothermal recombinase polymerase amplification and lateral flow analysis. *Malaria Journal, 13*, 99. doi: 10.1186/1475-2875-13-99

Khunthong, Sasiwarat, Jaroenram, Wansadaj, Arunrut, Narong, Suebsing, Rungkarn, Mungsantisuk, Idsada, & Kiatpathomchai, Wansika. (2013). Rapid and sensitive detection of shrimp yellow head virus by loop-mediated isothermal amplification combined with a lateral flow dipstick. *Journal of Virological Methods, 188*(1), 51-56.

Kim, Hyung-Seok, Ko, Hyuk, Kang, Min-Jung, & Pyun, Jae-Chul. (2010). Highly sensitive rapid test with chemiluminescent signal bands. *BioChip Journal, 4*(2), 155-160.

Kim, Tae-Hyeong, Park, Juhee, Kim, Chi-Ju, & Cho, Yoon-Kyoung. (2014). Fully integrated lab-on-a-disc for nucleic acid analysis of food-borne pathogens. *Analytical Chemistry, 86*(8), 3841-3848. doi: 10.1021/ac403971h

Kong, Y. Y., Thay, C. H., Tin, T. C., & Devi, S. (2006). Rapid detection, serotyping and quantitation of dengue viruses by taqman real-time one-step rt-pcr. *Journal of Virological Methods, 138*(1-2), 123-130. doi: 10.1016/j.jviromet.2006.08.003

Krebs, Matthew G., Metcalf, Robert L., Carter, Louise, Brady, Ged, Blackhall, Fiona H., & Dive, Caroline. (2014). Molecular analysis of circulating tumour cells[mdash]biology and biomarkers. *Nature Reviews: Clinical Oncology, 11*(3), 129-144. doi: 10.1038/nrclinonc.2013.253

Kudo, Takayuki, Oshima, Takeshi, Kure, Shigeo, Matsubara, Yoichi, & Ikeda, Katsuhisa. (2004). Mutation detection of gjb2 using isocode and real‐time quantitative polymerase chain reaction with sybr green i dye for newborn hearing screening. *The Laryngoscope, 114*(7), 1299-1304.

Kumanan, Vijayarani, Nugen, Sam R, Baeumner, Antje J, & Chang, Yung-Fu. (2009). A biosensor assay for the detection of mycobacterium avium subsp. Paratuberculosis in fecal samples. *Journal of Veterinary Science, 10*(1), 35-42.

Kumbhat, S., Sharma, K., Gehlot, R., Solanki, A., & Joshi, V. (2010a). Surface plasmon resonance based immunosensor for serological diagnosis of dengue virus infection. *Journal of Pharmaceutical and Biomedical Analysis, 52*(2), 255-259. doi: 10.1016/j.jpba.2010.01.001

Kumbhat, Sunita, Sharma, Kavita, Gehlot, Rakhee, Solanki, Aruna, & Joshi, Vinod. (2010b). Surface plasmon resonance based immunosensor for serological diagnosis of dengue virus infection. *Journal of Pharmaceutical and Biomedical Analysis, 52*(2), 255-259. doi: http://dx.doi.org/10.1016/j.jpba.2010.01.001

Laakso, Sanna, & Mäki, Minna. (2013). Assessment of a semi-automated protocol for multiplex analysis of sepsis-causing bacteria with spiked whole blood samples. *MicrobiologyOpen, 2*(2), 284-292. doi: 10.1002/mbo3.69

LaBarre, Paul, Hawkins, Kenneth R, Gerlach, Jay, Wilmoth, Jared, Beddoe, Andrew, Singleton, Jered, . . . Weigl, Bernhard. (2011). A simple, inexpensive device for nucleic acid amplification without electricity—toward instrument-free molecular diagnostics in low-resource settings. *PloS One, 6*(5), e19738.

Lange, V, Arndt, K, Schwarzelt, C, Boehme, I, Giani, AS, Schmidt, AH, . . . Wassmuth, R. (2014). High density fta plates serve as efficient long‐term sample storage for hla genotyping. *Tissue Antigens, 83*(2), 101-105.

Lau, Yee-Ling, Lai, Meng-Yee, Teoh, Boon-Teong, Abd-Jamil, Juraina, Johari, Jefree, Sam, Sing-Sin, . . . AbuBakar, Sazaly. (2015). Colorimetric detection of dengue by single tube reverse-transcription-loop-mediated isothermal amplification. *PloS One, 10*(9), e0138694.

Lee, Yu-Fang, Lien, Kang-Yi, Lei, Huan-Yao, & Lee, Gwo-Bin. (2009). An integrated microfluidic system for rapid diagnosis of dengue virus infection. *Biosensors and Bioelectronics, 25*(4), 745-752.

Li, Yuanyuan, Liu, Shoujie, Yao, Tao, Sun, Zhihu, Jiang, Zheng, Huang, Yuying, . . . Wei, Shiqiang. (2012). Controllable synthesis of gold nanoparticles with ultrasmall size and high monodispersity via continuous supplement of precursor. *Dalton Transactions, 41*(38), 11725-11730. doi: 10.1039/C2DT31270K

Liang, Xiao, Chigerwe, Munashe, Hietala, Sharon K, & Crossley, Beate M. (2014). Evaluation of fast technology analysis (fta) cards as an improved method for

specimen collection and shipment targeting viruses associated with bovine respiratory disease complex. *Journal of Virological Methods, 202*, 69-72.

Lien, Kang-Yi, Lee, Wan-Chi, Lei, Huan-Yao, & Lee, Gwo-Bin. (2006). *Micro reverse transcription polymerase chain reaction systems using super-paramagnetic beads for virus detection.* Paper presented at the Nano/Micro Engineered and Molecular Systems, 2006. NEMS'06. 1st IEEE International Conference on.

Lillis, Lorraine, Lehman, Dara, Singhal, Mitra C, Cantera, Jason, Singleton, Jered, Labarre, Paul, . . . Wood, Robert. (2014). Non-instrumented incubation of a recombinase polymerase amplification assay for the rapid and sensitive detection of proviral hiv-1 DNA. *PloS One, 9*(9), e108189.

Linnes, Jacqueline C, Fan, Andy, Rodriguez, Natalia M, Lemieux, Bertrand, Kong, Huimin, & Klapperich, Catherine M. (2014). Paper-based molecular diagnostic for chlamydia trachomatis. *RSC Advances, 4*(80), 42245-42251.

Liu, Changchun, Sadik, Mohamed M, Mauk, Michael G, Edelstein, Paul H, Bushman, Frederic D, Gross, Robert, & Bau, Haim H. (2014). Nuclemeter: A reaction-diffusion based method for quantifying nucleic acids undergoing enzymatic amplification. *Scientific Reports, 4*.

Liu, Haidong, Patil, Prabhamani, & Narusawa, Uichiro. (2007). On darcy-brinkman equation: Viscous flow between two parallel plates packed with regular square arrays of cylinders. *Entropy, 9*(3), 118.

Liu, Hong, & Crooks, Richard M. (2011). Three-dimensional paper microfluidic devices assembled using the principles of origami. *Journal of the American Chemical Society, 133*(44), 17564-17566.

Liu, Shan, Xie, Zhimei, Zhang, Weiwei, Cao, Xia, & Pei, Xiaofang. (2013). Risk assessment in chinese food safety. *Food Control, 30*(1), 162-167. doi: 10.1016/j.foodcont.2012.06.038

Liu, Zhi, Hu, Jie, Zhao, Yimeng, Qu, Zhiguo, & Xu, Feng. (2015). Experimental and numerical studies on liquid wicking into filter papers for paper-based diagnostics. *Applied Thermal Engineering, 88*, 280-287. doi: http://dx.doi.org/10.1016/j.applthermaleng.2014.09.057

Lourens, A., Jarvis, J. N., Meintjes, G., & Samuel, C. M. (2014). Rapid diagnosis of cryptococcal meningitis using the lateral flow assay on csf samples: The influence of the high dose "hook" effect. *Journal of Clinical Microbiology*. doi: 10.1128/jcm.01683-14

Lowe, Christopher R. (2007). Overview of biosensor and bioarray technologies. *Handbook of biosensors and biochips*.

Luo, Long, Li, Xiang, & Crooks, Richard M. (2014). Low-voltage origami-paper-based electrophoretic device for rapid protein separation. *Analytical Chemistry*.

Luong, John H. T., Male, Keith B., & Glennon, Jeremy D. (2008). Biosensor technology: Technology push versus market pull. *Biotechnol Adv, 26*(5), 492-500. doi: http://dx.doi.org/10.1016/j.biotechadv.2008.05.007

Lutz, Barry, Liang, Tinny, Fu, Elain, Ramachandran, Sujatha, Kauffman, Peter, & Yager, Paul. (2013). Dissolvable fluidic time delays for programming multi-step assays in instrument-free paper diagnostics. *Lab Chip, 13*(14), 2840-2847.

Lutz, Barry R, Trinh, Philip, Ball, Cameron, Fu, Elain, & Yager, Paul. (2011). Two-dimensional paper networks: Programmable fluidic disconnects for multi-step processes in shaped paper. *Lab Chip, 11*(24), 4274-4278.

Mao, X., Ma, Y., Zhang, A., Zhang, L., Zeng, L., & Liu, G. (2009). Disposable nucleic acid biosensors based on gold nanoparticle probes and lateral flow strip. *Analytical Chemistry, 81*(4), 1660-1668. doi: 10.1021/ac8024653

Martinez, A. W., Phillips, S. T., Whitesides, G. M., & Carrilho, E. (2010). Diagnostics for the developing world: Microfluidic paper-based analytical devices. *Anal Chem, 82*(1), 3-10.

Martinez, Andres W. (2011). Microfluidic paper-based analytical devices: From pocket to paper-based elisa. *Bioanalysis, 3*(23), 2589-2592.

Martinez, Andres W, Phillips, Scott T, & Whitesides, George M. (2008). Three-dimensional microfluidic devices fabricated in layered paper and tape. *Proceedings of the National Academy of Sciences, 105*(50), 19606-19611.

McFall, Sally M, Wagner, Robin L, Jangam, Sujit R, Yamada, Douglas H, Hardie, Diana, & Kelso, David M. (2015). A simple and rapid DNA extraction method from whole blood for highly sensitive detection and quantitation of hiv-1 proviral DNA by real-time pcr. *Journal of Virological Methods, 214*, 37-42.

Minnucci, Giulia, Amicarelli, Giulia, Salmoiraghi, Silvia, Spinelli, Orietta, Guinea Montalvo, Marie Lorena, Giussani, Ursula, . . . Rambaldi, Alessandro. (2012). A novel, highly sensitive and rapid allele-specific loop-mediated amplification assay for the detection of the jak2v617f mutation in chronic myeloproliferative neoplasms. *Haematologica, 97*(9), 1394-1400. doi: 10.3324/haematol.2011.056184

Moghadam, B. Y., Connelly, K. T., & Posner, J. D. (2015). Two orders of magnitude improvement in detection limit of lateral flow assays using isotachophoresis. *Anal Chem, 87*(2), 1009-1017. doi: 10.1021/ac504552r

Moher, D, Schulz, KF, & Altman, DG. (2001). The consort statement: Revised recommendations for improving the quality of reports of parallel-group randomized trials. *Annals of Internal Medicine, 134*, 657 - 662.

Morales-Narváez, Eden, Naghdi, Tina, Zor, Erhan, & Merkoçi, Arben. (2015). Photoluminescent lateral-flow immunoassay revealed by graphene oxide: Highly sensitive paper-based pathogen detection. *Analytical Chemistry, 87*(16), 8573-8577. doi: 10.1021/acs.analchem.5b02383

Mudanyali, Onur, Dimitrov, Stoyan, Sikora, Uzair, Padmanabhan, Swati, Navruz, Isa, & Ozcan, Aydogan. (2012). Integrated rapid-diagnostic-test reader platform on a cellphone. *Lab Chip, 12*(15), 2678-2686. doi: 10.1039/c2lc40235a

Nations, The United. (2015). The millennium development goals report 2015. New York: the Statistics Division of the United Nations Department of Economic and Social Affairs.

Ngo, Hoan T., Wang, Hsin-Neng, Fales, Andrew M., Nicholson, Bradly P., Woods, Christopher W., & Vo-Dinh, Tuan. (2014). DNA bioassay-on-chip using sers detection for dengue diagnosis. *Analyst, 139*(22), 5655-5659. doi: 10.1039/C4AN01077A

Nguyen, Binh Thi Thanh, Peh, Alister En Kai, Chee, Celine Yue Ling, Fink, Katja, Chow, Vincent TK, Ng, Mary ML, & Toh, Chee-Seng. (2012). Electrochemical impedance spectroscopy characterization of nanoporous alumina dengue virus biosensor. *Bioelectrochemistry, 88*, 15-21.

Nie, Ji, Zhang, De-Wen, Tie, Cai, Zhou, Ying-Lin, & Zhang, Xin-Xiang. (2014). G-quadruplex based two-stage isothermal exponential amplification reaction for label-free DNA colorimetric detection. *Biosensors and Bioelectronics, 56*, 237-242. doi: http://dx.doi.org/10.1016/j.bios.2014.01.032

Nie, Z., Nijhuis, C. A., Gong, J., Chen, X., Kumachev, A., Martinez, A. W., . . . Whitesides, G. M. (2010). Electrochemical sensing in paper-based microfluidic devices. *Lab Chip, 10*(4), 477-483. doi: 10.1039/b917150a

Niedl, Robert R, & Beta, Carsten. (2015). Hydrogel-driven paper-based microfluidics. *Lab Chip, 15*(11), 2452-2459.

Niemz, Angelika, Ferguson, Tanya M, & Boyle, David S. (2011). Point-of-care nucleic acid testing for infectious diseases. *Trends in Biotechnology, 29*(5), 240-250.

Nyachuba, D.G. (2010). Foodborne illness: Is it on the rise? *Nutrition reviews, 68*(5), 257-269.

Oberholster, Paul J, Myburgh, Jan G, Ashton, Pete J, Coetzee, Jan J, & Botha, Anna-Maria. (2012). Bioaccumulation of aluminium and iron in the food chain of lake loskop, south africa. *Ecotoxicology and Environmental Safety, 75*, 134-141.

Ortayli, Nuriye, Ringheim, Karin, Collins, Lynn, & Sladden, Tim. (2014). Sexually transmitted infections: Progress and challenges since the 1994 international conference on population and development (icpd). *Contraception, 90*(6), S22-S31.

Pai, Nitika Pant, Vadnais, Caroline, Denkinger, Claudia, Engel, Nora, & Pai, Madhukar. (2012). Point-of-care testing for infectious diseases: Diversity, complexity, and barriers in low-and middle-income countries. *PLoS Medicine, 9*(9), e1001306.

Pan-ngum, Wirichada, Blacksell, Stuart D, Lubell, Yoel, Pukrittayakamee, Sasithon, Bailey, Mark S, de Silva, H Janaka, . . . Limmathurotsakul, Direk. (2013). Estimating the true accuracy of diagnostic tests for dengue infection using bayesian latent class models. *PloS One, 8*(1), e50765.

Park, Jaenam, Park, Sojung, & Kim, Young-Kee. (2010). Multiplex detection of pathogens using an immunochromatographic assay strip. *BioChip Journal, 4*(4), 305-312.

Park, Seungkyung, Zhang, Yi, Lin, Shin, Wang, Tza-Huei, & Yang, Samuel. (2011). Advances in microfluidic pcr for point-of-care infectious disease diagnostics. *Biotechnol Adv, 29*(6), 830-839. doi: http://dx.doi.org/10.1016/j.biotechadv.2011.06.017

Parolo, Claudio, Medina-Sánchez, Mariana, de la Escosura-Muñiz, Alfredo, & Merkoçi, Arben. (2013). Simple paper architecture modifications lead to enhanced sensitivity in nanoparticle based lateral flow immunoassays. *Lab Chip, 13*(3), 386-390.

Peeling, R. W., Artsob, H., Pelegrino, J. L., Buchy, P., Cardosa, M. J., Devi, S., . . . Yoksan, S. (2010). Evaluation of diagnostic tests: Dengue. *Nat Rev Microbiol, 8*(12 Suppl), S30-38.

Peeling, R. W., & McNerney, R. (2014). Emerging technologies in point-of-care molecular diagnostics for resource-limited settings. *Expert Rev Mol Diagn, 14*(5), 525-534. doi: 10.1586/14737159.2014.915748

Perumal, Veeradasan, & Hashim, Uda. (2014). Advances in biosensors: Principle, architecture and applications. *Journal of Applied Biomedicine, 12*(1), 1-15. doi: http://dx.doi.org/10.1016/j.jab.2013.02.001

Pezzoli, N, Silvy, M, Woronko, A, Le Treut, T, Lévy-Mozziconacci, A, Reviron, D, . . . Picard, C. (2007). Quantification of mixed chimerism by real time pcr on whole blood-impregnated fta cards. *Leukemia Research, 31*(9), 1175-1183.

Pöhlmann, Christopher, Dieser, Irina, & Sprinzl, Mathias. (2014). A lateral flow assay for identification of escherichia coli by ribosomal rna hybridisation. *Analyst, 139*(5), 1063-1071.

Pok, Kwoon-Yong, Lai, Yee-Ling, Sng, Joshua, & Ng, Lee-Ching. (2010). Evaluation of nonstructural 1 antigen assays for the diagnosis and surveillance of dengue in singapore. *Vector-Borne and Zoonotic Diseases, 10*(10), 1009-1016.

Posthuma-Trumpie, GeertruidaA, Korf, Jakob, & van Amerongen, Aart. (2009). Lateral flow (immuno)assay: Its strengths, weaknesses, opportunities and threats. A literature survey. *Anal Bioanal Chem, 393*(2), 569-582. doi: 10.1007/s00216-008-2287-2

Pyrek, Kelly M. (2014). Emerging infectious diseases: Mers-cov, avian influenza remind us of the ongoing challenge.

Qin, Z., Chan, W. C., Boulware, D. R., Akkin, T., Butler, E. K., & Bischof, J. C. (2012). Significantly improved analytical sensitivity of lateral flow immunoassays by using thermal contrast. *Angewandte Chemie. International Ed. In English, 51*(18), 4358-4361. doi: 10.1002/anie.201200997

Qu, Z. G., He, X. C., Lin, M., Sha, B. Y., Shi, X. H., Lu, T. J., & Xu, F. (2013). Advances in the understanding of nanomaterial-biomembrane interactions and their mathematical and numerical modeling. *Nanomedicine (Lond), 8*(6), 995-1011. doi: 10.2217/nnm.13.81

Razali, Nornadiah Mohd, & Wah, Yap Bee. (2011). Power comparisons of shapiro-wilk, kolmogorov-smirnov, lilliefors and anderson-darling tests. *Journal of Statistical Modeling and Analytics, 2*(1), 21-33.

Rehermann, Barbara, & Nascimbeni, Michelina. (2005). Immunology of hepatitis b virus and hepatitis c virus infection. *Nature Reviews Immunology, 5*(3), 215-229.

Renault, Christophe, Li, Xiang, Fosdick, Stephen E, & Crooks, Richard M. (2013). Hollow-channel paper analytical devices. *Analytical Chemistry, 85*(16), 7976-7979.

Rigano, Luciano A, Malamud, Florencia, Orce, Ingrid G, Filippone, Maria P, Marano, Maria R, do Amaral, Alexandre Morais, . . . Vojnov, Adrian. (2014). Rapid and sensitive detection of candidatus liberibacter asiaticus by loop mediated isothermal amplification combined with a lateral flow dipstick. *BMC Microbiology, 14*(1), 86.

Rigano, Luciano A, Marano, María R, Castagnaro, Atilio P, Do Amaral, Alexandre M, & Vojnov, Adrian A. (2010). Rapid and sensitive detection of citrus bacterial canker by loop-mediated isothermal amplification combined with simple visual evaluation methods. *BMC Microbiology, 10*(1), 176.

Rivas, Lourdes, Medina-Sánchez, Mariana, de la Escosura-Muñiz, Alfredo, & Merkoçi, Arben. (2014). Improving sensitivity of gold nanoparticle-based lateral flow assays by using wax-printed pillars as delay barriers of microfluidics. *Lab Chip, 14*(22), 4406-4414.

Rodriguez, Natalia M, Linnes, Jacqueline C, Fan, Andy, Ellenson, Courtney K, Pollock, Nira R, & Klapperich, Catherine M. (2015). Paper-based rna extraction, in situ isothermal amplification, and lateral flow detection for low-cost, rapid diagnosis of influenza a (h1n1) from clinical specimens. *Analytical Chemistry, 87*(15), 7872-7879.

Rohrman, Brittany A, Leautaud, Veronica, Molyneux, Elizabeth, & Richards-Kortum, Rebecca R. (2012). A lateral flow assay for quantitative detection of amplified hiv-1 rna. *PloS One, 7*(9), e45611.

Rosenfeld, Tally, & Bercovici, Moran. (2014). 1000-fold sample focusing on paper-based microfluidic devices. *Lab Chip, 14*(23), 4465-4474.

Røsland, Gro Vatne, Svendsen, Agnete, Torsvik, Anja, Sobala, Ewa, McCormack, Emmet, Immervoll, Heike, . . . Lønning, Per Eystein. (2009). Long-term cultures of bone marrow–derived human mesenchymal stem cells frequently undergo spontaneous malignant transformation. *Cancer Research, 69*(13), 5331-5339.

Scallan, E., Griffin, P.M., Angulo, F.J., Tauxe, R.V., & Hoekstra, R.M. (2011a). Foodborne illness acquired in the united states—unspecified agents. *Emerging infectious diseases, 17*(1), 16.

Scallan, E., Hoekstra, R.M., Angulo, F.J., Tauxe, R.V., Widdowson, M.A., Roy, S.L., . . . Griffin, P.M. (2011b). Foodborne illness acquired in the united states—major pathogens. *Emerg Infect Dis, 17*(1).

Scharff, R.L. (2012). Economic burden from health losses due to foodborne illness in the united states. *Journal of Food Protection&# 174;, 75*(1), 123-131.

Schilling, S., Ludolfs, D., Van An, L., & Schmitz, H. (2004). Laboratory diagnosis of primary and secondary dengue infection. *Journal of Clinical Virology, 31*(3), 179-184. doi: 10.1016/j.jcv.2004.03.020

Shu, P. Y., Chen, L. K., Chang, S. F., Yueh, Y. Y., Chow, L., Chien, L. J., . . . Huang, J. H. (2003). Comparison of capture immunoglobulin m (igm) and igg enzyme-linked immunosorbent assay (elisa) and nonstructural protein ns1 serotype-specific igg elisa for differentiation of primary and secondary dengue virus infections. *Clinical and Diagnostic Laboratory Immunology, 10*(4), 622-630.

Siah, Ahmed, & McKenna, Patricia. (2013). Rapid detection assay for the invasive vase tunicate, ciona intestinalis, using loop-mediated isothermal amplification combined with lateral flow dipstick. *Management, 4*(1), 81-86.

Song, Chunmei, Liu, Cheng, Wu, Shuyan, Li, Haolin, Guo, Huiqin, Yang, Biao, . . . Liu, Qing. (2016). Development of a lateral flow colloidal gold immunoassay strip for the simultaneous detection of shigella boydii and escherichia coli o157:H7 in bread, milk and jelly samples. *Food Control, 59*, 345-351. doi: http://dx.doi.org/10.1016/j.foodcont.2015.06.012

Song, Chunmei, Zhi, Aimin, Liu, Qingtang, Yang, Jifei, Jia, Guochao, Shervin, Jahanian, . . . Xu, Chuanlai. (2013a). Rapid and sensitive detection of β-agonists using a portable fluorescence biosensor based on fluorescent nanosilica and a lateral flow test strip. *Biosensors and Bioelectronics, 50*, 62-65.

Song, Y., Zhang, Y., Bernard, P. E., Reuben, J. M., Ueno, N. T., Arlinghaus, R. B., . . . Qin, L. (2012). Multiplexed volumetric bar-chart chip for point-of-care diagnostics. *Nat Commun, 3*, 1283. doi: 10.1038/ncomms2292

Song, Yujun, Wang, Yuanchen, & Qin, Lidong. (2013b). A multistage volumetric bar chart chip for visualized quantification of DNA. *Journal of the American Chemical Society, 135*(45), 16785-16788. doi: 10.1021/ja4085397

Song, Yujun, Xia, Xuefeng, Wu, Xifeng, Wang, Ping, & Qin, Lidong. (2014). Integration of platinum nanoparticles with a volumetric bar-chart chip for biomarker assays. *Angewandte Chemie International Edition*, n/a-n/a. doi: 10.1002/anie.201404349

Stubbs, Samantha Licy, Hsiao, Sarah Tzu-Feng, Peshavariya, Hitesh Mahendrabhai, Lim, Shiang Yong, Dusting, Gregory James, & Dilley, Rodney James. (2011). Hypoxic preconditioning enhances survival of human adipose-derived stem cells and conditions endothelial cells in vitro. *Stem cells and development, 21*(11), 1887-1896.

Tai, Dar-Fu, Lin, Chung-Yin, Wu, Tzong-Zeng, & Chen, Li-Kuang. (2005). Recognition of dengue virus protein using epitope-mediated molecularly imprinted film. *Analytical Chemistry, 77*(16), 5140-5143.

Tamama, K., Kawasaki, H., Kerpedjieva, S. S., Guan, J., Ganju, R. K., & Sen, C. K. (2011). Differential roles of hypoxia inducible factor subunits in multipotential

stromal cells under hypoxic condition. *Journal of Cellular Biochemistry, 112*(3), 804-817. doi: 10.1002/jcb.22961

Tang, Ruihua, Yang, Hui, Choi, Jane Ru, Gong, Yan, Hu, Jie, Feng, Shangsheng, . . . Xu, Feng. (2016). Improved sensitivity of lateral flow assay using paper-based sample concentration technique. *Talanta, 152*, 269-276. doi: http://dx.doi.org/10.1016/j.talanta.2016.02.017

Teles, F. R. R., & Fonseca, L. P. (2008). Applications of polymers for biomolecule immobilization in electrochemical biosensors. *Materials Science and Engineering: C, 28*(8), 1530-1543. doi: http://dx.doi.org/10.1016/j.msec.2008.04.010

Teles, F. S. (2011). Biosensors and rapid diagnostic tests on the frontier between analytical and clinical chemistry for biomolecular diagnosis of dengue disease: A review. *Analytica Chimica Acta, 687*(1), 28-42. doi: 10.1016/j.aca.2010.12.011

Teoh, B. T., Sam, S. S., Tan, K. K., Danlami, M. B., Shu, M. H., Johari, J., . . . AbuBakar, S. (2015). Early detection of dengue virus by use of reverse transcription-recombinase polymerase amplification. *Journal of Clinical Microbiology, 53*(3), 830-837. doi: 10.1128/jcm.02648-14

Terao, Yoshitaka, Takeshita, Kana, Nishiyama, Yasutaka, Morishita, Naoki, Matsumoto, Takashi, & Morimatsu, Fumiki. (2015). Promising nucleic acid lateral flow assay plus pcr for shiga toxin–producing escherichia coli. *Journal of Food Protection®, 78*(8), 1560-1568.

Thongkao, Kanittada, Longyant, Siwaporn, Silprasit, Kun, Sithigorngul, Paisarn, & Chaivisuthangkura, Parin. (2013). Rapid and sensitive detection of vibrio harveyi by loop‐mediated isothermal amplification combined with lateral flow dipstick targeted to vhhp2 gene. *Aquaculture Research*.

Toley, Bhushan J, McKenzie, Brittney, Liang, Tinny, Buser, Joshua R, Yager, Paul, & Fu, Elain. (2013). Tunable-delay shunts for paper microfluidic devices. *Analytical Chemistry, 85*(23), 11545-11552.

Toumazou, Christofer, Shepherd, Leila M, Reed, Samuel C, Chen, Ginny I, Patel, Alpesh, Garner, David M, . . . Athanasiou, Panteleimon. (2013). Simultaneous DNA amplification and detection using a ph-sensing semiconductor system. *Nature methods, 10*(7), 641-646.

Umut, Evrim. (2013). *Surface modification of nanoparticles used in biomedical applications*.

Venkatesan, Bala Murali, & Bashir, Rashid. (2011). Nanopore sensors for nucleic acid analysis. *Nature Nanotechnology, 6*(10), 615-624.

Vickers, A. J. (2005). Parametric versus non-parametric statistics in the analysis of randomized trials with non-normally distributed data. *BMC Medical Research Methodology, 5*, 35. doi: 10.1186/1471-2288-5-35

Vickers, AJ. (2001). The use of percentage change from baseline as an outcome in a controlled trial is statistically inefficient: A simulation study. *BMC Medical Research Methodology, 1*, 6.

Vickers, AJ, Rees, RW, Zollman, CE, McCarney, R, Smith, CM, Ellis, N, . . . Haselen, RV. (2004). Acupuncture for chronic headache in primary care: Large, pragmatic, randomised trial. *BMJ, 328*, 744.

Waggoner, Jesse J, Abeynayake, Janaki, Sahoo, Malaya K, Gresh, Lionel, Tellez, Yolanda, Gonzalez, Karla, . . . Guo, Frances P. (2013). Single-reaction, multiplex, real-time rt-pcr for the detection, quantitation, and serotyping of dengue viruses. *PLoS Neglected Tropical Diseases, 7*(4), e2116.

Wang, C., Zhang, L., & Shen, X. (2013a). Development of a nucleic acid lateral flow strip for detection of hepatitis c virus (hcv) core antigen. *Nucleosides Nucleotides Nucleic Acids, 32*(2), 59-68. doi: 10.1080/15257770.2013.763976

Wang, J. H., Wang, C. H., & Lee, G. B. (2012). Sample pretreatment and nucleic acid-based detection for fast diagnosis utilizing microfluidic systems. *Annals of Biomedical Engineering, 40*(6), 1367-1383. doi: 10.1007/s10439-011-0473-4

Wang, L., Huang, G., Sha, B., Wang, S., Han, Y. L., Wu, J., . . . Xu, F. (2014). Engineering three-dimensional cardiac microtissues for potential drug screening applications. *Current Medicinal Chemistry, 21*(22), 2497-2509.

Wang, S., Inci, F., De Libero, G., Singhal, A., & Demirci, U. (2013b). Point-of-care assays for tuberculosis: Role of nanotechnology/microfluidics. *Biotechnol Adv, 31*(4), 438-449. doi: 10.1016/j.biotechadv.2013.01.006

Wang, S., Xu, F., & Demirci, U. (2010). Advances in developing hiv-1 viral load assays for resource-limited settings. *Biotechnol Adv, 28*(6), 770-781. doi: 10.1016/j.biotechadv.2010.06.004

Wanunu, Meni, Dadosh, Tali, Ray, Vishva, Jin, Jingmin, McReynolds, Larry, & Drndić, Marija. (2010). Rapid electronic detection of probe-specific micrornas using thin nanopore sensors. *Nature Nanotechnology, 5*(11), 807-814.

Webster, D. P., Farrar, J., & Rowland-Jones, S. (2009). Progress towards a dengue vaccine. *Lancet Infectious Diseases, 9*(11), 678-687. doi: 10.1016/s1473-3099(09)70254-3

WHO/UNICEF. (2015). Progress on sanitation and drinking water - 2015 update and mdg assessment. New York, USA: WHO/UNICEF Joint Monitoring Programme for Water Supply and Sanitation.

Wu, Grace, Srivastava, Jaya, & Zaman, Muhammad H. (2014). Stability measurements of antibodies stored on paper. *Analytical Biochemistry, 449*(0), 147-154. doi: http://dx.doi.org/10.1016/j.ab.2013.12.012

Wu, Tzong-Zeng, Su, Chih-Cheng, Chen, Li-Kuang, Yang, Hui-Hua, Tai, Dar-Fu, & Peng, Kou-Cheng. (2005). Piezoelectric immunochip for the detection of dengue fever in viremia phase. *Biosensors and Bioelectronics, 21*(5), 689-695.

Wu, Wei, Zhao, Shiming, Mao, Yiping, Fang, Zhiyuan, Lu, Xuewen, & Zeng, Lingwen. (2015). A sensitive lateral flow biosensor for escherichia coli o157:H7 detection based on aptamer mediated strand displacement amplification. *Analytica Chimica Acta, 861*, 62-68. doi: http://dx.doi.org/10.1016/j.aca.2014.12.041

Xu, Xiayu, Wang, Xuemin, Hu, Jie, Wang, Shuqi, Vanholsbeeck, Frédérique, Li, XiuJun, . . . Xu, Feng. Smartphone-based on-site quantitative detection of nucleic acids on lateral flow assays.

Xu, Zhiguang, Zhao, Yan, Dai, Liming, & Lin, Tong. (2014). Multi‐responsive janus liquid marbles: The effect of temperature and acidic/basic vapors. *Particle & Particle Systems Characterization, 31*(8), 839-842.

Yang, X., Forouzan, O., Brown, T. P., & Shevkoplyas, S. S. (2012). Integrated separation of blood plasma from whole blood for microfluidic paper-based analytical devices. *Lab Chip, 12*(2), 274-280. doi: 10.1039/c1lc20803a

Yetisen, Ali Kemal, Akram, Muhammad Safwan, & Lowe, Christopher R. (2013). Paper-based microfluidic point-of-care diagnostic devices. *Lab on a Chip, 13*(12), 2210-2251. doi: 10.1039/C3LC50169H

Yoshida, Wataru, Mochizuki, Eriko, Takase, Madoka, Hasegawa, Hijiri, Morita, Yo, Yamazaki, Hiroki, . . . Ikebukuro, Kazunori. (2009). Selection of DNA aptamers against insulin and construction of an aptameric enzyme subunit for insulin sensing. *Biosensors and Bioelectronics, 24*(5), 1116-1120.

Yu, A. C., Vatcher, G., Yue, X., Dong, Y., Li, M. H., Tam, P. H., . . . Lau, L. T. (2012a). Nucleic acid-based diagnostics for infectious diseases in public health affairs. *Front Med, 6*(2), 173-186.

Yu, AlbertCheung-Hoi, Vatcher, Greg, Yue, Xin, Dong, Yan, Li, MaoHua, Tam, PatrickH K., . . . Lau, Lok-Ting. (2012b). Nucleic acid-based diagnostics for infectious diseases in public health affairs. *Frontiers of Medicine, 6*(2), 173-186. doi: 10.1007/s11684-012-0195-5

Zaki, S. A., & Shanbag, P. (2010). Clinical manifestations of dengue and leptospirosis in children in mumbai: An observational study. *Infection, 38*(4), 285-291. doi: 10.1007/s15010-010-0030-3

Zaytseva, Natalya V, Montagna, Richard A, & Baeumner, Antje J. (2005). Microfluidic biosensor for the serotype-specific detection of dengue virus rna. *Analytical Chemistry, 77*(23), 7520-7527.

Zaytseva, Natalya V, Montagna, Richard A, Lee, Eun Mi, & Baeumner, Antje J. (2004). Multi-analyte single-membrane biosensor for the serotype-specific detection of dengue virus. *Anal Bioanal Chem, 380*(1), 46-53.

Zhang, Chunsun, Xu, Jinliang, Ma, Wenli, & Zheng, Wenling. (2006). Pcr microfluidic devices for DNA amplification. *Biotechnol Adv, 24*(3), 243-284. doi: http://dx.doi.org/10.1016/j.biotechadv.2005.10.002

Zhao, W., & van der Berg, A. (2008). Lab on paper. *Lab Chip, 8*(12), 1988-1991. doi: 10.1039/b814043j

Zhu, J., Zou, N., Zhu, D., Wang, J., Jin, Q., Zhao, J., & Mao, H. (2011). Simultaneous detection of high-sensitivity cardiac troponin i and myoglobin by modified sandwich lateral flow immunoassay: Proof of principle. *Clinical Chemistry, 57*(12), 1732-1738. doi: 10.1373/clinchem.2011.171694

Zimmermann, M., Schmid, H., Hunziker, P., & Delamarche, E. (2007). Capillary pumps for autonomous capillary systems. *Lab Chip, 7*(1), 119-125. doi: 10.1039/b609813d

PUBLICATIONS

1. **Choi, J. R.**, Tang, R., Wang, S., Wan Abas, W. A. B., Pingguan-Murphy, B*. & Xu F.* (2015). Paper-based Sample-to-Answer Molecular Diagnostic Platform for Point-of-Care Diagnostics. *Biosensors and Bioelectronics, 74,* 427-439.

2. **Choi, J. R.**, Hu, J., Feng, S., Wan Abas, W. A. B., Pingguan-Murphy, B., & Xu, F.* (2016). Paper-based Point-of-Care Testing for Diagnosis of Dengue Infections. *Critical Reviews in Biotechnology*, doi: 10.3109/07388551.2016.1139541.

3. **Choi, J. R.**, Hu, J., Feng, S., Wan Abas, W. A. B., Pingguan-Murphy, B.* & Xu, F.* (2016). Sensitive Biomolecule Detection in Lateral Flow Assay with A Portable Temperature-Humidity Control Device. *Biosensors and Bioelectronics, 79,* 98-107.

4. **Choi, J. R.**, Hu, J., Tang, R., Gong, Y., Feng, S., Ren, H.,… Xu, F.* (2016). An Integrated Paper-based Sample-to-Answer Biosensor for Nucleic Acid Testing at the Point of Care. *Lab on a Chip, 16,* 611-621.

5. **Choi, J. R.**, Hu, J., Gong, Y., Feng, S., Wan Abas, W. A. B., Pingguan-Murphy*, B. & Xu, F* (2016). An Integrated Lateral Flow Assay for Effective DNA Amplification and Detection at the Point of Care. *Analyst,* doi: 10.1039/C5AN02532J.

6. **Choi, J. R.**, Liu, Z., Hu, J., Tang, R., Gong, Y., Feng, S., . . . Xu, F*.(2016). Polydimethylsiloxane-Paper Hybrid Lateral Flow Assay for Highly Sensitive Point-of-Care Nucleic Acid Testing. *Analytical Chemistry,* doi: 10.1021/acs.analchem.6b00195.